Journal of Physical and Chemical Reference Data

Survey of Hyperfine Structure Measurements in Alkali Atoms

Cite as: J. Phys. Chem. Ref. Data **51**, 043102 (2022); https://doi.org/10.1063/5.0098061
Submitted: 04 May 2022 • Accepted: 09 September 2022 • Published Online: 09 November 2022

Maria Allegrini, Ennio Arimondo and Luis A. Orozco

AIP Publishing

Journal of Physical and Chemical Reference Data ARTICLE scitation.org/journal/jpr

Survey of Hyperfine Structure Measurements in Alkali Atoms

Cite as: J. Phys. Chem. Ref. Data 51, 043102 (2022); doi: 10.1063/5.0098061
Submitted: 4 May 2022 • Accepted: 9 September 2022 •
Published Online: 9 November 2022

Maria Allegrini,[1,2] Ennio Arimondo,[1,3] and Luis A. Orozco[4,a)]

AFFILIATIONS

[1] Dipartimento di Fisica "E. Fermi," Università di Pisa, Largo B. Pontecorvo 3, 56127 Pisa, Italy
[2] Istituto Nanoscienze-CNR, Piazza S. Silvestro 12, I-56127 Pisa, Italy
[3] Istituto Nazionale di Ottica-CNR, Via G. Moruzzi 1, 56124 Pisa, Italy
[4] Joint Quantum Institute, Department of Physics, University of Maryland and National Institute of Standards and Technology, College Park, Maryland 20742, USA

[a)] **Author to whom correspondence should be addressed:** ennio.arimondo@unipi.it

ABSTRACT

The spectroscopic hyperfine constants for all the alkali atoms are reported. For atoms from lithium to cesium, only the long lived atomic isotopes are examined. For francium, the measured data for nuclear ground states of all available isotopes are listed. All results obtained since the beginning of laser investigations are presented, while for previous works the data of Arimondo *et al.* [Rev. Mod. Phys. **49**, 31 (1977)] are recalled. Global analyses based on the scaling laws and the hyperfine anomalies are performed.

Published by AIP Publishing on behalf of the National Institute of Standards and Technology. https://doi.org/10.1063/5.0098061

Key words: Alkali atoms; Hyperfine structure; Atomic data.

CONTENTS

List of Tables

List of Figures

1. Introduction

Atomic spectroscopy was a key element in the original development of quantum mechanics theory at the beginning of the twentieth century. Its exploratory role continued after the Second World War when microwave sources, very stable Radio frequency generators, optical pumping, and later on lasers entered into the laboratories. The atomic contributions to quantum electrodynamics, parity violation, and the present searches for variation of the fundamental constants and for dark matter tests are noteworthy. In this scenery, the alkali atoms and their hyperfine splittings represent an important reference because of their rather simple energy level structure and their relatively easy laboratory exploration. Furthermore, they offer an opportunity to verify new experimental tools for a direct comparison within a wide research community. Very precise hyperfine constants of the alkalis are required for a large variety of atomic physics and quantum simulation experiments. More accurate hyperfine structure measurements have also revitalized their use in studies and tests of nuclear physics and fundamental symmetries in nature. Formidable progress achieved by atomic physics calculations supporting and also stimulating research on the above-mentioned advanced topics has refined its tools on the alkali hyperfine data.

A complete collection of hyperfine constants for alkali atoms was published by Arimondo *et al.* (1977) at the time when laser sources introduced high-resolution atomic spectroscopy. Since that time, new spectroscopy tools have been developed, and technological advances have produced extremely precise atomic measurements. This progress is the motivation of the present work. The most amazing example of the combination of scientific and technological progress is the atomic fountain proposed by Zacharias in 1953, unpublished but described by Ramsey (1956). Although it does not operate for room temperature atoms, it is very successful for launching ultracold ones, as exploited for hyperfine measurements based on atomic clocks [e.g., see Guéna *et al.* (2014) and Ovchinnikov *et al.* (2015)]. Using such a tool, the hyperfine ground states of rubidium and cesium are presently measured with such a precision that small variations of the fundamental constants can be tested. Recently, the use of frequency combs to perform absolute optical frequency measurements has provided alkali hyperfine values with a precision increased by a factor of up one thousand. In addition, some well assessed spectroscopy tools have been refined. For instance, in Bayram *et al.* (2014), the detection of delayed quantum beats at the hyperfine transition frequencies is used to determine very precise hyperfine coupling constants in several cesium excited states for which the precision of other techniques suffers from short lifetimes. These approaches have increased the precision for a large set of hyperfine measurements.

In another class of experiments, the hyperfine constants have been determined for excited states accessible only by laser sources covering new spectral regions or by multiple laser excitations. The most spectacular example is the alkali Rydberg states investigated for hyperfine structure up to levels with principal quantum number $n \approx 70$. For completeness, here we report a third class of hyperfine measurements of pre-laser times for alkali states not recently investigated. A very interesting example of this class is the ground state hyperfine structures of lithium and sodium for which the precise atomic-beam investigations of 1973–1974 remain the reference point. Certainly, atomic fountain experiments applied to those atoms could yield a precision comparable to that of the atomic clocks.

This work presents a complete overview of the measured hyperfine constants for the alkali atoms in ground or singly excited electronic states. It enlarges or supersedes the recent reviews of Das and Natarajan (2008), Kiran Kumar and Suryanarayana (2014), and Williams *et al.* (2018) that report a limited dataset for lighter alkalis. We also add data to the francium review of Sansonetti (2007). The main target is to provide to interested experimentalists and theoreticians the full set of hyperfine data in an easily accessible form. We have collected the hyperfine data of the stable alkali isotopes published after the review of Arimondo *et al.* (1977). In order to give a complete overview, our tables include measurements already reported in that review in all cases where new and more precise values are not available. We do not examine the unstable isotopes for the alkalis from lithium up to cesium as for them very limited

data were recently published. Instead, we review the full spectrum of the francium nuclear ground state isotopes because of the recent interest associated with this atom as a test of the nuclear structure owing to the large number of explored isotopes for this alkali. This review intends to cover the experimental investigations, while discussing theoretical results only briefly. However, it should be mentioned here that theoretical comparison has greatly progressed, and global analyses for a given alkali atom have produced a large set of theoretical values for the hyperfine constants.

For the experimentalists, this overview might stimulate investigations of specific atomic states for which the precision remains low. As advanced spectroscopic techniques are usually tested only on a few states, a large set of high precision data might boost the theoretical effort for global analyses. Based on Kramida (2022) "NIST atomic energy levels and spectra bibliographic database" (NIST stands for National Institute of Standards and Technology, USA), we have examined all articles that to the best of our knowledge have been published so far. However, we have disregarded publications that do not target the hyperfine splittings. For publications by the same research group reporting subsequent measurements with increasing precision our Tables include only the most recent value.

Section 2 presents the experimental tools exploited to measure the hyperfine constants. At first, the atomic sample is examined from vapor cells up to ultracold atomic clouds where the spatial and velocity confinement greatly increases the spectral resolution. In the following, the experiments are classified within some broad categories allowing a connection to the precision reached in ground and excited states. The core part of this review is Sec. 3. It is composed of tables reporting the hyperfine constants for each alkali isotope classified on the basis of the atomic state and for a given state in chronological order. Before presenting the tables, the basic theoretical concepts of the hyperfine interaction are briefly recalled. For each atom we discuss the main results and we mention large discrepancies, if any, between the data of a given state. For Rb and Cs atoms, where more data are available, Sec. 4 presents scaling laws vs the quantum number of the excited states. Such scaling is applied to determine or confirm the sign of the hyperfine constants for several states. The scaling law is applied also to the S states of francium isotopes for which few data are available. Hyperfine anomalies producing information on the nuclear structure are discussed, at least for the states measured with reasonable precision. A short section concludes this review.

2. Spectroscopic Tools

2.1. Samples

2.1.1. Atomic beam (AB)

In an atomic beam atoms propagate along a given direction with a small spread in the orthogonal plane, see Ramsey (1956). Usually, an exciting laser propagates perpendicularly to the beam propagation leading to a very small Doppler broadening.

2.1.2. Vapor cell (VC)

In a glass/quartz cell the atoms are in the vapor phase and their vapor pressure and the atomic density are controlled by the cell temperature.

2.1.3. Magneto-optical trap (MOT)

The combined action of laser cooling and magnetic field confinement produces dense atomic samples having a greatly reduced Doppler linewidth. Such samples allow to detect weak absorption features, as for highly excited states, and to perform experiments with long interaction times leading to increased precision.

2.1.4. Fountain (FOUNT)

In a fountain, atoms from a MOT are launched vertically by radiation pressure or a moving optical lattice [see Metcalf and van der Straten (1999)]. Excitation and detection take place at the same vertical position, the first one at the launching time and the second after the parabolic motion. Very high parabolic evolutions are used in order to increase the interrogation time. This approach is applied to the atomic clocks.

2.1.5. Optical dipole trap (ODT)

In the experiment by Neuzner *et al.* (2015) a single ^{87}Rb atom is trapped by an optical dipole trap created by a 2D optical lattice. Cavity-enhanced state detection of the optical absorption produces a good signal-to-noise ratio even for a single atom. Light-shift correction is carefully applied.

2.1.6. Thermoionic diode (TD)

In the presence of a weak electrical discharge in a VC, the light excited atoms are ionized by electron collisions. These ions diffuse into the space charge region of the diode, compensate partially the space charge, and increase the thermionic diode current, as described in Herrmann *et al.* (1985).

2.2. Spectroscopic techniques

The experimental techniques used to measure the reported hyperfine measurements are classified in the following. Several research groups have introduced a specific name for their technique. While our classification scheme is concise, detailed presentations of the techniques can be found in textbooks, such as Ramsey (1956), Kopfermann (1958), Foot (2005), Budker *et al.* (2008), and Inguscio and Fallani (2013).

2.2.1. Coherent-control spectroscopy (CCS)

This saturated absorption spectroscopy is based on copropagating pump and probe acting on a three-level V system. Similar to saturated absorption spectroscopy in a two-level system and to the electromagnetic-induced transparency in a Λ level scheme, a pump laser originates an atomic coherence in a branch of the V scheme. The absorption profile of a probe laser is modified. The frequency difference between pump and probe lasers furnishes the excited state energy splitting, as in Das and Natarajan (2005).

2.2.2. Delayed detection (DD)

The natural linewidth of a spectroscopic resonance is reduced by monitoring the atom evolution for times longer than the spontaneous emission lifetime. This refinement was

combined with other techniques, such as laser-induced fluorescence by Shimizu *et al.* (1987) or hyperfine quantum-beats by Deech *et al.* (1977), Krist *et al.* (1977), and Yei *et al.* (1993).

2.2.3. Double-resonance optical pumping (DROP)

A double-resonance optical excitation on a ladder three-level scheme is applied. An increased signal-to-noise ratio is obtained by detecting the population of the ground state rather than the excited state one. In the copropagating geometry, one laser excites zero velocity atoms on the lower transition and a second laser is scanned in frequency, as in Moon *et al.* (2009). In the counterpropagating geometry, it is often combined with electromagnetic-induced transparency.

2.2.4. Electromagnetic induced transparency (EIT)

This coupling/probe spectroscopy is based on the very narrow coherent feature produced in the absorption spectrum of three-level Λ or ladder systems. For the Λ scheme, a very narrow linewidth is determined by the long relaxation rate of the ground state coherence. Counterpropagating lasers and one laser locked to an atomic transition are used to produce sub-Doppler resolution, as presented in Krishna *et al.* (2005) and Wang *et al.* (2013, 2014a).

2.2.5. Frequency comb spectroscopy (FC)

The atomic absorption peaks are determined with a reference to a frequency comb. The absolute precision of the frequency readings is largely increased [see, for instance, Udem *et al.* (1999) and Das *et al.* (2006a)].

2.2.6. Frequency modulated laser (FML)

When the exciting laser is modulated at the hyperfine splitting frequency, cross-over resonances are induced in three-level Λ or V systems, as in Noble *et al.* (2006). The advantage of this technique is that only a single laser is required.

2.2.7. Hyperfine optical pumping and focus (HOPF)

Hyperfine transitions induced by microwaves or by optical pumping change the relative populations of the hyperfine levels of the ground state. In HOPF, this modification is detected by measuring the atomic beam intensity at the exit of a magnet that focuses or defocuses atoms with different magnetic quantum numbers. The focused atoms are analyzed by a mass spectrometer, as in Liberman *et al.* (1980).

2.2.8. Hyperfine quantum beats (HQB)

Quantum beats are based on coherent pulsed excitation of excited hyperfine levels producing a time decay of the excited state populations modulated by the hyperfine frequency splitting. Polarized excitation and detection are required, as in Deech *et al.* (1977). Bellini *et al.* (1997) applied delayed pulses of a frequency comb in order to probe the coherent hyperfine superposition of excited states.

2.2.9. Ion detection (ION)

This detection technique is very sensitive because a single ion can be detected. It is applied within different schemes, such as the resonant laser ionization (RIS), the selective electric field ionization of a Rydberg state, or the thermoionic diode operation.

2.2.10. Laser-induced fluorescence spectroscopy (LIF)

The emitted fluorescence is monitored as a function of the laser frequency. In Doppler spectroscopy, a high resolution is achieved by a careful analysis of the absorption lineshapes, as in Truong *et al.* (2015). In an AB with the laser propagation perpendicular to the atomic motion, the resolution is limited by the natural linewidth. By applying a sudden change to the laser phase and monitoring the atomic evolution at a later time T, subnatural width resolution reaching $\approx 1/(2T)$ is achieved in Shimizu *et al.* (1987). For short-lived atoms with low density using a fast beam and a collinear laser propagation, LIF is combined with nuclear decay to increase the signal to noise ratio as in Duong *et al.* (1987) and Lynch *et al.* (2016).

2.2.11. Level crossing by magnetic or electric fields

An energy crossings of excited state levels vs an external parameter, either magnetic field (MLC) or electric field (ELC), is monitored [see, for instance, Nagourney *et al.* (1978) and Auzinsh *et al.* (2007)]. A precise determination of the applied field is required.

2.2.12. Maser (MA)

The emission frequency of a maser operating on a hyperfine ground state transition is measured in Tetu *et al.* (1976).

2.2.13. Magnetic field decoupling (MFD)

Starting from an initial anisotropic Zeeman sublevel population distribution, the hyperfine constants are derived from the polarization of the fluorescent emission monitored vs an applied magnetic field decoupling the nuclear and electronic angular momenta, as presented in van Wijngaarden and Sagle (1991b).

2.2.14. Microwave spectroscopy (MWS)

The population modifications induced by transitions between hyperfine levels, mainly in the microwaves, are detected. In order to increase the signal-to-noise ratio, MWS is combined to other techniques, such as HOPF, LIF, or selective electric field ionization for Rydberg states as in Goy *et al.* (1982). The FOUNT+MWS combination applied to optical clocks leads to an extremely high precision, as in Guéna *et al.* (2014) and Ovchinnikov *et al.* (2015). A Ramsey optical interferometer is used for the potassium ground state measurement of Arias *et al.* (2019) and Peper *et al.* (2019).

2.2.15. Optical radio frequency or microwave double resonance (ORFDR)

The radio frequency induced transitions between excited states are detected through the modification of the LIF, either in its spectrum or in its polarization, as in Farley *et al.* (1977) and Lam *et al.* (1980). Optical pumping is applied to modify the population distribution and increase the detected signal.

2.2.16. Optical–optical double-resonance (OODR)

A two-color excitation via an intermediate step produces the population of excited states. The sub-Doppler resolution is obtained by operating in a MOT in Fort *et al.* (1995a), by applying the lasers in a counterpropagating geometry in Stalnaker *et al.* (2010), by a counterpropagating laser geometry selecting a single class of velocities different from zero in Lee and Moon (2015), or by using saturated

absorption to lock on the first transition and excite only the atoms at zero velocity in Yang *et al.* (2016). Detection is based mainly on the spontaneous emission from the intermediate or final state. In the presence of an optical pumping process, the population distribution perturbed by the second step excitation is monitored, as in Wang *et al.* (2014b).

2.2.17. Optical spectroscopy (OS)

Doppler limited high optical resolution spectroscopy from an alkali cell as in Truong *et al.* (2015) or Doppler-free in a MOT as in Antoni-Micollier *et al.* (2017) and Arias *et al.* (2019).

2.2.18. Resonant ionization spectroscopy (RIS)

Atoms in specific states are ionized by multistep laser absorption, and the ions are detected. It was introduced by Andreev *et al.* (1987) for measuring of the ground state hyperfine structure in francium. The resonant tuning of the intermediate step provides the spectroscopic resolution of its hyperfine structure. High resolution and sensitivity due to ion detection are associated with this technique as in the MOT experiment by Gabbanini *et al.* (1999) or for exotic isotopes in an atomic beam of exotic isotopes using the collinear laser spectroscopy as in Lynch *et al.* (2014). These last authors directed the ion to an alpha-decay detection station for clear identification in order to reduce isobaric and ground state contamination in their francium isotopes studies. In order to increase the frequency resolution, in recent francium accelerated atomic beam experiments [Neugart *et al.* (2017)], the excitation laser is split into two beams, copropagating and counterpropagating, with the atoms in order to increase the frequency resolution.

2.2.19. Saturated absorption spectroscopy (SAS)

This technique is based on a pump and probe laser applied to the same transition. It produces spectra with a natural linewidth resolution. The counterpropagating geometry compensates for the Doppler broadening. Main limitations are imposed by the laser stability, as analyzed in Das and Natarajan (2008) and Glaser *et al.* (2020).

2.2.20. Stark spectroscopy (SS)

Stark spectroscopy is based on the electric field shift of atomic level energies. It is used mainly for Rydberg states as in Stevens *et al.* (1995). Information on lower energy states may be derived by the difference in level Stark shifts.

2.2.21. Two-photon sub-Doppler spectroscopy (TPSDS)

A single-color two photon not-resonant excitation explores highly excited states. The sub-Doppler resolution is obtained by operating with counterpropagating beams in a VC as described by Herrmann *et al.* (1985) and Hagel *et al.* (1999) or in a MOT as in Georgiades *et al.* (1994).

3. Hyperfine Theory

The hyperfine structure Hamiltonian H_{hyp} of an atom having a single valence electron outside the closed shells consists of the magnetic dipole H_{dip}, the electric quadrupole H_{quadr} and the octupole H_{octup} terms

$$H_{hyp} = H_{dip} + H_{quadr} + H_{octup}. \tag{1}$$

H_{dip} describes the interaction of the nuclear magnetic moment with the magnetic field generated by the electrons. For the electron angular momentum $\boldsymbol{J}$ and the nuclear angular momentum $\boldsymbol{I}$, it is given by

$$H_{dip} = hA\boldsymbol{I}\cdot\boldsymbol{J}, \tag{2}$$

where A is the magnetic dipole constant and h is the Planck constant.

The electric quadrupole term originates from the Coulomb interaction between the electron and a nonspherically symmetric nucleus. It is given by

$$H_{quadr} = hB\frac{3(\boldsymbol{I}\cdot\boldsymbol{J})^2 + \frac{3}{2}\boldsymbol{I}\cdot\boldsymbol{J} - I(I+1)J(J+1)}{2I(2I-1)J(2J-1)}, \tag{3}$$

where B is the electric quadrupole moment coupling constant. This expression is valid for nuclear spins $I \geq 1$ and is zero otherwise.

The octupole Hamiltonian H_{octup} presented in Armstrong (1971) depends on the electron and nuclear tensor operators of rank 3, requires an electron angular momentum at least equal to 3/2, and is characterized by the hyperfine C constant. The explicit dependence on the atomic quantum numbers is detailed in Gerginov *et al.* (2003).

Hyperfine interactions decrease rapidly for higher-lying states. Kopfermann (1958) showed that the hyperfine constants are proportional to the expectation value of $1/r^3$, where r is the distance between the nucleus and valence electron. For highly excited electrons, the valence electron is far from the core electrons and $\langle 1/r^3\rangle$ is well approximated by the hydrogenic result

$$\langle 1/r^3\rangle \propto \frac{1}{(n^*)^3}\left(1 - \frac{\partial\sigma}{\partial n}\right), \tag{4}$$

where n^* is the effective principal quantum number, n is the principal quantum number, and the difference $\sigma(n) = n - n^*$ is the quantum defect. In a more refined treatment, by expressing the Schrödinger wavefunction at the nucleus position through the effective nuclear charge Z_I in the inner region where the orbit penetrates, and setting $Z_0 = 1$ for the net charge of the ion around which the single electron moves, the modified Fermi–Segre formula for the dipolar constant of the state with angular momentum l is derived in Kopfermann (1958)

$$A = \frac{8}{3}R_\infty \alpha^2 g_I \frac{Z_i Z_0^2}{(n^*)^3} F_{r,J}(n,l,Z)(1-\epsilon)(1-\delta), \tag{5}$$

with R_∞ being the Rydberg constant, α the fine structure constant, and g_I the gyromagnetic ratio of the nuclear magnetic moment. The relativistic effects are expressed by the factor $F_{r,J}(n,l,Z)$ near unity for light atoms and different from unity for large Z numbers. The $1-\epsilon$ factor is the change in the electronic wave function for distributions of the nuclear charge over its volume. The $1-\delta$ factor is the change in the electron–nuclear interaction by the distribution of the magnetic moment, which is called the Breit–Weisskopf effect.

For the quadrupole coupling constant B, the following expression is derived in Kopfermann (1958):

$$B = \frac{1}{h}\frac{e^2}{4\pi\epsilon_0}\frac{2J-1}{2J+2}Q\left\langle\frac{1}{r^3}\right\rangle R_{r,J}(n,l,Z), \tag{6}$$

with e the charge of the electron, ϵ_0 the vacuum permittivity, Q the quadrupole nuclear moment, and $R_{r,J}(n,l,Z)$ a relativistic

correction factor. From Eq. (4) for $1/r^3$, it follows that the B constant is also proportional to $1/(n^*)^3$.

On the basis of the above expressions, where the nucleus is represented by a point charge, the following scaling is derived in Kopfermann (1958) for the magnetic dipole and magnetic quadrupole constants A and B associated with two different isotopes

$$\frac{A^i}{A^j} = \frac{g_I^i}{g_I^j}, \tag{7}$$

$$\frac{B^i}{B^j} = \frac{Q^i}{Q^j}, \tag{8}$$

where g_I^i and Q^i represent the nuclear gyromagnetic factor g and the quadrupole moment of the isotope i, respectively. Deviations from these isotopic scaling laws represent the hyperfine anomalies presented in Subsection 5.2.

The dipolar and quadrupolar hfs Hamiltonians, involving the interaction of spin and orbital angular momenta with the nuclear moments, have matrix elements diagonal over the hyperfine quantum numbers, but also off-diagonal ones ($A_{J,J-1}$) connecting fine-structure states with different J values as presented in Arimondo *et al.* (1977). These off-diagonal couplings produce a mixing of the eigenstates and a shift of the energies. For fine structure states far apart in energy, a perturbation of the hyperfine constants includes the influence of the off-diagonal matrix elements, as for the 6^2P Cs doublet in Johnson *et al.* (2004). In the opposite case, such as the 2^2P ^{7}Li doublet, the hyperfine splittings are expressed through the $a_i, (i = c, d, o)$ parameters of an effective hyperfine-splitting Hamiltonian: contact, dipolar, and orbital, respectively, as derived in Lyons and Das (1970). In the first perturbation order and using the one-electron theory, the different hyperfine constants are written as

$$\begin{aligned} A(^2P_{1/2}) &= -a_c - 10a_d + 2a_o, \\ A(^2P_{3/2}) &= a_c + a_d + a_o, \\ A(^2P_{3/2}, {}^2P_{1/2}) &= -a_c + \frac{5}{4}a_d + \frac{1}{2}a_o. \end{aligned} \tag{9}$$

These relations have been used by experimentalists for their data analysis. Higher perturbation order corrections to the Li constants were derived in Beloy and Derevianko (2008) and Puchalski and Pachucki (2009). The mixing produced by off-diagonal hyperfine interactions plays an important role in the cesium measurements for parity nonconservation, as in the experiments of Gilbert *et al.* (1986) and Bouchiat and Guéna (1988) and in the theoretical analysis of Dzuba and Flambaum (2000). It is expected to be even more important in francium.

Equation (5) predicts the following scaling law:

$$A \propto \frac{1}{(n^*)^3}. \tag{10}$$

A similar one applies to B on the basis of Eqs. (4) and (6).

For the ^{87}Rb low-n states, the A dependence on n^* was tested in 1976 by Belin *et al.* (1976b) using the $1/(n^*)^2$ dependence of the fine structure data. The A scaling law was later verified for ^{85}Rb high D states within 2% by van Wijngaarden *et al.* (1993). More recently, with the very high-n^* values having been precisely derived from laser spectroscopy, the scaling was tested for the ^{85}Rb Rydberg states between $n = 27$ and $n = 33$ in Li *et al.* (2003) and Ramos *et al.* (2019). The ^{87}Rb data obtained by Li *et al.* (2003) were reexamined for the scaling in Mack *et al.* (2011). In Saßmannshausen *et al.* (2013) the scaling law was verified for the Cs $^2S_{1/2}$ and $^2P_{1/2}$ Rydberg states in the $n = 10$–80 range.

The theoretical determination of the hyperfine constants has greatly evolved within the last few years. Instead of focusing on a few atomic states, the more recent calculations target a very large number of states. While in 1999 a few hyperfine constants of different alkalis were calculated, e.g., in Safronova *et al.* (1999), more recently Safronova and coworkers in [Johnson *et al.* (2008); Safronova and Safronova (2008, 2011) and Auzinsh *et al.* (2007)] have produced a global derivation of the constants for ^{7}Li, ^{39}K, ^{87}Rb, and ^{133}Cs. Later, the hyperfine data for all the K isotopes were carefully examined by Singh *et al.* (2012), for Rb and Cs by Grunefeld *et al.* (2019), for Cs by Tang *et al.* (2019), and for Fr by Sahoo *et al.* (2015), Lou *et al.* (2019), and Grunefeld *et al.* (2019). The global analysis by Singh *et al.* (2012) has derived precise values for the nuclear quadrupole moments of the potassium isotopes demonstrating a good internal consistency of the hyperfine data. The development led by Marianna Safronova to provide both experimental and theoretical energy level information for a large variety of atoms is a welcome addition to the data compilation. It is currently available online [see Barakhshan *et al.* (2022)].

The hyperfine interaction and the weak interaction that gives rise to parity-nonconservation (PNC) in atoms both happen because the electron density overlaps with the nucleus. From a particle physics point of view, the exchange of the Z^0 boson carries the weak interaction with its PNC. Atomic PNC interest comes from its unique possibility to test the standard model at low energy. The structure of the nucleus is key to the details of nuclear-spin-independent PNC, where the electron axial–vector–current interacts with the nucleon vector–current. The nuclear-spin-dependent PNC, where the nucleon axial–vector–current interacts with the electron vector–current also depends on nuclear structure and is primarily due to the nuclear anapole moment. As noted by Flambaum and Khriplovich (1985) and confirmed by Bouchiat and Piketty (1991) and Johnson *et al.* (2003), the hyperfine interaction leads to the nuclear spin dependence of the matrix element in the atomic PNC. Cs measurements by Wood *et al.* (1997) reached enough sensitivity to measure the anapole moment in the nuclear-spin-dependent part of the PNC interaction. A new generation of atomic parity violation experiments is under way, e.g., see Gwinner and Orozco (2022). These experiments are made with francium atoms. The PNC effects in Fr with respect to Cs are estimated to be 18 times larger for the nuclear-spin-independent and 11 times larger for the nuclear-spin-dependent part.

The determination of the parity-conserving quantities in both high precision experiments and *ab initio* calculations, such as transition matrix elements, lifetimes, polarizabilities, and hyperfine constants, is essential for PNC studies. The hyperfine constants test in quantitative ways the quality of the electronic wavefunction near the nucleus. This unique combination between theory and experiment has greatly favored the heaviest alkali atoms and has stimulated a large search effort for the hyperfine structures in their isotopes as presented in Safronova *et al.* (2018).

4. Measured Hyperfine Constants

In the following, we present several tables for the measured A and B constants of the alkali atoms. In a few cases, we derive the A constant from the measured hyperfine splitting reported by the authors using the formula for the hyperfine energies given by Kopfermann (1958). In each Table, the atomic states are listed in order of increasing n, then of increasing L, increasing J, and finally chronologically. Two columns report the acronyms determining the atomic sample and the spectroscopic technique applied in the measurement. The reference to the original publication is in the last column. The spectroscopic technique column reports the "From" notation for the data taken from Arimondo *et al.* (1977), for which a critical examination or a weighted averaging over several measurements was performed, leading to a recommended value. When the hyperfine value reported in that reference remains the only one available, or its error bar is smaller than later measurements, the original work is directly quoted in the table. Within the table's B column, the entry "0." denotes that the authors have assumed the quadrupole constant equal to zero.

A few techniques, such as the HQB, are not able to resolve the sign of the constants for the explored state. On the basis of the above scaling laws applied to different atoms within Sec. 5.1, we have produced a dependable sign assignment for most states. If the sign was not identified, the absolute value is reported.

The measurement uncertainties are reported in the text and tables in parentheses after the value, in units of the last decimal place of the value. For example, 153.3(11) means 153.3 ± 1.1. Most authors specify their uncertainty on the level of one standard deviation. If a different convention is used, it is mentioned in the text.

For each atomic species, we mention in the text the states where a very high precision is obtained or where a disagreement between the measured values exists. When several (n) measurements are associated with a single state, the tables include a weighted average, w.a., representing a reference for further work. We follow the procedure of the Particle Data Group in Zyla *et al.* (2020) in the Introduction, Sec. 5.2.2, *Unconstrained averaging*, to find the weighted error (w.e.). We calculate it first based on the n individual errors (e_i), w.e. = $(1/\sum 1/e_i^2)^{1/2}$. We also calculate the reduced χ-squared $(\chi^2_{\rm red})$ with $n-1$ degrees of freedom to test the size of the w.e. If $(\chi^2_{\rm red})$ is greater than unity by more than one standard deviation $(2/(n-1))^{1/2}$, then we increase the w.e. of the w.a. by the factor $(\chi^2_{\rm red})^{1/2}$ so that the weighted enhanced error (w.e.e.) is w.e.e. = $(\chi^2_{\rm red})^{1/2}\times$ w.e. We report in the table either the w.a. with its w.e. or the w.e.e., which we explicitly state. Such averaging is not performed when the precision of one measurement is greater than all the remaining ones, which is then denoted by "Recommended" in the table's last column. The last column contains a "See text" statement, if one or more values are not included into the w.a.

A different way of averaging developed by Rukhin (2009, 2019) evaluates the clustering of the data and assigns individual hidden uncertainties to the measurements from different groups. These uncertainties are then added in quadrature to the stated uncertainties. w.a.s and w.e.s calculated by this cluster maximum likelihood estimator (CMLE) are not always identical to the values reported in our tables. For completeness, whenever a table recommended value includes a w.e.e. derived from the $(\chi^2_{\rm red})^{1/2}$ analysis, we have used the CMLE method to calculate the corresponding w.a.$_{\rm CMLE}$ weighted average and w.e.e.$_{\rm CMLE}$ weighted enhanced error. The comparison between the recommended values obtained by these two approaches shows that, in almost all the 28 cases, the w.a. of the two analyses agrees within two times the w.e.e. There are only two cases with a greater difference, associated with a large $(\chi^2_{\rm red})^{1/2}$ value as an indicator of an anomalous scatter of the data. The interested reader can find results and plots in the supplementary material of this review.

4.1. Lithium

Data for this atom are reported in Table 1. As for all alkalis, several spectroscopic investigations are stimulated by the interest in laser cooling, but only a few experiments are performed in a MOT. The recent ^{6}Li MOT experiments by Wu *et al.* (2018), Li *et al.* (2020), and Rui *et al.* (2021) at Shanghai may open a new trend. For the ground state of both lithium isotopes, the "old" atomic beam measurements based on MWS report the highest precision, not reached by the several ones based on laser spectroscopy. Otto *et al.* (2002) performed measurements for a few high-n states of ^{7}Li, as well as for other alkalis.

For the ^{6,7}Li $2^2P_{1/2,3/2}$ state measurements by Umfer *et al.* (1992), the error bar is derived on the basis of Eq. (9) from the off-diagonal constants presented in the following. For the A value of the $3^2S_{1/2}$ state of both isotopes measured by Lien *et al.* (2011), we estimated the error bar not reported by the authors.

A wide experimental effort concentrates on the $2^2P_{1/2}$ state of both isotopes. Instead, the $2^2P_{3/2}$ state of ^{6}Li remains with the data obtained before laser spectroscopy. For ^{7}Li, three experimental investigations of this doublet, by Orth *et al.* (1975), Nagourney *et al.* (1978), and Umfer *et al.* (1992), consider the contribution of the off-diagonal hyperfine couplings linked to the small fine-structure splitting. Orth *et al.* (1975) include in their analysis the previous level crossing data by Brog *et al.* (1967). The analysis by Nagourney *et al.* (1978) combines their own data and the previous ones. Umfer *et al.* (1992), acquired enough data for their own analysis. Orth *et al.* (1975) using Eq. (9) and their measured $A_{3/2,1/2}$ = 11.85(35) MHz found $a_c = -9.838(48)$, $a_d = -1.876(12)$, and $a_o = 8.659(37)$. Nagourney *et al.* (1978) reported $a_c = -9.838(48)$, $a_d = -1.975(22)$, and $a_o = 8.659(37)$, and Umfer *et al.* (1992) obtained $a_c = -9.93(37)$, $a_d = -1.72(20)$, $a_o = 8.69(31)$ (all in MHz). For the same doublet, Beloy and Derevianko (2008) performed an accurate evaluation of the off-diagonal hyperfine couplings. They produced corrections to the measured dipole constant in the $A(^2P_{1/2})$ accurately measured by Orth *et al.* (1975), Walls *et al.* (2003), and Das and Natarajan (2008). For this last one, the 27.0 kHz correction should be compared to the author's original 3 kHz experimental uncertainty.

A disagreement exceeding the error bars exists for the $3^2S_{1/2}$ ^{7}Li hyperfine constant A measured in Stevens *et al.* (1995), compared to those of Bushaw *et al.* (2003) and Lien *et al.* (2011). We do not include that measurement in the w.a.

The discrepancy for the $3^2P_{3/2}$ ^{7}Li constants between the previous values by Budick *et al.* (1966), Isler *et al.* (1969), and

TABLE 1. Measured *A* and *B* values for Li isotopes

State	A (MHz)	B (MHz)	Sample	Technique	References
			^{6}Li		
$2^2S_{1/2}$	152.136 840 7(20)	⋯	AB	MWS	From Arimondo *et al.* (1977)
	151.(3)	⋯	VC	ION	Lorenzen and Niemax (1982)
	153.3(11)	⋯	AB	LIF	Windholz *et al.* (1990)
	152.109(43)	⋯	AB	LIF	Walls *et al.* (2003)
	152.121(57)	⋯	AB	FML	Noble *et al.* (2006)
	152.143(11)	⋯	AB	LIF+FC	Sansonetti *et al.* (2011)
	152.134 3(9)	⋯	MOT	LIF	Wu *et al.* (2018) and Li *et al.* (2020)
	152.136 840 7(20)	⋯	⋯	⋯	Recommended
$2^2P_{1/2}$	17.375(18)	⋯	VC	ORFDR	Orth *et al.* (1974)
	17.8(3)	⋯	VC	MLC	Nagourney *et al.* (1978)
	16.81(70)	⋯	AB	LIF	Windholz *et al.* (1990)
	17.386(31)	⋯	AB	LIF	Walls *et al.* (2003)
	17.407(37)	⋯	AB	FML	Noble *et al.* (2006)
	17.394(4)	⋯	AB	LIF	Das and Natarajan (2008)
	17.407(10)	⋯	AB	LIF+FC	Sansonetti *et al.* (2011)
	17.402 1(9)	⋯	MOT	LIF	Li *et al.* (2020) and Rui *et al.* (2021)
	17.408(13)	⋯	MOT	LIF+DD	Li *et al.* (2021)
	17.401 7(9)	⋯	⋯	⋯	w.a.
$2^2P_{3/2}$	−1.155(8)	−0.10(14)	AB	ORFDR	Orth *et al.* (1974)
$3^2S_{1/2}$	34.(13)	⋯	VC	ION	Vadla *et al.* (1987)
	35.263(15)	⋯	AB	TPSDS+RIS	Bushaw *et al.* (2003)
	35.283(10)	⋯	AB	RIS	Ewald *et al.* (2004)
	35.20(20)	⋯	AB	LIF	Lien *et al.* (2011)
	35.267(14)	⋯	AB	RIS	Nörtershäuser *et al.* (2011)
	35.274(7)	⋯	⋯	⋯	w.a.
$3^2P_{1/2}$	5.3(4)	⋯	VC	MLC	Nagourney *et al.* (1978)
$3^2P_{3/2}$	−0.40(2)	0	VC	MLC	Isler *et al.* (1969)
$4^2S_{1/2}$	13.1(13)	⋯	AB	LIF	Kowalski *et al.* (1978)
	15.(3)	⋯	VC	ION	Lorenzen and Niemax (1982)
	13.5(8)	⋯	AB	LIF	DeGraffenreid and Sansonetti (2003)
	13.5(7)	⋯	⋯	⋯	w.a.
			^{7}Li		
$2^2S_{1/2}$	401.752 043 3(5)	⋯	AB	MWS	Beckmann *et al.* (1974)
	401.(5)	⋯	VC	ION	Lorenzen and Niemax (1982)
	401.81(25)	⋯	AB	LIF	Windholz *et al.* (1990)
	401.767(39)	⋯	AB	LIF	Walls *et al.* (2003)
	401.772(33)	⋯	AB	MFL	Noble *et al.* (2006)
	401.747(7)	⋯	AB	LIF+FCS	Sansonetti *et al.* (2011)
	401.755(8)	⋯	AB	LIF	Huang *et al.* (2013)
	401.752 043 3(5)	⋯	⋯	⋯	Recommended
$2^2P_{1/2}$	45.914(25)	⋯	AB	ORFDR	Orth *et al.* (1974)
	46.05(30)	⋯	AB	LIF	Windholz *et al.* (1990)
	46.175(2980)	⋯	AB	MLC	Umfer *et al.* (1992)
	46.010(25)	⋯	AB	LIF	Walls *et al.* (2003)
	45.893(26)	⋯	AB	FML	Noble *et al.* (2006)
	46.024(3)	⋯	AB	LIF	Das and Natarajan (2008)
	46.047(3)	⋯	VC	SAS	Singh *et al.* (2010)
	45.938(5)	⋯	AB	LIF+FCS	Sansonetti *et al.* (2011)
	45.946(4)	⋯	AB	LIF	Huang *et al.* (2013)
	46.005(16)	⋯	⋯	⋯	w.a. (w.e.e.)

TABLE 1. (*Continued*)

State	A (MHz)	B (MHz)	Sample	Technique	References
	−3.055(14)	−0.221(29)	AB	ORFDR	Orth *et al.* (1975)
	−2.95(4)	0	VC	MLC	Nagourney *et al.* (1978)
	−3.08(4)	−0.16(10)	AB	LIF+DD	Shimizu *et al.* (1987)
$2^2P_{3/2}$	−3.18(10)	−0.8(7)	AB	LIF	Windholz *et al.* (1990)
	−3.08(8)	−0.20(27)	AB	HQB	Carlsson and Sturesson (1989)
	−2.96(88)	−0.1(5)	AB	MLC	Umfer *et al.* (1992)
	−3.050(16)	−0.22(3)	···	···	w.a.
	95.(10)	···	VC	ION	Vadla *et al.* (1987)
	94.68(22)	···	AB	SS	Stevens *et al.* (1995)
	93.106(11)	···	AB	TPSDS+RIS	Bushaw *et al.* (2003)
$3^2S_{1/2}$	93.117(25)	···	AB	RIS	Ewald *et al.* (2004)
	93.13(20)	···	AB	LIF	Lien *et al.* (2011)
	93.103(11)	···	AB	RIS	Nörtershäuser *et al.* (2011)
	93.095(52)	···	AB	SAS	Kumar and Natarajan (2017)
	93.105(7)	···	···	···	See text w.a.
	13.5(2)	···	VC	MLC	Budick *et al.* (1966)
$3^2P_{1/2}$	13.7(12)	···	VC	MLC	Nagourney *et al.* (1978)
	13.5(2)	···	···	···	Recommended
	−0.96(13)	0	VC	MLC	Budick *et al.* (1966)
$3^2P_{3/2}$	−0.965(20)	−0.019(22)	VC	MLC	Isler *et al.* (1969)
	−1.036(16)	−0.094(10)	VC	MLC	Nagourney *et al.* (1978)
	−1.01(2)	−0.081(28)	···	···	w.a. (w.e.e.)
	0.843(41)	0	AB	TPSDS	Burghardt *et al.* (1988)
$3^2D_{3/2}$	1.14(49)	0	VC	TPSDS	Otto *et al.* (2002)
	0.843(41)	0	···	···	Recommended
	0.343 6(10)	0	AB	TPSDS	Burghardt *et al.* (1988)
$3^2D_{5/2}$	0.31(13)	0	VC	TPSDS	Otto *et al.* (2002)
	0.342 6(10)	0	···	···	Recommended
	36.4(40)	···	AB	LIF	Kowalski *et al.* (1978)
	38.(3)	···	VC	ION	Lorenzen and Niemax (1982)
$4^2S_{1/2}$	35.32(72)	···	VC	TPSDS	Otto *et al.* (2002)
	34.9(4)	···	AB	LIF	DeGraffenreid and Sansonetti (2003)
	35.05(35)	···	···	···	w.a.
$4^2P_{3/2}$	−0.41(4)	0	VC	MLC	Isler *et al.* (1969)
$6^2S_{1/2}$	38.0(15)	···	VC	TPSDS	Otto *et al.* (2002)
$7^2S_{1/2}$	9.2(25)	···			

Nagourney *et al.* (1978) ones remains unexplained as pointed out by these authors. Therefore, instead of the recommended value from Arimondo *et al.* (1977), we consider all the previous measurements. The χ^2_{red} correction is applied to the statistical error. An analysis of the off-diagonal elements was performed by Nagourney *et al.* (1978) for the 3^2P ^{7}Li doublet, leading to $a_c = -3.10(67)$, $a_d = -0.54(27)$, and $a_o = 2.61(40)$.

4.2. Sodium

The sodium results of Table 2 are emblematic of the progress achieved in hyperfine constant measurements. In chronological order, the two-photon sub-Doppler spectroscopy was applied in 1978 to probe the 4^2D excited states, by Biraben and Beroff (1978) and Burghardt *et al.* (1978), extended by this last research group to the 3^2D states in Burghardt *et al.* (1988). In 1989, Kasevich *et al.* (1989) published the first hyperfine ground state determination in an atomic fountain with 1 mHz precision, close to the previous best atomic beam value of Table 2, opening the road to further amazing improvements in fountain atomic clocks. Zhu *et al.* (1993) performed the first hyperfine constant measurement in a MOT exploring the 5^2P states with a relative precision $\approx 1 \times 10^{-4}$ among the best ones for excited states. In the same year, Yei *et al.* (1993) performed subnatural linewidth measurements of hyperfine coupling constants using the delayed detection in polarization quantum beat spectroscopy. In 2003, the excitation of ultracold atoms in a MOT on the 3^2P–4^2P electric quadrupole transition allowed Bhattacharya *et al.* (2003) to perform high resolution spectroscopy of the $4^2P_{1/2}$ level. Das and Natarajan (2006b) introduced the CCS approach for the first excited state,

TABLE 2. Measured *A* and *B* values for ^{23}Na

State	A (MHz)	B (MHz)	Sample	Technique	References
$3^2S_{1/2}$	885.813 064 4(5)	···	AB	MWS	From Arimondo *et al.* (1977)
	885.70(25)	···	VC	SAS	Pescht *et al.* (1977)
	885.813 065(1)	···	FOUNT	RIS	Kasevich *et al.* (1989)
	885.813 064 4(5)	···	···	···	Recommended
$3^2P_{1/2}$	94.25(15)	···	VC	SAS	Pescht *et al.* (1977)
	94.47(1)	···	AB	LIF	Griffith *et al.* (1977)
	94.05(20)	···	AB	LIF	Umfer *et al.* (1992)
	94.42(19)	···	AB	HQB	Carlsson *et al.* (1992)
	94.44(13)	···	AB	LIF	van Wijngaarden and Li (1994)
	94.7(2)	···	AB	LIF	Scherf *et al.* (1996)
	94.349(7)	···	VC	SAS	Das and Natarajan (2008)
	94.39(2)	···	···	···	w.a. (w.e.e.)
$3^2P_{3/2}$	18.64(6)	2.77(6)	AB	HQB	Krist *et al.* (1977)
	18.69(6)	2.83(10)	AB	HQB	Carlsson and Sturesson (1989)
	18.78(8)	2.60(41)	AB	LIF	Umfer *et al.* (1992)
	18.534(15)	2.724(30)	VC	HQB+DD	Yei *et al.* (1993)
	18.62(21)	2.11(52)	AB	LIF	van Wijngaarden and Li (1994)
	18.8(1)	2.7(2)	AB	LIF	Scherf *et al.* (1996)
	18.79(12)	2.75(12)	AB	HQB	Volz *et al.* (1996)
	18.572(24)	2.723(55)	AB	LIF	Gangrsky *et al.* (1998)
	18.530(3)	2.721(8)	VC	CCS	Das *et al.* (2006b)
	18.532(6)	2.722(7)	···	···	w.a. (w.e.e); w.a.
$3^2D_{3/2}$	0.527(25)	0	AB	TPSDS	Burghardt *et al.* (1988)
$3^2D_{5/2}$	0.108 5(24)	0			
$4^2S_{1/2}$	203.6(2)	···	VC	TPSDS+LIF	Arqueros (1988)
$4^2P_{1/2}$	30.4(5)	···	VC	ORFDR	Grundevik and Lundberg (1978)
	30.6(1)	···	MOT	OODR+RIS	Bhattacharya *et al.* (2003)
	30.6(1)	···	···	···	w.a.
$4^2P_{3/2}$	6.022(61)	0.97(6)	VC	LC+ORFDR	From Arimondo *et al.* (1977)
	0.23(12)	0	VC	TPSDS	Biraben and Beroff (1978)
$4^2D_{3/2}$	0.215(15)	0	AB	TPSDS	Burghardt *et al.* (1978)
	0.215(15)	0	···	···	Recommended
$4^2D_{5/2}$	$<\|0.28\|$	0	VC	TPSDS	Biraben and Beroff (1978)
	0.029(6)	0	AB	TPSDS	Burghardt *et al.* (1978)
	0.029(6)	0	···	···	Recommended
$5^2S_{1/2}$	77.6(2)	···	VC	ORFDR	Tsekeris *et al.* (1976)
	77.2(2)	···	MOT	TPSDS+RIS	Marcassa *et al.* (1998)
	77.40(14)	···	···	···	w.a.
$5^2P_{1/2}$	13.3(2)	···	VC	ORFDR	Grundevik and Lundberg (1978)
	13.468 7(42)	···	MOT	SAS	Zhu *et al.* (1993)
	13.468 7(42)	···	···	···	Recommended
$5^2P_{3/2}$	2.64(1)	0.38(3)	AB	HQB	Grundevik *et al.* (1979)
	2.636 0(23)	0.370 4(77)	MOT	SAS	Zhu *et al.* (1993)
	2.636 0(23)	0.370 4(77)	···	···	Recommended
$6^2S_{1/2}$	37.5(2)	···	VC	ORFDR	Lundberg *et al.* (1977)
	34.5(45)	···	AB	SS	Hawkins *et al.* (1977)
	37.5(2)	···	···	···	Recommended
$6^2P_{3/2}$	1.39(1)	0.21(2)	AB	HQB	Grundevik *et al.* (1979)
	20.9(1)	···	AB	ORFDR	Lundberg *et al.* (1977)
$7^2S_{1/2}$	23.3(65)	···	AB	SS	Hawkins *et al.* (1977)
	20.9(1)	···	···	···	Recommended
$7^2P_{3/2}$	0.82(1)	0.13(3)	VC	QBS	Jiang *et al.* (1982)
$8^2S_{1/2}$	12.85(10)	···	VC	ORFDR	Lundberg *et al.* (1977)
$8^2P_{3/2}$	0.535(15)	0.070(25)	VC	QBS	Jiang *et al.* (1982)
$9^2P_{3/2}$	0.36(1)	0.045(15)			

$3^2P_{3/2}$. However, no competitive new data for the ground state are available.

The $3^2P_{1/2,3/2}$ states have been examined by several authors, with an increasing precision and a good agreement among the different results. For the 4^2D states of Biraben and Beroff (1978) and for the 7, 8, and $9^2P_{3/2}$ ones of Jiang *et al.* (1982), the sign has been determined here from the scaling law. In sodium, there is not enough data for a global analysis. For the large majority of excited states above the 5^2P ones, no new data have been published after 1982.

4.3. Potassium

Our previous Li and Na remarks on the ground state values do not apply to the ^{39}K ground state, as shown in Table 3. For this atom, several recent measurements exist, with the frequency comb spectral resolution applied to determine the absolute transition frequencies, and from them, the fine and hyperfine splittings. A high precision is achieved, usually with a good agreement among data from different research groups, e.g., for several $n = 5$–$8^2S_{1/2}$ states with

TABLE 3. Measured *A* and *B* values for K isotopes

State	A (MHz)	B (MHz)	Sample	Technique	Referernces
			^{39}K		
	<|1.8|	0	VC	ORFDR	Lam *et al.* (1980)
$3^2D_{3/2}$	0.96(4)	0.37(8)	VC	HQB+DD	Sieradzan *et al.* (1997)
	0.96(4)	0.37(8)	···	···	Recommended
	<|2.2|	0	VC	ORFDR	Lam *et al.* (1980)
$3^2D_{5/2}$	−0.62(4)	⟨|0.3|	VC	HQB+DD	Sieradzan *et al.* (1997)
	−0.62(4)	0	···	···	Recommended
	230.859 860 1(3)	···	AB	MWS	From Arimondo *et al.* (1977)
	231.0(3)	···	AB	LIF	Touchard (1982)
	230.859 9(1)	···	AB	MWS	Duong *et al.* (1993)
	213.0(3)	···	AB	LIF	Papuga *et al.* (2014)
$4^2S_{1/2}$	230.859 858(6)	···	MOT	MWS	Arias *et al.* (2019)
	230.859 850(3)	···	MOT	MWS	Peper *et al.* (2019)
	231.1(3)	···	AB	RIS	Koszorús *et al.* (2019)
	230.859 860 1(3)	···	···	···	Recommended
	28.85(30)	···	AB	MWS	Buck and Rabi (1957)
	27.80(15)	···	AB	FML	Bendali *et al.* (1981) and Duong (1982)
	27.5(4)	···	AB	LIF	Touchard et al. (1982)
	28.859(15)	···	VC	SAS	Banerjee *et al.* (2004)
$4^2P_{1/2}$	27.775(42)	···	AB	LIF+FC	Falke et al. (2006)
	28.848(5)	···	VC	CCS	Das and Natarajan (2008)
	27.8 (2)	···	AB	LIF	Papuga *et al.* (2014)
	27.793(71)	···	···	···	See text w.a. (w.e.e.)
	6.093(25)	2.786(71)	AB	LIF+FC	Falke *et al.* (2006)
$4^2P_{3/2}$	6.077(23)	2.875(55)	VC	CCS	Das and Natarajan (2008)
	6.084(17)	2.842(43)	···	···	w.a.
$5^2S_{1/2}$	55.50(60)	···	VC	ORFDR	Gupta *et al.* (1973)
	9.02(17)	···	VC	ORFDR	From Arimondo *et al.* (1977)
$5^2P_{1/2}$	8.93(69)	···	VC	SAS	Halloran *et al.* (2009)
	9.01(17)	···	···	···	w.a.
$5^2P_{3/2}$	1.969(13)	0.870(22)	VC	MLC	From Arimondo *et al.* (1977)
$5^2D_{3/2}$	0.44(10)	0	VC	ORFDR	Belin *et al.* (1975b)
$5^2D_{5/2}$	−0.24(7)	0			
	21.81(18)	···	VC	ORFDR	Gupta *et al.* (1973)
	20.4(23)	···	TD	TPSDS	Thompson *et al.* (1983)
$6^2S_{1/2}$	21.8(5)	···	VC	TPSDS	Kiran Kumar and Suryanarayana (2011)
	21.93(11)	···	VC	OODR+FC	Stalnaker *et al.* (2017)
	21.89(9)	···	···	···	w.a.
$6^2P_{1/2}$	4.05(7)	···	VC	ORFDR	Belin *et al.* (1975b)
$6^2P_{3/2}$	0.886(8)	0.370(15)	VC	MLC	From Arimondo *et al.* (1977)
$6^2D_{3/2}$	0.25(1)	0.05(2)	VC	HQB+MFD	Głódó and Kraińska-Miszczak (1985a)

TABLE 3. (*Continued*)

State	A (MHz)	B (MHz)	Sample	Technique	Referernces
$6^2D_{5/2}$	−0.12(4)	0			
	10.79(5)	⋯	VC	ORFDR+MLC	From Arimondo *et al.* (1977)
$7^2S_{1/2}$	12.7(24)	⋯	TD	TPSDS	Thompson *et al.* (1983)
	10.41(93)	⋯	VC	TPSDS	Otto *et al.* (2002)
	10.79(5)	⋯	⋯	⋯	w.a.
$7^2P_{1/2}$	2.18(5)	⋯			
$7^2P_{3/2}$	0.49(4)	0	VC	ORFDR	Belin *et al.* (1975b)
	5.99(8)	⋯			
$8^2S_{1/2}$	6.8(12)	⋯	VC	TPSDS	Thompson *et al.* (1983)
	6.2(12)	⋯	VC	TPSDS	Otto *et al.* (2002)
	5.99(8)	⋯	⋯	⋯	Recommended
$9^2S_{1/2}$	4.0(11)	⋯	TPSDS	⋯	Otto *et al.* (2002)
	2.41(5)	⋯	VC	MLC	Belin *et al.* (1975a) also in Arimondo *et al.* (1977)
$10^2S_{1/2}$	2.6(12)	⋯	VC	TPSDS	Otto *et al.* (2002)
	2.41(5)	⋯	⋯	⋯	Recommended
$11^2S_{1/2}$	2.1(9)	⋯			
$12^2S_{1/2}$	1.5(12)	⋯	VC	TPSDS	Otto *et al.* (2002)
$13^2S_{1/2}$	1.9(14)	⋯			
$14^2S_{1/2}$	1.0(16)	⋯			
			^{40}**K**		
$3^2D_{3/2}$	|1.07(2)|	|0.4(1)|	VC	HQB+DD	Sieradzan *et al.* (1997)
$3^2D_{5/2}$	|0.71(4)|	|0.8(8)|			
$4^2S_{1/2}$	−285.730 8(24)	⋯	AB	MWS	From Arimondo *et al.* (1977)
	−34.49(11)	⋯	AB	FML	Bendali *et al.* (1981)
$4^2P_{1/2}$	−34.523(25)	⋯	AB	LIF+FC	Falke *et al.* (2006)
	−34.523(25)	⋯	⋯	⋯	Recommended
	−7.59(6)	−3.5(5)	VC	MLC	Ney *et al.* (1968)
$4^2P_{3/2}$	−7.48(6)	−3.23(50)	AB	FML	Bendali *et al.* (1981)
	−7.585(10)	−3.445(90)	AB	LIF+FC	Falke *et al.* (2006)
	−7.585(10)	−3.445(90)	⋯	⋯	Recommended
$5^2P_{1/2}$	−12.0(9)	⋯	VC	SAS	Behrle *et al.* (2011)
$5^2P_{3/2}$	−2.45(2)	−1.16(22)	VC	MLC	From Arimondo *et al.* (1977)
			^{41}**K**		
$3^2D_{3/2}$	|0.55(3)|	|0.51(8)|	VC	HQB+DD	Sieradzan *et al.* (1997)
$3^2D_{5/2}$	|0.40(2)|	<|0.2|			
$4^2S_{1/2}$	127.006 935 2(6)	⋯	AB	MWS	From Arimondo *et al.* (1977)
	126.9(8)	⋯	AB	LIF	Touchard *et al.* (1982)
	127.006 935 2(6)	⋯	⋯	⋯	Recommended
$4^2P_{1/2}$	15.19(21)	⋯	VC	FML	Bendali *et al.* (1981)
	15.1(8)	⋯	AB	LIF	Touchard *et al.* (1982)
	15.245(42)	⋯	AB	LIF+FC	Falke *et al.* (2006)
	15.245(42)	⋯	⋯	⋯	Recommended
$4^2P_{3/2}$	3.40(8)	3.34(24)	VC	MFD	Ney (1969)
	3.43(5)	0	VC	MFD	Kraińska-Miszczak (1981)
	3.325(15)	3.230(23)	VC	HQB	Sieradzan *et al.* (1995)
	3.363(25)	3.351(71)	AB	LIF+FC	Falke *et al.* (2006)
	3.342(12)	3.242(22)	⋯	⋯	w.a.
$5^2S_{1/2}$	30.75(75)	⋯	VC	ORFDR	Gupta *et al.* (1973)
$5^2P_{1/2}$	4.96(17)	⋯	VC	MLC	Ney (1969)

TABLE 3. (*Continued*)

State	A (MHz)	B (MHz)	Sample	Technique	Referernces
$5^2P_{3/2}$	1.08(2)	1.06(4)	VC	MLC	Ney (1969)
	12.03(40)	⋯	VC	ORFDR	Gupta *et al.* (1973)
$6^2S_{1/2}$	11.8(13)	⋯	VC	TPSDS	Kiran Kumar and Suryanarayana (2011), also in Kiran Kumar *et al.* (2014)
	12.03(40)	⋯	⋯	⋯	Recommended
$6^2D_{3/2}$	|0.14(2)|	|0.05(2)|	VC	HQB	Głódó and Kraińska-Miszczak (1985b)
	9.0(9)	⋯	TD	TPSDS	Thompson *et al.* (1983)
$7^2S_{1/2}$	6.5(10)	⋯	VC	TPSDS	Otto *et al.* (2002)
	7.9(12)	⋯	⋯	⋯	w.a. (w.e.e.)
	2.9(8)	⋯	TD	TPSDS	Thompson *et al.* (1983)
$8^2S_{1/2}$	3.5(13)	⋯	VC	TPSDS	Otto *et al.* (2002)
	3.1(7)	⋯	⋯	⋯	w.a.
$9^2S_{1/2}$	2.6(13)	⋯			
$10^2S_{1/2}$	2.0(24)	⋯	VC	TPSDS	Otto *et al.* (2002)
$11^2S_{1/2}$	2.0(11)	⋯			

measurements performed over a long time span. Otto *et al.* (2002) explored the ^2S states of the 39 and 41 isotopes up to $n = 14$ using two-photon sub-Doppler spectroscopy.

The spatial dependence of the HQB polarized fluorescence intensity in a given magnetic field was used by Głódó and Kraińska-Miszczak (1985a) to derive for the first time the signs of the A constants in the 6^2D states of ^{39}K. For other ^2D states, the investigations by Belin *et al.* (1975b), Sieradzan *et al.* (1997), and Głódó and Kraińska-Miszczak (1985b) produced only the absolute sign of the A and B constants. Their signs are determined here on the basis of the scaling laws.

4.3.1. ^{39}K

The ground $4^2S_{1/2}$ state was measured in three MOT experiments by Antoni-Micollier *et al.* (2017), Arias *et al.* (2019), and Peper *et al.* (2019). Peper *et al.* (2019) obtained a value close to the old atomic beam experiments with a difference in the 10 Hz range. Arias *et al.* (2019) claimed that their small discrepancy with the previous AB measurement can be accounted for by the 16(6) Hz quadratic Zeeman shift of the bias field and by the differential ac Stark shift in the optical dipole trap. Table 3 value takes into account such shift. Antoni-Micollier *et al.* (2017) reported an all-optical measurement of the hyperfine splitting with a low statistical uncertainty, but there were uncontrolled systematical errors in their work, according to Peper *et al.* (2019).

A large disagreement exists between the measured A values of the $4^2P_{1/2}$ states, some of them having been reported with high precision. The data are centered on two separate values 27.78(4) and 28.849(5) MHz with a separation larger than the reported precision. The lower values are by Bendali *et al.* (1981), Touchard *et al.* (1982), Duong (1982), and Papuga *et al.* (2014), (all of them with low precision) and by Falke *et al.* (2006) with higher precision. The greater values were obtained in an AB magnetic resonance experiment by Buck and Rabi (1957) with a low precision and in two recent measurements by the Bangalore research group Banerjee *et al.* (2004) and Das and Natarajan (2008) used the accurate CCS technique. The χ^2_{red} for the full dataset leads to a very large error bar. Light shifts corrections, an important issue for several recent publications, were taken into account by the Bangalore group. They stated, "we do not have a satisfactory explanation for such a large discrepancy." Such a discrepancy does not exist for the $4^2P_{3/2}$ values determined at the same time by Falke *et al.* (2006) and Das and Natarajan (2008). Falke *et al.* (2006) compared their ^{6,7}Li D optical transition values to those by Banerjee *et al.* (2004) and attributed the discrepancies to systematic errors in the laser calibration, more precisely to phase shifts in the wavelength (not frequency) comparison of the atomic excitation lasers. In Das and Natarajan (2008), the driving frequency of an acousto-optical modulator gives a direct measurement of the hyperfine interval and the calibration issue should have been resolved. For the discrepancies in those optical frequencies, Brown *et al.* (2013) pointed out the important role of quantum interference and light polarization effects. For the $4^2P_{1/2}$ state Table 3 reports a w.a. excluding the Banerjee *et al.* (2004) and Das and Natarajan (2008) values.

For the $6^2S_{1/2}$ state, the A value referred to Thompson *et al.* (1983) in Table 3 was derived from their hyperfine splitting in Stalnaker *et al.* (2017).

4.3.2. ^{41}K

The $7^2S_{1/2}$ values by Thompson *et al.* (1983) and by Otto *et al.* (2002) have a large disagreement. The first value is not consistent with the $1/(n^*)^3$ scaling law applied to the $n^2S_{1/2}$ states of this isotope. The Otto *et al.* (2002) value is the "Recommended" one.

4.4. Rubidium

The long list of recent spectroscopic data for this atom is the result of the laser cooling research in worldwide spread laboratories. For both the 85 and 87 isotopes, the ultracold atomic samples have produced very precise measurements of several hyperfine splittings, in particular, for the ground state and the Rydberg ones from $n = 26$ to $n = 46$. Note that ^{87}Rb has 50 neutrons, the exact magic number that makes it a closed shell.

Entries with very high precision and good agreement are presented in Tables 4 and 5 for ^{85}Rb and ^{87}Rb, respectively. The tables report the w.a. of the two published measured values for the ^{87}Rb $6^2P_{1/2}$ state by Nyakang'o *et al.* (2020), while for the ^{85,87}Rb $5^2S_{1/2}$, and $6^2P_{1/2}$ states, the reported average was communicated by Shiner *et al.* (2007). The error bars of the $6^2S_{1/2}$ hyperfine constants for both isotopes measured by Orson *et al.* (2021) and the measurements with a 30 kHz precision of McLaughlin *et al.* (2022)

TABLE 4. Measured *A* and *B* values for ^{85}Rb isotope

State	A (MHz)	B (MHz)	Sample	Technique	References
	7.3(5)	0	VC	ORFDR	Lam *et al.* (1980)
$4^2D_{3/2}$	7.329(35)	4.52(23)	VC	OODR	Moon *et al.* (2009)
	7.329(35)	4.52(23)	···	···	Recommended
	−5.2(3)	0	VC	ORFDR	Lam *et al.* (1980)
	−5.06(10)	7.42(15)	MOT	OODR	Sinclair *et al.* (1994)
$4^2D_{5/2}$	−4.978(4)	6.560(52)	VC	OODR+EIT	Wang *et al.* (2014b)
	−5.008(9)	7.15(15)	VC	OODR+FC	Lee and Moon (2015)
	−4.983(7)	6.70(21)	···	···	w.a. (w.e.e.)
	1 011.910 813(2)	···	AB	MA	Tetu *et al.* (1976)
	1 011.894(9)	···	VC	SAS	Barwood *et al.* (1991)
$5^2S_{1/2}$	1 011.910 8(3)	···	AB	LIF	Duong *et al.* (1993)
	1 011.914(12)	···	VC	SAS+FC	Shiner *et al.* (2007)
	1 011.910 814 940 6(1)	···	FOUNT	MWS	Wang *et al.* (2019)
	1 011.910 814 940 6(1)	···	···	···	Recommended
	120.72(25)	···	VC	OS	Beacham and Andrew (1971)
	120.499(10)	···	VC	SAS	Barwood *et al.* (1991)
	120.64(2)	···	VC	SAS	Banerjee *et al.* (2004)
$5^2P_{1/2}$	120.645(5)	···	VC	SAS	Das and Natarajan (2006a)
	120.500(13)	···	MOT	LIF+FC	Maric *et al.* (2008)
	120.79(29)	···	VC	SAS	Rupasinghe *et al.* (2022)
	120.605(29)	···	···	···	w.a. (w.e.e.)
	25.009(22)	25.88(3)	VC	ORFDR	From Arimondo *et al.* (1977)
	25.3 (4)	21.4 (40)	AB	LIF	Thibault *et al.* (1981b)
	24.988 (31)	25.693 (31)	VC	SAS	Barwood *et al.* (1991)
$5^2P_{3/2}$	25.038(5)	26.011(22)	VC	SAS	Rapol *et al.* (2003)
	25.041(6)	26.013(25)	VC	SAS	Banerjee *et al.* (2003)
	25.040 3(11)	26.008 4(49)	VC	SAS	Das and Natarajan (2008)
	25.040 1(11)	26.000(22)	···	···	w.a.; w.a. (w.e.e).
	4.269 9(2)	1.910 6(8)	VC	TPSDS	Nez *et al.* (1993, 1994)
$5^2D_{3/2}$	4.43(28)	1.7(24)	MOT	OODR+RIS	Gabbanini *et al.* (1999)
	4.269 9(2)	1.910 6(8)	···	···	Recommended
	−2.211 2(12)	2.680 4(200)	VC	TPSDS	Nez *et al.* (1993, 1994)
	−2.196(52)	2.51(53)	VC	TPSDS	Grove *et al.* (1995)
$5^2D_{5/2}$	−2.31(23)	2.7(27)	MOT	OODR+RIS	Gabbanini *et al.* (1999)
	−2.222 (19)	2.664(130)	VC	EIT	Yang *et al.* (2017)
	−2.211 2(12)	2.680 4(200)	···	···	Recommended
	239.18(3)	···	VC	FML	Pérez Galván *et al.* (2007) also in Pérez Galván *et al.* (2008)
$6^2S_{1/2}$	234.(30)	···	VC	TPSDS	Orson *et al.* (2021)
	239.057(10)	···	VC	TPSDS	McLaughlin *et al.* (2022)
	239.069(26)	···	···	···	w.a. (w.e.e.)
	39.11(3)	···	VC	ORFDR	Feiertag and zu Putlitz (1973)
$6^2P_{1/2}$	39.123(9)	···	VC	SAS+FC	Shiner *et al.* (2007)
	39.470(32)	···	VC	SAS+FC	Glaser *et al.* (2020)
	39.122(9)	···	···	···	See text w.a.
	8.179(12)	8.190(49)	VC	ORFDR+MLC	From Arimondo *et al.* (1977)
$6^2P_{3/2}$	8.220(3)	5.148(3)	VC	SAS	Zhang *et al.* (2017)
	8.166 7(94)	8.126(54)	VC	SAS+FC	Glaser *et al.* (2020)
	8.171(7)	8.161(36)	···	···	See text w.a.

TABLE 4. (*Continued*)

State	A (MHz)	B (MHz)	Sample	Technique	References
	2.28(6)	0	VC	MLC	Hogervorst and Svanberg (1975)
$6^2D_{3/2}$	2.32(6)	1.62(6)	VC	HQB	van Wijngaarden *et al.* (1986)
	2.30(4)	1.62(6)	···	···	w.a.
$6^2D_{5/2}$	−1.069(18)	−0.41(41)	VC	OODR	Brandenberger and Lindley (2015)
	94.7(1)	···	MOT	TPSDS	Snadden *et al.* (1996)
	94.2(6)	···	MOT	OODR	Gomez *et al.* (2004)
	94.085(18)	···	VC	EIT	Krishna *et al.* (2005)
	94.658(19)	···			Chui *et al.* (2005)
$7^2S_{1/2}$	94.680 7(37)	···			Barmes *et al.* (2013)
	94.678 4(23)	···	VC	TPSDS+FC	Morzyński *et al.* (2013) and Morzyński *et al.* (2014)
	94.684(2)	···			Morgenweg *et al.* (2014)
	94.681 3(15)	···	···	···	See text w.a.
$7^2P_{1/2}$	17.68(8)	···	VC	ORFDR	Feiertag and zu Putlitz (1973)
$7^2P_{3/2}$	3.71(1)	3.68(8)			Bucka *et al.* (1961)
	1.34(1)	0	VC	MLC	Hogervorst and Svanberg (1975)
$7^2D_{3/2}$	1.415(30)	0.31(6)	VC	HQB	van Wijngaarden and Sagle (1991a)
	1.40(10)	0	VC	TPSDS	Otto *et al.* (2002)
	1.35(2)	0.31(6)	···	···	w.a. (w.e.e.)
$7^2D_{5/2}$	−0.55(10)	0	VC	MLC	Hogervorst and Svanberg (1975)
	45.2(20)	···	VC	ORFDR	Gupta *et al.* (1973)
$8^2S_{1/2}$	47.1(20)	···	VC	TPSDS	Otto *et al.* (2002)
	46.1(14)	···	···	···	w.a.
$8^2P_{3/2}$	1.99(2)	1.98(12)	VC	ORFDR	zu Putlitz and Venkataramu (1968)
	0.84(1)	0	VC	MLC	Hogervorst and Svanberg (1975)
$8^2D_{3/2}$	0.879(8)	0.15(2)	VC	HQB	van Wijngaarden *et al.* (1993)
	0.864(19)	0.15(2)	···	···	w.a. (w.e.e); w.a.
$8^2D_{5/2}$	−0.35(7)	0	VC	MLC	Hogervorst and Svanberg (1975)
	30.(2)	···	TD	TPSDS	Stoicheff and Weinberger (1979)
$9^2S_{1/2}$	33.5(15)	···	VC	TPSDS	Otto *et al.* (2002)
	32.2(12)	···	···	···	w.a.
$9^2D_{3/2}$	0.561(11)	0.20(3)	VC	HQB	Kraińska-Miszczak (1994)
	23.(3)	···	TD	TPSDS	Stoicheff and Weinberger (1979)
$10^2S_{1/2}$	22.2(16)	···	VC	TPSDS	Otto *et al.* (2002)
	22.4(14)	···	···	···	w.a.
$10^2D_{3/2}$	0.393(8)	0.141(13)	VC	HQB	Głódó and Kraińska-Miszczak (1993)
	13.(6)	···	TD	TPSDS	Stoicheff and Weinberger (1979)
$11^2S_{1/2}$	17.1(19)	···	VC	TPSDS	Otto *et al.* (2002)
	16.7(18)	···	···	···	w.a.
$11^2D_{3/2}$	0.283(6)	0.100(11)	VC	HQB	Głódó and Kraińska-Miszczak (1993)
$12^2S_{1/2}$	7.3(2)	···	TD	TPSDS	Stoicheff and Weinberger (1979)
$13^2S_{1/2}$	8.3(4)	···			
$28^2S_{1/2}$	0.322(26)	···			
$29^2S_{1/2}$	0.280(26)	···			
$30^2S_{1/2}$	0.224(20)	···	MOT	MWS	Li *et al.* (2003)
$31^2S_{1/2}$	0.252(31)	···			
$32^2S_{1/2}$	0.209(22)	···			
$33^2S_{1/2}$	0.182(21)	···			
$43^2S_{1/2}$	0.080 4(2)	···			
$44^2S_{1/2}$	0.074 3(3)	···	MOT	MWS	Ramos *et al.* (2019)
$45^2S_{1/2}$	0.070 3(7)	···			
$46^2S_{1/2}$	0.065 3(1)	···			

TABLE 4. (*Continued*)

State	A (MHz)	B (MHz)	Sample	Technique	References
$50^2S_{1/2}$	0.057(13)	⋯			
$51^2S_{1/2}$	0.057(12)	⋯			
$52^2S_{1/2}$	0.053(10)	⋯			
$53^2S_{1/2}$	0.050(10)	⋯			
$54^2S_{1/2}$	0.050(10)	⋯	AB	MWS	Meschede (1987)
$55^2S_{1/2}$	0.047(10)	⋯			
$56^2S_{1/2}$	0.041(8)	⋯			
$57^2S_{1/2}$	0.040(7)	⋯			
$58^2S_{1/2}$	0.036(7)	⋯			
$59^2S_{1/2}$	0.036(3)	⋯			

TABLE 5. Measured *A* and *B* values for ^{87}Rb isotope

State	A (MHz)	B (MHz)	Sample	Technique	References
	25.1(9)	0	VC	ORFDR	Otto *et al.* (2002)
$4^2D_{3/2}$	24.75(12)	2.19(11)	VC	OODR	Moon *et al.* (2009)
	24.75(12)	2.19(11)	⋯	⋯	Recommended
	−16.9(6)	0	VC	ORFDR	Otto *et al.* (2002)
	−16.747(10)	4.149(59)	VC	SAS+FC	Lee *et al.* (2007, 2015)
$4^2D_{5/2}$	−16.801(5)	3.645(30)	VC	OODR+EIT	Wang *et al.* (2014b)
	−16.779(6)	4.112(52)	VC	OODR+FC	Lee and Moon (2015)
	−16.786(10)	3.82(16)	⋯	⋯	w.a. (w.e.e.)
	3 417.330 (7)	⋯	VC	SAS	Barwood *et al.* (1991)
	3 417.341 5(5)	⋯	AB	LIF	Duong *et al.* (1993)
	3 417.341 305 452 156(4)	⋯	⋯	⋯	CCTF (2012)
$5^2S_{1/2}$	3 417.353(19)	⋯	VC	SAS+FC	Shiner *et al.* (2007)
	3 417.341 305 452 156(3)	⋯	MOT	FOUNT	Guéna *et al.* (2014)
	3 417.341 305 452 154(2)	⋯	MOT	FOUNT	Ovchinnikov *et al.* (2015)
	3 417.341 305 452 154 8(15)	⋯	⋯	⋯	w.a.
	406.2(8)	⋯	VC	OS	Beacham and Andrew (1971)
	408.328(15)	⋯	VC	SAS	Barwood *et al.* (1991)
	406.147(15)	⋯	VC	SAS	Banerjee *et al.* (2004)
	406.119(7)	⋯	VC	SAS	Das and Natarajan (2006a)
$5^2P_{1/2}$	408.330(56)	⋯	MOT	LIF+FC	Maric *et al.* (2008)
	408.3(1)	⋯	ODT	OS	Neuzner *et al.* (2015)
	407.75(50)	⋯	VC	SAS	Rupasinghe *et al.* (2022)
	406.48(33)	⋯	⋯	⋯	w.a. (w.e.e.)
	84.29(50)	12.2(20)	VC	SAS	Thibault *et al.* (1981b)
	84.676(28)	12.475(28)	VC	SAS	Barwood *et al.* (1991)
	84.718 5(20)	12.496 5(37)	MOT	SAS	Ye *et al.* (1996)
$5^2P_{3/2}$	84.718 9(22)	12.494 2(43)	MOT	SAS	Gerginov *et al.* (2009)
	84.720 0(16)	12.497 0(35)	VC	SAS	Das and Natarajan (2008)
	84.745(6)	12.528(10)	VC	SAS	Chang *et al.* (2017)
	84.720(3)	12.497(2)	⋯	⋯	w.a. (w.e.e.)
	14.430 3(5)	0.932 0(17)	VC	TPSDS	Nez *et al.* (1993, 1994)
$5^2D_{3/2}$	14.64(30)	0.8(8)	MOT	OODR+RIS	Gabbanini *et al.* (1999)
	14.430 3(5)	0.932 0(17)	⋯	⋯	Recommended

TABLE 5. (*Continued*)

State	A (MHz)	B (MHz)	Sample	Technique	References
$5^2D_{5/2}$	−7.460 5(3)	1.271 3(20)	VC	TPSDS	Nez *et al.* (1993, 1994)
	−7.45(21)	0.462(1088)	MOT	OODR	Grove *et al.* (1995)
	−7.51(28)	2.7(24)	MOT	OODR+RIS	Gabbanini *et al.* (1999)
	−7.460 5(3)	1.271 3(20)	⋯	⋯	Recommended
$6^2S_{1/2}$	807.66(8)	⋯	VC	FML	Pérez Galván *et al.* (2007) also in Pérez Galván *et al.* (2008)
	797.(30)	⋯	VC	TPSDS	Orson *et al.* (2021)
	807.341(15)	⋯			McLaughlin *et al.* (2022)
	807.35(4)	⋯	⋯	⋯	w.a.(w.e.e.)
$6^2P_{1/2}$	132.56(3)	⋯	VC	ORFDR	Feiertag and zu Putlitz (1973)
	132.559(13)	⋯	VC	SAS+FC	Shiner *et al.* (2007)
	132.583(141)	⋯	VC	OODR+EIT	Nyakang'o *et al.* (2020)
	133.24(28)	⋯	VC	SAS+FC	Glaser *et al.* (2020)
	132.569(9)	⋯	⋯	⋯	See text w.a.
$6^2P_{3/2}$	27.700(17)	3.953(24)	VC	ORFDR	From Arimondo *et al.* (1977)
	27.710(15)	4.030(42)	VC	SAS+FC	Glaser *et al.* (2020)
	27.706(11)	3.972(33)	⋯	⋯	w.a. (w.e.e. for *B*)
$6^2D_{3/2}$	7.84(5)	0.53(6)	VC	MLC	Svanberg and Tsekeris (1975)
	−3.4(5)	0	VC	ORFDR+MLC	Hogervorst and Svanberg (1975)
$6^2D_{5/2}$	−3.61(6)	−0.20(20)	VC	OODR	Brandenberger and Lindley (2015)
	−3.61(6)	−0.20(20)	⋯	⋯	Recommended
$7^2S_{1/2}$	319.7(1)	⋯	MOT	TPSDS	Snadden *et al.* (1996)
	319.174(45)	⋯	VC	EIT	Krishna *et al.* (2005)
	319.702(65)	⋯	MOT		Marian *et al.* (2005)
	319.759(28)	⋯	VC		Chui *et al.* (2005)
	319.751 8(51)	⋯	VC	TPSDS+FC	Barmes et al. (2013)
	319.747 9(23)	⋯	VC		Morzyński *et al.* (2013) also in Morzyński *et al.* (2014)
	319.762(6)	⋯	VC		Morgenweg *et al.* (2014)
	319.750 0(20)	⋯	⋯	⋯	See text w.a.
$7^2P_{1/2}$	59.92(9)	⋯	VC	ORFDR	Feiertag and zu Putlitz (1973)
$7^2P_{3/2}$	12.57(1)	1.762(16)	VC	ORFDR+MLC	From Arimondo *et al.* (1977)
	4.53(3)	0.26(4)	VC	MLC	Svanberg and Tsekeris (1975)
$7^2D_{3/2}$	4.69(23)	0	VC	TPSDS	Otto *et al.* (2002)
	4.53(3)	0.26(4)	⋯	⋯	Recommended
$7^2D_{5/2}$	−2.0(3)	0	VC	ORFDR+MLC	Hogervorst and Svanberg (1975)
	−1.85(80)	0	VC	TPSDS	Otto *et al.* (2002)
	−1.98(28)	0	⋯	⋯	w.a.
$8^2S_{1/2}$	159.2(15)	⋯	VC	ORFDR	Tsekeris and Gupta (1975)
	159.3(30)	⋯	VC	TPSDS	Otto *et al.* (2002)
	159.2(13)	⋯	⋯	⋯	w.a.
$8^2P_{1/2}$	32.12(11)	⋯	VC	ORFDR	Tsekeris *et al.* (1975)
$8^2P_{3/2}$	6.739(15)	0.935(22)	VC	ORFDR+MLC	From Arimondo *et al.* (1977)
$8^2D_{3/2}$	2.840(15)	0.17(2)	VC	MLC+ORFDR	Belin *et al.* (1976b)
	−1.20(15)	0	VC	ORFDR+MLC	Hogervorst and Svanberg (1975)
$8^2D_{5/2}$	−1.00(13)	0	VC	TPSDS	Otto *et al.* (2002)
	−1.09(10)	0	⋯	⋯	w.a.
$9^2S_{1/2}$	90.9(8)	⋯	VC	ORFDR	Tsekeris and Gupta (1975)
	106.(3)	⋯	TD	TPSDS	Stoicheff and Weinberger (1979)
	91.6(47)	⋯	VC	TPSDS	Belin *et al.* (1976b)
	90.9(8)	⋯	⋯	⋯	Recommended
$9^2P_{3/2}$	4.05(3)	0.55(3)	VC	ORFDR	Belin *et al.* (1976b)

TABLE 5. (*Continued*)

State	A (MHz)	B (MHz)	Sample	Technique	References
	1.90(1)	0.11(3)	VC	MLC+ORFDR	Belin *et al.* (1976b)
$9^2D_{3/2}$	2.01(17)	0	VC	TPSDS	Otto *et al.* (2002)
	1.90(1)	0.11(3)	⋯	⋯	Recommended
	−0.80(15)	0	VC	MLC+ORFDR	Otto *et al.* (2002)
$9^2D_{5/2}$	−0.740(12)	0.160(15)	VC	HQB	Głódó and Kraińska-Miszczak (1990)
	−0.740(12)	0.160(15)	⋯	⋯	Recommended
	56.3(2)	⋯	VC	ORFDR	Farley *et al.* (1977)
$10^2S_{1/2}$	70.(3)	⋯	TD	TPSDS	Stoicheff and Weinberger (1979)
	56.1(23)		VC	TPSDS	Otto *et al.* (2002)
	56.3(2)	⋯	⋯	⋯	Recommended
$10^2P_{3/2}$	2.60(8)	0	VC	ORFDR	Belin *et al.* (1976b)
$10^2D_{3/2}$	1.315(17)	0.070(11)	VC	HQB	Głódó and Kraińska-Miszczak (1991)
$10^2D_{5/2}$	−0.510(10)	0.098(11)			Głódó and Kraińska-Miszczak (1987)
	37.4(3)	⋯	VC	ORFDR	Farley *et al.* (1977)
$11^2S_{1/2}$	54.(10)	⋯	TD	TPSDS	Stoicheff and Weinberger (1979)
	37.2(35)		VC	TPSDS	Otto *et al.* (2002)
	37.4(3)	⋯	⋯	⋯	Recommended
$11^2D_{3/2}$	0.955(11)	0.049(6)	VC	HQB	Głódó and Kraińska-Miszczak (1991)
$11^2D_{5/2}$	−0.361(7)	0.071(11)			Głódó and Kraińska-Miszczak (1989)
$12^2S_{1/2}$	27.(8)	⋯	TD	TPSDS	Stoicheff and Weinberger (1979)
$12^2D_{3/2}$	0.715(12)	0.037(8)	VC	HQB	Głódó and Kraińska-Miszczak (1991)
$12^2D_{5/2}$	−0.266(9)	0.063(14)			Głódó and Kraińska-Miszczak (1989)
$13^2S_{1/2}$	23.(8)	⋯	TD	TPSDS	Stoicheff and Weinberger (1979)
$13^2D_{5/2}$	−0.20(1)	0.05(2)	VC	HQB	Głódó and Kraińska-Miszczak (1989)
$20^2S_{1/2}$	3.891(2)	⋯			
$21^2S_{1/2}$	3.249(2)	⋯	VC	EIT	Tauschinsky *et al.* (2013)
$22^2S_{1/2}$	2.721(3)	⋯			
$23^2S_{1/2}$	2.390(4)	⋯			
$24^2S_{1/2}$	2.115(5)	⋯			
$28^2S_{1/2}$	1.07(5)	⋯			
$29^2S_{1/2}$	0.97(5)	⋯			
$30^2S_{1/2}$	0.78(4)	⋯	MOT	MWS	Li *et al.* (2003)
$31^2S_{1/2}$	0.81(7)	⋯			
$32^2S_{1/2}$	0.71(5)	⋯			
$33^2S_{1/2}$	0.63(4)	⋯			
$50^2S_{1/2}$	0.185(20)	⋯			
$51^2S_{1/2}$	0.170(18)	⋯			
$52^2S_{1/2}$	0.165(18)	⋯			
$53^2S_{1/2}$	0.160(10)	⋯			
$54^2S_{1/2}$	0.145(18)	⋯	AB	MWS	Meschede (1987)
$55^2S_{1/2}$	0.145(15)	⋯			
$56^2S_{1/2}$	0.142(13)	⋯			
$57^2S_{1/2}$	0.135(13)	⋯			
$58^2S_{1/2}$	0.111(13)	⋯			
$59^2S_{1/2}$	0.105(10)	⋯			

were communicated privately by Lindsay. For the A constants of the 57 and 58 $^2S_{1/2}$ states measured by Meschede (1987) for the ^{87}Rb the missing error bar is assumed equal to the ^{85}Rb ones.

For n^2D $(n \geq 6)$ states the investigations by Svanberg and Tsekeris (1975) and van Wijngaarden *et al.* (1993) and by Głódó and Kraińska-Miszczak (1987, 1990, 1991) and Kraińska-Miszczak (1994) produced only the relative signs of the A and B constants. Their signs are determined here on the basis of the scaling laws presented in Fig. 3 of Sec. 5.1.

For the 85 isotope in Table 4, the ground state hyperfine measurement in a maser by Tetu *et al.* (1976) agrees with and supersedes the atomic beam MWS results reported in Arimondo *et al.* (1977). The following table entries based on saturated absorption spectroscopy by Barwood *et al.* (1991) and Shiner *et al.* (2007) or atomic beam laser spectroscopy by Duong *et al.* (1993) have a lower precision. They are superseded by the clock measurements in an optical fountain by Wang *et al.* (2019). The ^{87}Rb fountain progress was summarized in 2012 by the International Committee for Weights and Measures with their recommended Table 5 value. Later observations by Guéna *et al.* (2014) and Ovchinnikov *et al.* (2015) improved its precision.

Data for the $5^2P_{1/2}$ level of both isotopes are classified in two groups. The first one includes Barwood *et al.* (1991) and Maric *et al.* (2008), while the second one includes the optical spectroscopy determination by Beacham and Andrew (1971) recommended in Arimondo *et al.* (1977), Banerjee *et al.* (2004), Das and Natarajan (2006a) data from the Bangalore research team, and the Rupasinghe *et al.* (2022) value. The agreement of the results within each group is good. However, the first group compared to the second one derives the ^{85}Rb A constant lower by 0.146(13) MHz, and the ^{87}Rb A value higher by 2 202(33) MHz. The data of both groups lead to peculiar values for the hyperfine anomaly. The higher measured values for ^{87}Rb are closer to the theoretical predictions by Safronova and Safronova (2011) of 408.53 MHz and by Grunefeld *et al.* (2019) of 410.06 MHz. The only theoretical prediction for ^{85}Rb by Pal *et al.* (2007) of 119.192 MHz is off by a few MHz above both group results. The search for similar systematic errors as discussed for the case of the ^{39}K $4^2P_{1/2}$ state combined with the present restricted dataset does not resolve the discrepancy. For this state, the w.a. entry in both Tables 4 and 5 is reported with a large error bar determined from the χ^2_{red} approach.

For the ^{85}Rb $5^2P_{3/2}$ state, excellent agreement exists for the A value. This is not the case for the B constant, where the SAS measurement by Barwood *et al.* (1991) considered as a reference point increases greatly the χ^2 and as a consequence the error bar. An agreement within less than 30 kHz is reached for most data of the ^{87}Rb $5^2P_{3/2}$ state. An excellent relative precision of 2×10^{-5} was reached by two separate measurements on the ^{87}Rb isotope by Ye *et al.* (1996) and Das and Natarajan (2008). In Table 6, the Ye *et al.* (1996) data reexamined by Gerginov *et al.* (2009) bring evidence of the octupole contribution to the Rb hyperfine interactions.

Another example of large discrepancies is found for the ^{85}Rb $6^2P_{1/2}$ state. The 39.470(32) MHz SAS+FC measurement by Glaser *et al.* (2020) presents a difference exceeding the error bar, compared to the values reported by Shiner *et al.* (2007) based on the same SAS+FC technique, and also the ORFDR measurement by Feiertag and zu Putlitz (1973) and the OODR-EIT measurement by Nyakang'o *et al.* (2020). Our derivation of the hyperfine splitting from the measured optical frequencies of Glaser *et al.* (2020) leads to the 39.11(22) MHz value in good agreement with other ones. Therefore, the Glaser *et al.* (2020) entry is not included in the w.a.

TABLE 6. Measured C values for ^{87}Rb and ^{133}Cs

State	C (kHz)	Sample	Technique	References
		^{87}Rb		
$5^2P_{3/2}$	−0.12(9)	MOT	SAS	Gerginov *et al.* (2009)
		^{133}Cs		
$6^2P_{3/2}$	0.56(7)	AB	LIF	Gerginov *et al.* (2003)
	0.87(32)	VC	CCS	Das and Natarajan (2005)
$6^2D_{3/2}$	4.3(10)	VC	TPSDS	Chen *et al.* (2018)

In contrast, the $6^2P_{3/2}$ Glaser *et al.* (2020) data for both isotopes are in very good agreement with the earlier radio frequency and level-crossing data. For that state in ^{85}Rb, the A value derived by Zhang *et al.* (2017) on the basis of saturated absorption and EIT measurements is close to those of other references. However, that experiment produced a B constant with a large deviation from other values, probably because the hyperfine lines were not well resolved. Both their A and B values are not included into the w.a.

The $7^2S_{1/2}$ state of both isotopes has received a wide attention because of the large probability for the two-photon excitation from the ground state. Precision at the 1×10^{-6} level is reached in the 87 isotope and at the 2×10^{-5} level in the 85 one, limited by the 2 kHz resolution of the frequency comb in Krishna *et al.* (2005), Chui *et al.* (2005), Barmes *et al.* (2013), and Morzyński *et al.* (2013). However, in both isotopes the EIT results by Krishna *et al.* (2005) are lower than the other ones by ≈400 kHz, while their claimed precision is ≈20 kHz precision. The presence of light shifts originated by the intense control laser producing the EIT signal was not tested. The w.a. are performed excluding the Krishna *et al.* (2005) values.

For the $n = (9–13)\,^2S_{1/2}$ states, the optical spectra recorded by Stoicheff and Weinberger (1979) produce hyperfine constants in good agreement with more recent ones, but only for the 85 isotope. Their $n = (9–11)$ data for the 87 isotope are very far off and not included in the w.a.

4.5. Cesium

Considering the large set of measured values that cover up Rydberg states with high n numbers, cesium is a favorite atom for hyperfine spectroscopy. In addition, there is a good (or very good) agreement for the large majority of states.

The use of frequency combs in order to perform absolute optical frequency measurements produces very precise values for the explored states. For instance, the $6^2P_{1/2}$ A constant was reported with a $\approx 3 \times 10^{-4}$ precision in Arimondo *et al.* (1977), while it reached $\approx 3 \times 10^{-6}$ in Gerginov *et al.* (2006). A similar spectacular improvement is associated with the $8^2S_{1/2}$ state, object of several investigations owing to its large two-photon excitation probability.

The nuclear magnetic octupole dipole moment was measured for the first time in the $6^2P_{3/2}$ state by Gerginov *et al.* (2003) with the value of $C = 0.56(7)$ kHz, and remeasured as $C = 0.87(32)$ kHz

by Das and Natarajan (2008), as shown in Table 6. The first reference reaches a higher precision, but leads to a B constant in poor agreement with the values by the second reference and by Tanner and Wieman (1988). For the $6^2D_{3/2}$ state, the octupole moment was recently measured by Chen *et al.* (2018) with the value of $C = 4.3(10)$ kHz, much larger than the above value for the $6^2P_{3/2}$ state.

Off-diagonal elements between $6P_{1/2}$ and $6P_{3/2}$ levels derived theoretically in Johnson *et al.* (2004) at the level of ≈40 Hz are negligible even at the high precision level of the $6P_{3/2}$ state hyperfine data.

For several high nD, with $n \geq 10$, states, the investigations by Svanberg and Belin (1974), Belin *et al.* (1976a), Deech *et al.* (1977), Nakayama *et al.* (1981), Sagle and van Wijngaarden (1991), and Głódó and Kraińska-Miszczak (1987, 1990, 1991) produced only the absolute value of the A constant. Their signs are determined here on the basis of the scaling laws. All B values for those states were assumed equal zero.

The inversion of the $^2D_{5/2}$ hyperfine states is basically due to core-polarization and electron-correlation effects induced by the valence electron, as initially pointed out by Fredriksson *et al.* (1980) and carefully examined recently in Auzinsh *et al.* (2007), Grunefeld *et al.* (2019), and Tang *et al.* (2019).

The $6^2S_{1/2}$ A coefficient corresponding to the ground state hyperfine splitting is not listed in Table 7 because it is related, as the 2 298.157 943 MHz frequency, to the Bureau International des Poids et Mesures definition of the second.

For the $6^2D_{3/2}$ state, Table 7 reports the value by Kortyna *et al.* (2006) because the remeasured value in Kortyna *et al.* (2011) using a different method is less precise. The A and B values measured by Cheng *et al.* (2017) are not included into the calculation of the w.a. because their fit does not reproduce all

TABLE 7. Measured A and B values for ^{133}Cs

State	A (MHz)	B (MHz)	Sample	Technique	References
$5^2D_{3/2}$	48.6(2)	0.0(8)	AB	LIF	Fredriksson *et al.* (1980)
	48.8(3)	0	VC	HQB	Ryschka and Marek (1981)
	48.78(7)	0.1(7)	VC	HQB+DD	Yei *et al.* (1998)
	48.78(7)	0.(7)	···	···	Recommended
$5^2D_{5/2}$	−21.2(2)	0.0(10)	AB	LIF	Fredriksson *et al.* (1980)
	−22.1(5)	0	VC	ORFDR	Lam *et al.* (1980)
	−21.24(5)	0.2(5)	VC	HQB+DD	Yei *et al.* (1998)
	−21.24(5)	0.2(5)	···	···	Recommended
$5^2F_{5/2}$ $5^2F_{7/2}$	<|0.7| <|1.0|	0	VC	ORFDR	Svanberg *et al.* (1973)
$6^2P_{1/2}$	291.90(12)	···	VC	ORFDR	Abele (1975a)
	291.3(7)	···	AB	ORFDR	Coc *et al.* (1987)
	291.885(80)	···	AB	LIF	Rafac and Tanner (1997)
	291.922(20)	···	VC	SAS+FCS	Udem *et al.* (1999)
	291.918(8)	···	VC	SAS	Das *et al.* (2006a)
	291.913 5(15)	···	VC	SAS	Das and Natarajan (2006b)
	291.930 9(12)	···	AB	LIF +FC	Gerginov *et al.* (2006)
	291.929(1)	···	VC	OS	Truong *et al.* (2015)
	291.926 3(25)	···	···	···	w.a. (w.e.e.)
$6^2P_{3/2}$	50.15(8)	−1.35(80)	AB	HOPF	Thibault *et al.* (1981a)
	50.275(3)	−0.53(2)	AB	LIF	Tanner and Wieman (1988)
	50.288 27(23)	−0.493 4(17)	AB	LIF	Gerginov *et al.* (2003)
	50.281 63(86)	−0.526 6(57)	VC	CCS	Das and Natarajan (2005)
	50.287 8(11)	−0.496(6)	···	···	w.a .(w.e.e.)
$6^2D_{3/2}$	16.30(15)	0	VC	TPSDS	Tai *et al.* (1975)
	16.17(17)	0.11(127)	VC	TPSDS	Ohtsuka et al. (2005)
	16.34(3)	−0.1(2)	VC	OODR	Kortyna *et al.* (2006)
	16.333 1(80)	−0.36(1)	VC	OODR	Cheng *et al.* (2017)
	16.338(3)	−0.136(24)	VC	TPSDS	Chen *et al.* (2018)
	16.338(3)	−0.136(24)	···	···	See text recommended
$6^2D_{5/2}$	−4.69(4)	0.18(73)	MOT	TPSDS	Georgiades *et al.* (1994)
	−4.56(9)	−0.35(183)	VC	TPSDS	Ohtsuka et al. (2005)
	−4.66(4)	0.9(8)	VC	OODR	Kortyna *et al.* (2006)
	−4.59(6)	−0.78(66)	VC	OODR	Wang *et al.* (2020a)
	−4.629(14)	−0.10(15)	VC	TPSDS	Herd *et al.* (2021)

TABLE 7. (*Continued*)

State	A (MHz)	B (MHz)	Sample	Technique	References
	−4.629(11)	−0.10(15)	⋯	⋯	Recommended
	545.90(9)	⋯	AB	LIF	Gilbert *et al.* (1983)
	545.818(16)	⋯	VC	OODR	Yang *et al.* (2016) and Ren *et al.* (2016)
$7^2S_{1/2}$	545.90(32)	⋯	MOT	TPSDS	Tian *et al.* (2019)
	545.87(1)	⋯	VC	OODR+EIT	He *et al.* (2020)
	545.856(14)	⋯	⋯	⋯	w.a. (w.e.e.)
	94.35(4)	⋯	VC	ORFDR	Feiertag *et al.* (1972)
	94.2(5)	⋯	VC	SAS	Gerhardt *et al.* (1978)
$7^2P_{1/2}$	94.40(5)	⋯	VC	SAS	Williams *et al.* (2018)
	94.37(3)	⋯	⋯	⋯	w.a.
	16.605(6)	−0.15(3)	VC	VR	From Arimondo *et al.* (1977)
	16.6(3)	0	VC	HQB	Deech *et al.* (1977)
$7^2P_{3/2}$	16.605(6)	−0.19(5)	VC	SAS	Williams *et al.* (2018)
	16.605(4)	−0.16(3)	⋯	⋯	w.a.
	7.36(3)	−0.1(2)	AB	OODR	Kortyna *et al.* (2008)
	7.386(15)	−0.18(16)	VC	OODR+FC	Stalnaker *et al.* (2010)
	7.36(7)	−0.88(87)	VC	TPSDS	Lee *et al.* (2011)
$7^2D_{3/2}$	7.38(1)	−0.18(10)	VC	TPSDS	Kiran Kumar *et al.* (2013)
	7.38(19)	−0.15(21)	VC	OODR+FC	Jin *et al.* (2013)
	7.39(6)	−0.19(18)	VC	TPSDS	Wang *et al.* (2021)
	7.380(8)	−0.17(7)	⋯	⋯	w.a.
	−1.56(9)	0	VC	ELC	Auzinsh *et al.* (2007)
	−1.717(15)	−0.18(52)	VC	OODR+FC	Stalnaker *et al.* (2010)
	−1.81(5)	1.01(106)	VC	TPSDS	Lee *et al.* (2011)
$7^2D_{5/2}$	−1.70(3)	−0.77(58)	VC	OODR+EIT	Wang *et al.* (2020b)
	−1.79(5)	1.05(29)	VC.	TPSDS	Wang *et al.* (2021)
	−1.717(15)	−0.18(52)	⋯	⋯	See text recommended
	225.(15)	⋯	VC	LOF	Campani *et al.* (1978)
	219.3(2)	⋯	TD	TPSDS	Herrmann *et al.* (1985)
	219.(1)	⋯	MOT	OODR	Fort *et al.* (1995a)
	220.(1)	⋯	VC	TPSDS	Fort *et al.* (1995b)
	205.(15)	⋯	VC	FC+QBS	Bellini *et al.* (1997)
	219.12(1)	⋯	VC	TPSDS	Hagel *et al.* (1999)
$8^2S_{1/2}$	219.125(4)	⋯	VC	TPSDS+FC	Fendel *et al.* (2007)
	219.14(11)	⋯	VC	OODR+FC	Stalnaker *et al.* (2010)
	219.124(7)	⋯	VC	SAS	Wu *et al.* (2013)
	219.08(12)	⋯	VC	OODR+EIT	Wang *et al.* (2013, 2014a)
	219.137(11)	⋯	VC	OODR+FC	Jin *et al.* (2013)
	219.125(3)	⋯	⋯	⋯	w.a.
$8P_{1/2}$	42.95 (15)	⋯	AB	SAS	Liu and Baird (2000)
	42.97(10)	⋯	VC	ORFDR+MFD	Tai *et al.* (1973)
$8^2P_{1/2}$	42.9(3)	⋯	VC	SAS	Cataliotti *et al.* (1996)
	42.96(9)	⋯	⋯	⋯	w.a.
	7.55(5)	0.63(35)	VC	ORFDR	Barbey and Geneux (1962)
	7.626(5)	−0.049(42)	VC	ORFDR	Bucka and von Oppen (1962)
	7.58(1)	−0.14(5)	VC	ORFDR	Faist *et al.* (1964)
$8^2P_{3/2}$	7.644(25)	0	VC	ORFDR	Abele (1975b)
	7.42(6)	0.14(29)	VC	HQB+DD	Bayram *et al.* (2014)
	7.58(3)	−0.14(5)	⋯	⋯	See text w.a. (w.e.e); recommended
	3.94(8)	0	VC	MLC+HQB	From Arimondo *et al.* (1977)
	3.92(7)	0	VC	HQB	Deech et al. (1977)
$8^2D_{3/2}$	3.92(10)	0	VC	MFD	van Wijngaarden and Sagle (1991b)
	3.95(1)	0	VC	HQB	Sagle and van Wijngaarden (1991)
	3.95(1)	0	⋯	⋯	Recommended

TABLE 7. (*Continued*)

State	A (MHz)	B (MHz)	Sample	Technique	References
$8^2D_{5/2}$	−0.85(20)	0	VC	ORFDR+MLC	From Arimondo *et al.* (1977)
	110.1(5)	···	VC	ORFDR	Farley *et al.* (1977)
	109.93(9)	···	VC	OODR+FC	Stalnaker *et al.* (2010)
$9^2S_{1/2}$	109.7(3)	···	VC	TPSDS	Kiran Kumar and Suryanarayana (2012)
	110.150(13)	···	VC	OODR+FC	Jin *et al.* (2013)
	109.999(3)	···	VC	TPSDS+FC	Morgenweg *et al.* (2014)
	110.999(3)	···	···	···	Recommended
$9^2P_{1/2}$	23.19(15)	···	VC	ORFDR	Tsekeris *et al.* (1975)
$9^2P_{3/2}$	4.123(3)	−0.051(25)	VC	MLC	Rydberg and Svanberg (1972)
	2.35(4)	0	VC	MLC+HQB	From Arimondo *et al.* (1977)
$9^2D_{3/2}$	2.32(4)	0	VC	HQB	Deech *et al.* (1977)
	2.38(1)	0	VC	HQB	Sagle and van Wijngaarden (1991)
	2.375(10)	0	···	···	w.a.
$9^2D_{5/2}$	−0.43(4)	0	VC	ELC	Auzinsh *et al.* (2007)
$10^2S_{1/2}$	63.2(3)	···	VC	ORFDR	Tsekeris *et al.* (1974)
$10^2P_{1/2}$	13.9(2)	···	VC	ORFDR	Farley *et al.* (1977)
$10^2P_{3/2}$	2.481(9)	−0.025(8)	VC	MLC	Rydberg and Svanberg (1972)
	1.52(3)	0	VC	MLC	Svanberg and Tsekeris (1975)
	1.51(2)	0	VC	HQB	Deech *et al.* (1977)
$10^2D_{3/2}$	1.54(2)	0	VC	HQB	Sagle and van Wijngaarden (1991)
	1.503(91)	0	VC	TPSDS	Otto *et al.* (2002)
	1.524(13)	0	···	···	w.a.
$10^2D_{5/2}$	−0.34(3)	0	VC	ELC	Auzinsh *et al.* (2007)
	39.4(2)	···	VC	ORFDR	Tsekeris *et al.* (1974)
$11^2S_{1/2}$	39.4(17)	···	VC	TPSDS	Otto *et al.* (2002)
	38.81(23)	···	VC	OODR+EIT	He *et al.* (2012)
	39.15(15)	···	···	···	w.a. (w.e.e.)
$11^2P_{3/2}$	1.600(15)	0	VC	ORFDR	Belin and Svanberg (1974)
	1.055(15)	0	VC	MLC	Svanberg and Belin (1974)
	1.05(4)	0	VC	HQB	Deech *et al.* (1977)
$11^2D_{3/2}$	1.11(11)	0	VC	TPSDS	Otto *et al.* (2002)
	1.053 0(69)	0	VC	TPSDS+FC	Quirk *et al.* (2022a)
	1.053 0(69)	0	···	···	Recommended
	−0.24(6)	0	VC	ORFDR	Svanberg and Belin (1974)
$11^2D_{5/2}$	−0.21(6)	0	VC	TPSDS+FC	Quirk *et al.* (2022a)
	−0.225(41)	0	···	···	w.a.
	26.31(10)	···	VC	ORFDR	Tsekeris and Gupta (1975)
$12^2S_{1/2}$	26.4(16)	···	VC	TPSDS	Otto *et al.* (2002)
	26.318(15)	···	VC	TPSDS+FC	Quirk *et al.* (2022a)
	26.318(15)	···	···	···	Recommemded
$12^2P_{3/2}$	1.10(3)	0	VC	ORFDR	Belin *et al.* (1976a)
	0.758(12)	0	VC	MLC	Svanberg and Belin (1974)
$12^2D_{3/2}$	0.75(2)	0	VC	HQB	Deech *et al.* (1977)
	0.758(12)	0	···	···	Recommended
$12^2D_{5/2}$	−0.19(5)	0	VC	ORFDR	Svanberg and Belin (1974)
	18.4(1)	···	VC	ORFDR	Farley *et al.* (1977)
$13^2S_{1/2}$	18.6(18)	···	VC	TPSDS	Otto *et al.* (2002)
	18.431(10)	···	VC	TPSDS+FC	Quirk *et al.* (2022a)
	18.431(10)	···	···	···	Recommended

TABLE 7. (*Continued*)

State	A (MHz)	B (MHz)	Sample	Technique	References
$13^2P_{3/2}$	0.77(5)	0	VC	ORFDR	Belin *et al.* (1976a)
	0.556(8)	0	VC	MLC	Svanberg and Belin (1974)
$13^2D_{3/2}$	0.55(4)	0	VC	HQB	Deech *et al.* (1977)
	0.556(8)	0	···	···	Recommemded
$13^2D_{5/2}$	−0.14(4)	0	VC	ORFDR	Svanberg and Belin (1974)
	13.4(1)	···	VC	ORFDR	Farley *et al.* (1977)
$14^2S_{1/2}$	13.9(15)	···	VC	TPSDS	Otto *et al.* (2002)
	13.4(1)	···	···	···	Recommended
	0.425(7)	0	VC	MLC	Belin *et al.* (1976a)
$14^2D_{3/2}$	0.40(5)	0	VC	HQB	Deech *et al.* (1977)
	0.425(7)	0	···	···	Recommended
$15^2S_{1/2}$	10.1(1)	···	VC	ORFDR	Farley *et al.* (1977)
	0.325(8)	0	VC	MLC	Belin *et al.* (1976a)
$15^2D_{3/2}$	0.31(2)	0	VC	HQB	Nakayama *et al.* (1981)
	0.325(8)	0	···	···	Recommended
$16^2S_{1/2}$	7.73(5)	···	VC	ORFDR	Farley *et al.* (1977)
	0.255(12)	0	VC	MLC	Belin *et al.* (1976a)
$16^2D_{3/2}$	0.24(2)	0	VC	HQB	Nakayama *et al.* (1981)
	0.255(12)	0	···	···	Recommended
$17^2S_{1/2}$	6.06(10)	···	VC	ORFDR	Farley *et al.* (1977)
$17^2D_{3/2}$	0.190(12)	0	VC	MLC	Belin *et al.* (1976a)
$18^2D_{3/2}$	0.160(10)	0			
$23^2S_{1/2}$	2.3(2)	···			
$23^2P_{1/2}$	0.56(5)	···			
$25^2S_{1/2}$	1.5(2)	···			
$25^2P_{1/2}$	0.40(5)	···	AB	OODR+MWS	Raimond *et al.* (1981), also in
$26^2S_{1/2}$	1.4(2)	···			Goy *et al.* (1982)
$26^2P_{1/2}$	0.31(5)	···			
$28^2S_{1/2}$	1.2(2)	···			
$28^2P_{1/2}$	0.28(5)	···			
$45^2P_{3/2}$	0.010 3(27)	0			
$49^2S_{1/2}$	0.147(4)	···			
$59^2P_{3/2}$	0.004 7(10)	0			
$67^2P_{3/2}$	0.003 0(17)				
$68^2S_{1/2}$	0.052 0(13)	···	MOT	MWS	Saßmannshausen *et al.* (2013)
$72^2P_{3/2}$	0.002 1(36)	0			
$81^2S_{1/2}$	0.031 8(19)	···			
$90^2S_{1/2}$	0.022 7(28)	···			
$66^2D_{3/2}$	0.002 6(5)	0			
$66^2D_{5/2}$	0.000 10(45)	0			

the measured hyperfine frequencies within the reported error bar.

For the $7^2D_{5/2}$ state, several A values were measured with good overall agreement. This is not the case for the B values, where large discrepancies are reported. The small values of the hyperfine constants limit the frequency resolution. Three experiments [Lee *et al.* (2011) and Wang *et al.* (2020b, 2021)] measured a restricted number of hyperfine splittings with a limited agreement of their frequency. Stalnaker *et al.* (2010) reported a full high-resolution spectrum and a careful study of systematic errors. Having observed a dependence of the B value on the applied magnetic field, they increase the error bar of their B measurement in order to cover both negative and positive values. Their A and B values are recommended in Table 7.

For the $8^2P_{3/2}$ state, the A and B values examined by Arimondo *et al.* (1977) were based on early ORFDR investigations by Barbey and Geneux (1962), Bucka and von Oppen (1962), and Faist *et al.* (1964), all suffering from radio frequency shifts as discussed in this last reference. All of them are reported in Table 7. Arimondo *et al.* (1977) recommended the Faist *et al.* (1964) values, where the shift corrections were included. That A value and the one by Bayram *et al.* (2014) agree at 0.15 MHz level. Table 7 reports the w.a. of Faist *et al.* (1964) and Bayram *et al.* (2014) with χ^2_{red} correction. The B values by Faist *et al.* (1964) and Bayram *et al.* (2014) are identical except for their sign. Bayram *et al.* (2014) defended their positive value on the basis of their earlier Na $3P_{3/2}$ hyperfine constants by Yei *et al.* (1993) using a similar technique and agreeing with the best other measurements as in Table 2. A negative B value is confirmed by the scaling law of Fig. 1. Despite w.a. being −0.12(5), Table 7 recommends the value of Faist *et al.* (1964).

For the measured constant of $9^2S_{1/2}$, the high reported precision of Jin *et al.* (2013) leads to an anomalously large contribution to χ^2_{red}. When that value is excluded from the w.a., the error bar is greatly reduced. It is worth noting that the $8^2S_{1/2}$ and $7^2D_{3/2}$ values presented by the same authors with a similar precision match very well those by other authors. The $9^2S_{1/2}$ recommended value is the Morgenweg *et al.* (2014) measurement having a 2×10^{-5} precision.

The 9 and 10 $^2P_{3/2}$ values by Rydberg and Svanberg (1972) are corrected for the g_j value in Arimondo *et al.* (1977). Rydberg and Svanberg (1972) derive the $10^2P_{3/2}$ B value on the basis of the average measured ratio $B/A = -0.010(3)$ in the lower n $^2P_{3/2}$ levels.

We have received privately from Deiglmayr the A values for the $^2S_{1/2}$, $^2P_{1/2}$ states with n between 43 and 81 measured by Saßmannshausen *et al.* (2013).

4.6. Francium

In the 1980–1987 years, the Orsay group at the ISOLDE atomic beam facility in CERN measured several hyperfine constants of different Fr isotopes reported in Liberman *et al.* (1980), Coc *et al.* (1985, 1987), and Duong *et al.* (1987). Francium spectroscopy has reached a higher precision level with the preparation of a cold atom MOT in 1996–1997 by Simsarian *et al.* (1996) and Lu *et al.* (1997). Two years later, the important information on the nuclear structure associated with the $^2P_{1/2}$ hyperfine structure pointed out by Grossman *et al.* (1999) has triggered a new interest leading to several more recent experimental investigations.

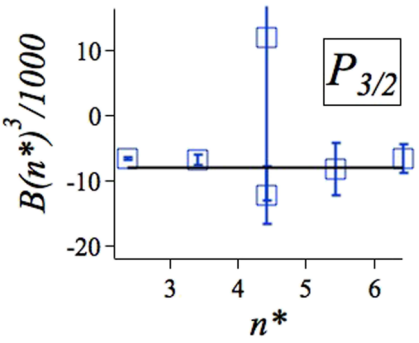

FIG. 1. For Cs $^2P_{3/2}B(n^*)^3$ scaling test, with B in MHz, vs the n number in logarithmic scale states. For the $n = 8$ state, one negative and one positive value are reported here from Table 7. The quantum defect parameters are derived from Lorenzen and Niemax (1984). The continuous horizontal line represents a fit of the negative values based on the $1/(n^*)^3$ scaling.

Table 8 reports all results for the Fr nuclear ground state configuration, avoiding duplicates when the same value was published more than once. The table does not include the francium data published by Voss *et al.* (2013), where systematic errors are unaccounted, since updates and corrections of these measurements were presented by Voss *et al.* (2015); see Table 1 of that paper. Table 8 evidences that a very large set of isotopes was investigated, all of them targeted at the nuclear structure exploration. The agreement between different hyperfine values is not exceptional, in several cases, the differences being greater than the error bars. Because for most isotopes the explored energy levels are limited in number, usually only the lower levels for each L series, global analyses are not efficient. A partial spectroscopic information is associated with the S series in the 210 and 212 isotopes composed by three explored states, with both $n = 8$ and $n = 9$ hyperfine values missed out in the second isotope. The inconsistency in Gomez *et al.* (2008) between the number in Table 1 and that reported in the text and the abstract is resolved by using the number reported in the text and the abstract as checked against the original data by one of us (LAO).

5. Data Analysis

5.1. Quantum number scaling law

The present level of high precision for the theoretical computations leads to agreement with selected experimental results up to 0.1 percent, also for high quantum numbers. Even at that precision level, semi-empirical laws, such as the scaling ones, remain useful for verifying or predicting data, or confirming the presence of perturbations for specific atomic states.

We have tested the scaling laws of Eq. (10) for A and similar one of B, for the overall S, P, and D states of potassium, rubidium, cesium, and francium using the quantum defect parameters from Lorenzen and Niemax (1983), Li *et al.* (2003), Lorenzen and Niemax (1984), Simsarian *et al.* (1999), and Peper *et al.* (2019). As examples, we report in Fig. 2 the A dipole constant results for both Rb isotopes, in (a) for ^2S states, and in (b), (c) for the ^2D ones. Panel (d) of that figure reports the data for the ^2S and ^2P states of Cs and for the ^2D ones. The $^2Sn = (12–13)$ ^{87}Rb data by Stoicheff and Weinberger (1979) with large error bars are not plotted. Note that the $A(n^*)^3$ values are plotted vs n enhancing the deviations from the scaling law. The validity of the scaling law is tested by the horizontal lines derived from data fits. For the ^2D states in (b) and (c), the ^{85}Rb data have been scaled to the ^{87}Rb ones by supposing the validity of the g_J scaling of Eq. (7), leading to a precise superposition of the two isotope values. Similar results are obtained for all the ^{39}K states and the ^2S states of ^{41}K.

For the ^2S states, the ^{87}Rb theoretical results by Grunefeld *et al.* (2019) reproduce very closely the experimental A values for all quantum numbers, as shown by the black dots in the (a) panel of the figure. The A scaling law was tested theoretically for the ^2S, ^2P, and ^2D Rb states in the log/log plot of

TABLE 8. Measured *A* and *B* values for Fr isotopes with g next to the isotope to indicate the nucleus ground state

State	A (MHz)	B (MHz)	Sample	Technique	References
			^{202g}**Fr**		
$7^2S_{1/2}$	12 800.(50)	···	AB	LIF	Flanagan *et al.* (2013), also in Lynch *et al.* (2014)
			^{203g}**Fr**		
	8 180.(30)	···	AB	RIS	Lynch *et al.* (2014)
$7^2S_{1/2}$	8 187.(2)	···	AB	LIF	Wilkins *et al.* (2017)
	8 187.(2)	···	···	···	w.a.
$8^2P_{3/2}$	29.5(2)	−39.1(20)	···	···	Wilkins *et al.* (2017)
			^{204g}**Fr**		
	12 990.(30)	···	AB	RIS	Lynch *et al.* (2014)
$7^2S_{1/2}$	13 146.7(7)	···	AB	LIF	Voss *et al.* (2015)
	13 146.6(36)	···	···	···	w.a. (w.e.e)
$7^2P_{3/2}$	141.7(3)	−37.1(19)	···	···	Voss *et al.* (2015)
			^{205g}**Fr**		
	8 355.0(11)	···	AB	LIF	Voss *et al.* (2013, 2015)
$7^2S_{1/2}$	8 400.(30)	···	AB	RIS	Lynch *et al.* (2014)
	8 355.0(11)	···	···	···	Recommended
$7^2P_{3/2}$	89.7(4)	−81.0(48)	AB	LIF	Voss *et al.* (2015)
			^{206g}**Fr**		
	13 052.2(18)	···			Voss *et al.* (2015)
$7^2S_{1/2}$	13 057.8(10)	···	AB	RIS	Lynch *et al.* (2016)
	13 056.5(24)	···	···	···	w.a. (w.e.e.)
$7^2P_{1/2}$	1 716.90(16)	···	MOT	FML	Zhang *et al.* (2015)
$7^2P_{3/2}$	139.1(8)	−66.8(50)	AB	LIF	Voss *et al.* (2015)
$8^2P_{3/2}$	47.5(10)	−29.8(10)	AB	LIF	Lynch *et al.* (2016)
			^{207g}**Fr**		
	8 484.(1)	···	AB	HOPF	Coc *et al.* (1985)
$7^2S_{1/2}$	8 480.(30)	···	AB	LIF	Lynch *et al.* (2014)
	8 482.(2)	···	AB	LIF	Wilkins *et al.* (2017)
	8 483.6(9)	···	···	···	w.a.
$7^2P_{1/2}$	1 111.81(11)	···	MOT	FML	Zhang *et al.* (2015)
$7^2P_{3/2}$	90.7(6)	−42.(13)	AB	HOPF	Coc *et al.* (1985)
$8^2P_{3/2}$	30.4(2)	−20.0(16)	AB	LIF	Wilkins *et al.* (2017)
			^{208g}**Fr**		
	6 639.7(70)	···	AB	HOPF	Liberman *et al.* (1980)
$7^2S_{1/2}$	6 650.7(8)	···	AB	HOPF	Coc *et al.* (1985)
	6 653.7(4)	···	AB	LIF	Voss *et al.* (2015)
	6 653.1(10)	···	···	···	w.a.(w.e.e.)
$7^2P_{1/2}$	874.8(3)	···	MOT	FML	Grossman *et al.* (1999)
	72.8(5)	8.9(75)	AB	HOPF	Liberman *et al.* (1980)
$7^2P_{3/2}$	72.4(5)	1.(10)	AB	HOPF	Coc *et al.* (1985)
	71.9(2)	13.6(29)	AB	LIF	Voss *et al.* (2015)
	72.1(2)	6.9(59)	···	···	w.a.

TABLE 8. (*Continued*)

State	A (MHz)	B (MHz)	Sample	Technique	References
			^{209g}**Fr**		
	8 590.5(105)	⋯	AB	HOPF	Liberman *et al.* (1980)
$7^2S_{1/2}$	8 606.7(9)	⋯	AB	HOPF	Coc *et al.* (1985)
	8 606.6(9)	⋯	⋯	⋯	w.a.
	1 127.9(2)	⋯	MOT	FML	Grossman *et al.* (1999)
$7^2P_{1/2}$	1 127.67(11)	⋯	MOT	FML	Zhang *et al.* (2015)
	1 127.72(10)	⋯	⋯	⋯	w.a.
	93.1(6)	−61.0(58)	AB	HOPF	Liberman *et al.* (1980)
$7^2P_{3/2}$	93.3(5)	−62.(5)	AB	HOPF	Coc *et al.* (1985)
	93.2(4))	−62.(4)	⋯	⋯	w.a.
$7^2D_{5/2}$	−21.(1)	−81.(22)	MOT	LIF	Agustsson *et al.* (2017)
			^{210g}**Fr**		
	7 182.4(81)	⋯	AB	HOPF	Liberman *et al.* (1980)
$7^2S_{1/2}$	7 195.1(4)	⋯	AB	HOPF	Coc *et al.* (1985)
	7 195.1(6)	⋯	⋯	⋯	w.a.
	945.6(58)	⋯	AB	HOPF	Coc *et al.* (1987)
$7^2P_{1/2}$	946.3(2)	⋯	MOT	FML	Grossman *et al.* (1999)
	946.3(2)	⋯	⋯	⋯	w.a.
	77.9(2)	47.6(22)	AB	HOPF	Liberman *et al.* (1980)
$7^2P_{3/2}$	78.0(2)	51.(4)	AB	HOPF	Coc *et al.* (1985)
	77.95(14)	48.4(19)	⋯	⋯	w.a.
$7^2D_{3/2}$	22.3(5)	0	MOT	OODR	Grossman *et al.* (2000)
$7^2D_{5/2}$	−17.8(8)	64.(17)			
$8^2S_{1/2}$	1 577.8(11)	⋯	MOT	TCSDS	Simsarian *et al.* (1999)
$9^2S_{1/2}$	622.25(36)	⋯	MOT	TCSDS	Gomez *et al.* (2008)
			^{211g}**Fr**		
	8 698.2(105)	⋯	AB	HOPF	Liberman *et al.* (1980)
$7^2S_{1/2}$	8 713.9(8)	⋯	AB	HOPF	Coc *et al.* (1985)
	8 700.(60)	⋯	AB	RIS	Lynch *et al.* (2014)
	8 713.8(8)	⋯	⋯	⋯	w.a.
$7^2P_{1/2}$	1 142.1(2)	⋯	MOT	FML	Grossman *et al.* (1999)
	94.7(2)	−55.3(34)	AB	HOPF	Liberman *et al.* (1980)
$7^2P_{3/2}$	94.9(3)	−51.(7)	AB	HOPF	Coc *et al.* (1985)
	94.8(2)	−54.5(31)	⋯	⋯	w.a.
			^{212g}Fr		
	9 051.3(95)	⋯	AB	HOPF	Liberman *et al.* (1980)
$7^2S_{1/2}$	9 064.2(2)	⋯	AB	HOPF	Coc *et al.* (1985)
	9 064.4(15)	⋯	AB	LIF	Duong *et al.* (1987)
	9 064.2(2)	⋯	⋯	⋯	w.a.
	1 189.1(46)	⋯	AB	HOPF	Coc *et al.* (1987)
$7^2P_{1/2}$	1 187.1(68)	⋯	AB	LIF	Duong *et al.* (1987)
	1 192.0(2)	⋯	MOT	FML	Grossman *et al.* (1999)
	1 192.0(2)	⋯	⋯	⋯	w.a.
	99.1(9)	−35.3(155)	AB	HOPF	Liberman *et al.* (1980)
$7^2P_{3/2}$	97.2(1)	−26.(2)	AB	LIF	Coc *et al.* (1985)
	97.2(1)	−26.0(2)	AB	LIF	Duong *et al.* (1987)
	97.21(10)	−26.0(2)	⋯	⋯	w.a. (w.e.e); w.a.

TABLE 8. (*Continued*)

State	A (MHz)	B (MHz)	Sample	Technique	References
$8^2P_{1/2}$	373.0(1)	⋯	AB	LIF	Duong *et al.* (1987)
$8^2P_{3/2}$	32.8(1)	−7.7(9)	AB		
$8^2D_{3/2}$	13.0(6)	0	AB	LIF	Arnold *et al.* (1990)
$8^2D_{5/2}$	−7.2(6)	0	AB		
$9^2D_{3/2}$	7.1(7)	0	AB		
$9^2D_{5/2}$	−3.6(4)	0	AB		
$10^2S_{1/2}$	401.(5)	⋯	AB		
$11^2S_{1/2}$	225.(3)	⋯	AB		
			^{213g}Fr		
$7^2S_{1/2}$	8 744.9(105)	⋯	AB	HOPF	Liberman *et al.* (1980)
	8 759.9(6)	⋯	AB	HOPF	Coc *et al.* (1985)
	8 757.4(19)	⋯	AB	LIF	Duong *et al.* (1987)
	8 759.6(6)	⋯	⋯	⋯	w.a.
$7^2P_{1/2}$	1 150.5(75)	⋯	AB	HOPF	Coc *et al.* (1987)
	1 147.89(11)	⋯	MOT	FML	Zhang *et al.* (2015)
	1 147.89(11)	⋯	⋯	⋯	Recommended
$7^2P_{3/2}$	94.5(16)	−20.7(170)	AB	HOPF	Liberman *et al.* (1980)
	95.3(3)	−36.(5)	AB	HOPF	Coc *et al.* (1985)
	95.3(3)	−36.0(5)	AB	LIF	Duong *et al.* (1987)
	95.3(2)	−36.0(5)	⋯	⋯	w.a.
$8^2P_{3/2}$	31.6(1)	−7.0(25)	AB	LIF	Duong *et al.* (1987)
			^{214g}Fr		
$7^2S_{1/2}$	2 370.(150)	⋯	AB	RIS	Farooq-Smith *et al.* (2016a; 2016b)
			^{219g}Fr		
$7^2S_{1/2}$	6 820.(30)	⋯	AB	RIS	Budinčević *et al.* (2014)
	6 851.(1)	⋯	AB	RIS	de Groote *et al.* (2015)
	6 851.(1)	⋯	⋯	⋯	Recommended
$8^2P_{3/2}$	24.7(5)	−104.(1)	⋯	⋯	de Groote *et al.* (2015)
			^{220g}Fr		
$7^2S_{1/2}$	−6 549.4(9)	⋯	AB	HOPF	Coc *et al.* (1985)
	−6 549.2(12)	⋯	AB	LIF	Duong *et al.* (1987)
	−6 500.(40)	⋯	AB	RIS	Lynch *et al.* (2014)
	−6 549.3(7)	⋯	⋯	⋯	w.a.
$7^2P_{3/2}$	−73.2(5)	126.8(5)	AB	HOPF	Coc *et al.* (1985)
	−68.5(62)	123.(9)	AB	HOPF	Coc *et al.* (1987)
	−73.2(5)	125.9(44)	⋯	⋯	w.a.
$8^2P_{3/2}$	−23.3(1)	41.4(14)	AB	LIF	Duong *et al.* (1987)
			^{221g}Fr		
$7^2S_{1/2}$	6 204.6(8)	⋯	AB	HOPF	Coc *et al.* (1985)
	6 100.(200)	⋯	AB	HOPF	Andreev *et al.* (1986)
	6 205.6(17)	⋯	AB	HOPF	Coc *et al.* (1987)
	6 209.9(10)	⋯	AB	LIF	Duong *et al.* (1987)
	6 200.(30)	⋯	AB	RIS	Lynch *et al.* (2014)
	6 209.(1)	⋯	AB	RIS	de Groote *et al.* (2015)
	6 207.2(11)	⋯	⋯	⋯	w.a. (w.e.e.)

TABLE 8. (*Continued*)

State	A (MHz)	B (MHz)	Sample	Technique	References
$7^2P_{1/2}$	808.(12)	···	AB	HOPF	Coc *et al.* (1987)
	811.0(13)	···	MOT	LIF	Lu *et al.* (1997)
	810.3(18)	···	MOT	FML	Zhang *et al.* (2015)
	810.7(10)	···	···	···	w.a.
$7^2P_{3/2}$	65.5(6)	−264.(3)	AB	HOPF	Coc *et al.* (1985)
	65.4(29)	−259.(16)	AB	HOPF	Coc *et al.* (1987)
	66.5(9)	−260.(48)	MOT	LIF	Lu *et al.* (1997)
	65.8(49)	−264.(3)	···	···	w.a.
$8^2P_{3/2}$	22.4(1)	−85.7(8)	AB	LIF	Duong *et al.* (1987)
	22.3(5)	−87.(2)	AB	RIS	de Groote *et al.* (2015)
	22.40(10)	−86.9(3)	···	···	w.a.; w.a. (w.e.e.)
			^{222g}Fr		
$7^2S_{1/2}$	3 070.(3)	···	AB	HOPF	Coc *et al.* (1985)
$7^2P_{3/2}$	33.(1)	133.(9)			
			^{223g}Fr		
$7^2S_{1/2}$	7 654.(2)	···	AB	HOPF	Coc *et al.* (1985)
$7^2P_{3/2}$	83.3(9)	308.(3)			
			^{224g}Fr		
$7^2S_{1/2}$	3 876.(1)	···	AB	HOPF	Coc *et al.* (1985)
$7^2P_{3/2}$	42.1(7)	136.(1)			
			^{225g}Fr		
$7^2S_{1/2}$	6 980.(1)	···	AB	HOPF	Coc *et al.* (1985)
	6 980.1(75)	···	AB	HOPF	Coc *et al.* (1987)
	6 980.(1)	···	···	···	Recommended
$7^2P_{3/2}$	77.1(5)	347.(2)	AB	HOPF	Coc *et al.* (1985)
	77.2(30)	346.(13)	AB	HOPF	Coc *et al.* (1987)
	77.1(5)	347.(2)	···	···	w.a.
			^{226g}Fr		
$7^2S_{1/2}$	699.4	···	AB	HOPF	Coc *et al.* (1985)
	698.107 1(20)	···			Duong *et al.* (1986)
	698.107(2)	···	···	···	w.a.
$7^2P_{3/2}$	7.(1)	−356.(4)	···	···	Coc *et al.* (1985)
			^{227g}Fr		
$7^2S_{1/2}$	29 458.(4)	···	···	···	Coc *et al.* (1985)
$7^2P_{3/2}$	316.(2)	0	···	···	
			^{228g}Fr		
$7^2S_{1/2}$	−3 731.(4)	···	···	···	Coc *et al.* (1985)
$7^2P_{3/2}$	−41.(2)	627.(12)	···	···	
			^{229g}Fr		
$7^2S_{1/2}$	30 080.(110)	···	AB	RIS	Budinčević *et al.* (2014)
			^{231g}Fr		
$7^2S_{1/2}$	30 770.(130)	···	···	···	···

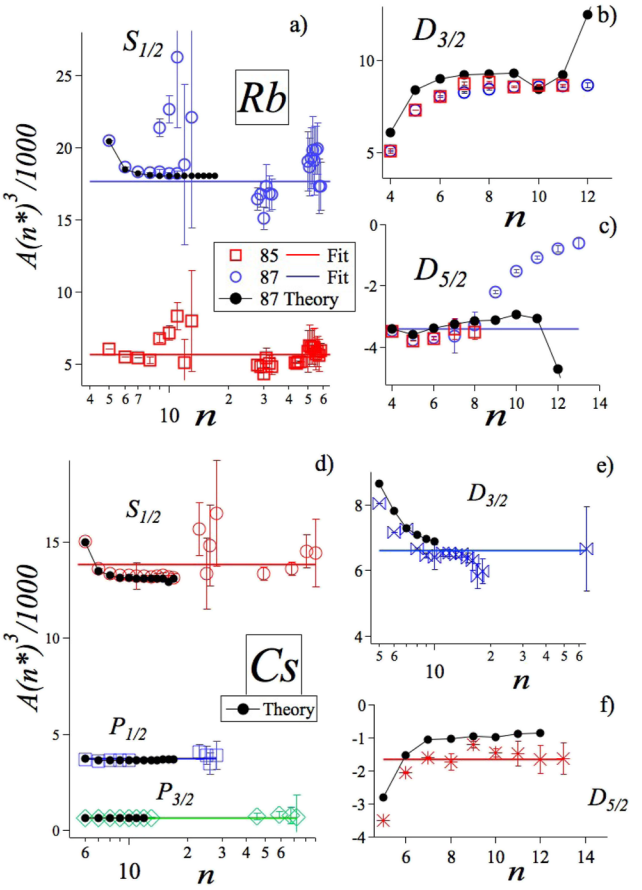

FIG. 2. $A(n^*)^3$ scaling test, with A in MHz, vs n number. Experimental result with their error bars are shown in colors, while black dots represent the theoretical predictions. Experimental and theoretical data: (a) data for Rb $^2S_{1/2}$ states, and (b) and (c) for $^2D_{3/2,5/2}$ ones, with red open squares for ^{85}Rb and blue circles for ^{87}Rb; (d) data for Cs $^2S_{1/2}$ and $^2P_{1/2,3/2}$, (e) and (f) for Cs $^2D_{3/2}$ and $^2D_{5/2}$, respectively. Panel (f) plot does not include the $n = 66$ value of Table 7 owing to its very large error bar. ^{85}Rb ^{2}D states data are scaled to the ^{87}Rb ones by assuming the validity of the isotope g_I scaling of Eq. (10). Note the logarithmic horizontal scale in (a), (d), and (e). The continuous horizontal lines represent fits based on the $1/(n^*)^3$ scaling. Theoretical predictions are for ^{87}Rb $^2S_{1/2}$ by Grunefeld *et al.* (2019) and $^2D_{3/2,5/2}$ by Safronova and Safronova (2011); for Cs $^2S_{1/2}$ and $^2P_{1/2}$ states by Grunefeld *et al.* (2019), $^2P_{3/2}$ and $^2D_{3/2,5/2}$ by Tang *et al.* (2019); for the Cs $^2D_{5/2}$ states, the data by Auzinsh *et al.* (2007) appear superimposed.

Safronova and Safronova (2011). In panels (b) and (c) of Fig. 2, the black dots depict those theoretical predictions for the $^2D_{3/2}$ states. For the values up to $n \approx 9$, the differences between theoretical and experimental results are small. For higher n values, the differences are significant because of the limitation in the computer codes at that time. A good agreement with experimental data exists for the Grunefeld *et al.* (2019) predictions of the Cs $^2S_{1/2}$ and $^2P_{1/2}$ states, as shown in (d). For Cs, there are additional theoretical results for the $^2P_{3/2}$ states by Tang *et al.* (2019) for $^2D_{3/2}$ by Auzinsh *et al.* (2007) and for $^2D_{5/2}$ by Tang *et al.* (2019). For the ^2D states, the data by Auzinsh *et al.* (2007) cannot be distinguished on the figure scale. In addition, they cover a short range of n values.

In most cases, the A scaling law is verified in both experimental and theoretical data, and its validity is used to assign the sign of the A values reported in the tables of the previous section. For the Cs $^2P_{1/2,3/2}$ and $^2D_{3/2,5/2}$ states in a large range of n values, the horizontal fits are good. The scaling validity applies to the high-n states, as for the $(n = 40, 90)$ $^2S_{1/2}$ and $^2P_{3/2}$ data of Saßmannshausen *et al.* (2013) as seen in panel (d). For the ^{87}Rb and Cs ^2S states, the scaling does not apply precisely to low-n values because of additional contributions to A in Eq. (5). In contrast, the ^{85}Rb values satisfy the $1/(n^*)^3$ scaling. The low-n difference between the two isotopes produces the deviation from the g_I scaling, linked to the hyperfine anomalies discussed in the following subsection. For the low-n ^2D states, large deviations from the scaling lead to lower A values in Rb and higher A ones in Cs for both experimental and theoretical data. These deviations are equivalent for the two Rb isotopes. They originate from the pair-correlation and core-polarization, as explained in Auzinsh *et al.* (2007) and Tang *et al.* (2019).

We have verified the validity of the $1/(n^*)^3$ scaling law also for the B constants. Figure 3 reports the $B(n^*)^3$ constants of both Rb isotopes for the $^2P_{3/2}$ and $^2D_{3/2}$ states. The continuous horizontal lines indicate that the scaling law is valid for the ^{87}Rb B constants of both states. For the ^{85}Rb isotope, deviations appear in Fig. 3(b) for the $^2D_{3/2}$ states at intermediate n values. The B theoretical predictions by Safronova and Safronova (2011) denoted by black dots indicate a good agreement between the theory and experiments. The B scaling applies also to the Cs $^2P_{3/2}$ states. For the Rb $^2D_{5/2}$ and Cs ^2D states, a definitive conclusion cannot be reached owing to the limited number of data. For the $^2P_{3/2}$ states, the ^{85}Rb B data are precisely scaled to the ^{87}Rb ones by assuming the validity of the quadrupole moment dependence of Eq. (8), with the Q values

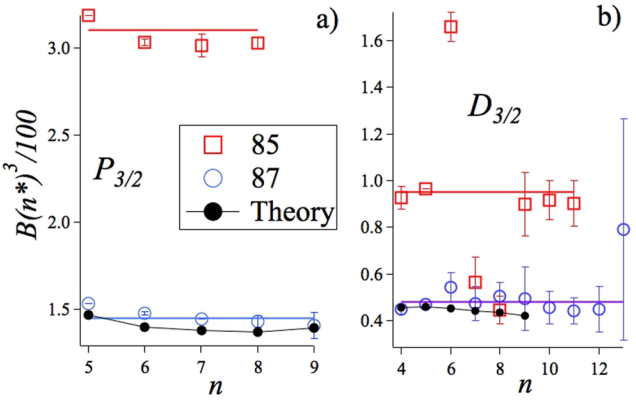

FIG. 3. $B(n^*)^3$ scaling, with B in MHz, for Rb isotopes versus n, with open blue circles for the ^{87}Rb data, and open red squares for the ^{85}Rb data, with error bars for the experiments. (a) $^2P_{3/2}$ data; (b) $^2D_{3/2}$ data. The continuous horizontal lines represent fits based on the $(n^*)^{-3}$ scaling law. For the ^{85}Rb $^2D_{3/2}$ data, the fit does not include the $n = 6, 7$ states. The black dots joined by a line represent the theoretical predictions by Safronova and Safronova (2011) for ^{87}Rb.

of Raghavan (1989). This Q proportionality applies also to the $^2D_{3/2}$ data, where the n^* scaling is valid.

Since the data for each Fr isotope are very limited in number, the application of the quantum number scaling law is not very efficient. Nevertheless, its validity test is useful to verify the present level of knowledge. The law is also useful for the experimental determination of the hyperfine constants in states not yet explored. While the francium effective quantum numbers may be derived from the quantum defects of Arnold *et al.* (1990), Simsarian *et al.* (1999), and Huang and Sun (2010), we rely on those of Simsarian *et al.* (1999) based on the full spectrum of the francium absorption lines compiled by Sansonetti (2007). The francium table evidences that hyperfine sequences are available only for the ^2S states of the 210 and 212 isotopes, each sequence limited to three entries. Figure 4 presents those experimental results in a $A(n^*)^3$ plot. The dipole constant for the 211 isotope 7^2S state is also plotted. The dots joined by continuous lines represent the theoretical data for ^{210}Fr by Sahoo *et al.* (2015), ^{211}Fr by Grunefeld *et al.* (2019), and ^{212}Fr by Lou *et al.* (2019). On the figure scale, equivalent results are obtained using the quantum defect numbers of all the above references. For the experimental and theoretical data on the ^{210,212}Fr isotopes, the deviations from the scaling law for the lowest $n = 7$ number are similar to those presented for the Rb and Cs low-n^2S and ^2D states in Fig. 2. Such deviation from the scaling law does not appear in the ^{211}Fr theoretical data by Grunefeld *et al.* (2019), while their prediction for the ^2S Cs and Rb states match very closely the experimental data as shown in Fig. 2. An acquisition of more experimental data is required in order to progress with this exploration. The program highlighted by Grunefeld *et al.* (2019) and Roberts and Ginges (2020) focuses on the importance of having more hyperfine splitting information for higher excited levels to better understand not only the Fr atom but also the properties of the different nuclear isotopes.

5.2. Anomalies

The hyperfine anomalies, first introduced by Bohr and Weisskopf (1950), are defined as the A deviations from Eq. (7) produced by the finite size of the nucleus. As a measure of the finite structure

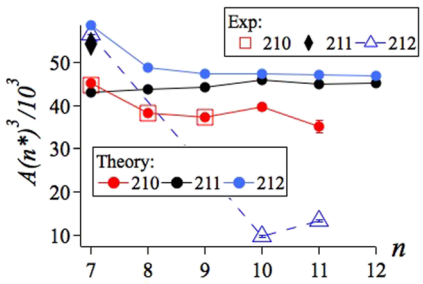

FIG. 4. $A(n^*)^3$ scaling, with A in MHz, vs n for the 210, 211, and 212 Fr isotopes. Experimental data: red open squares for ^{210}Fr, black diamond for the ^{211}Fr single value, and blue open triangles for ^{212}Fr, joined by a dashed line. Theoretical predictions with colored dots joined by a continuous line for ^{210}Fr by Sahoo *et al.* (2015), ^{211}Fr by Grunefeld *et al.* (2019), and ^{212}Fr by Lou *et al.* (2019). Error bars for experiment and theory are too small to be visible. The effective quantum numbers are derived from the quantum defects of Simsarian *et al.* (1999). The ^{211}Fr theoretical data follow closely a horizontal line of the $1/(n^*)^3$ scaling law.

influence on the dipole constants of isotopes 1 and 2, following Persson (2013) the expression for the $^1\Delta^2$ hyperfine anomaly is

$$^1\Delta^2 = \frac{A^1}{A^2}\frac{g_I^2}{g_I^1} - 1, \tag{11}$$

where (A^i, g_I^i) are the hyperfine magnetic dipole constant and the nuclear gyromagnetic ratio, respectively, of the $i = (1,2)$ isotopes. For a point-like nucleus, the hyperfine anomaly is null. The article of Persson (2013) represents the most recent review of the atomic anomalies. Those of the $6^2S_{1/2}$ Fr states are examined in Zhang *et al.* (2015). Recent theoretical studies of Fr anomalies can be found in Konovalova *et al.* (2018), Konovalova *et al.* (2020), and Roberts and Ginges (2020).

Anomalies can be derived from measured A constants and accurate values of the nuclear g-ratio. This is the case for light alkali atoms with their precise values in the gas phase determined in the 1960s and 1970s, as discussed in Arimondo *et al.* (1977). Anomalies for those atoms are reported in Table 9, derived from the weighted mean values and variances of the dipole constants reported in the tables of the previous section. Only anomalies with a value significantly different from zero are presented in Table 9. For the $5^2P_{1/2}$ state of the Rb isotopes, where a very large discrepancy between the measured values was noted in Subsection 4, the value is missed because none reasonable anomaly is associated to the different set of data. The Rb values of Table 9 are in good agreement with those derived by Pérez Galván *et al.* (2007), Pérez Galván *et al.* (2008), and Wang *et al.* (2014b) for ^2S and ^2D states. For the Rydberg S states, enormous anomalies are obtained, $\approx -50(5)$ percent, a quite surprising result, because the interaction of a Rydberg electron with the nucleus should be comparable to that of low orbitals. The fairly constant anomaly for all the ^2S states of the Rb isotopes was pointed out by Pérez Galván *et al.* (2007). For Rb ^2P states, the situation is not well defined, with the $5^2P_{1/2}$ value reflecting the discording results associated with this state, and for the $^2P_{3/2}$ states the quadrupole interaction playing an important role. The constant value of the $4^2P_{1/2}$ anomaly applies also to the K isotopes.

The francium case is different because the list of isotope data is quite long, and therefore, interesting information about the nuclear structures could be derived from the anomaly determinations. However, for francium, an important element is missing in Eq. (11) because a direct measurement of the nuclear gyromagnetic ratio is available only for ^{211}Fr in Stone (2005). For the remaining isotopes, the g_I ratios are derived by assuming a zero anomaly [see Raghavan (1989)]. In the recent theoretical studies of Fr anomalies by Konovalova et al. (2018), Roberts and Ginges (2020), and Konovalova *et al.* (2020), the information on the nuclear structure is replaced by derivations of the radial nuclear structure and of the nuclear radius. In order to obtain the anomalies without relying on such theoretical analyses, Grossman *et al.* (1999), following Persson (1998), concentrated their attention to the $7^2S_{1/2}$ and $7^2P_{1/2}$ states. The $^2P_{1/2}$ electron probes the nucleus with a more uniform radial dependence of the interaction than does the $^2S_{1/2}$ electron. They introduced the following $R(S/P)$ ratio of their hyperfine constants:

$$R(S/P) = \frac{A(S_{1/2})}{A(P_{1/2})} \tag{12}$$

TABLE 9. Light alkali hyperfine anomalies $^1\Delta^2$ with states listed in order of increasing L, then of increasing n and finally of increasing J

Element	Isotope 1	Isotope 2	State	$^1\Delta^2$(%)
			$2S_{1/2}$	0.006 806 7(8)
Li	6	7	$2P_{1/2}$	−0.173 4(2)
			$2P_{3/2}$	−0.155(8)
			$4S_{1/2}$	0.467(2)
K	39	40	$4P_{1/2}$	3.90(13)
			$4S_{1/2}$	−0.229 37(13)
K	39	41	$4P_{1/2}$	3.9(3)
			$5S_{1/2}$	0.351 41(2)
			$6S_{1/2}$	0.361(19)
			$7S_{1/2}$	0.342(3)
			$5P_{1/2}$	0.55(8)
			$5P_{3/2}$	0.168(5)
Rb	85	87	$6P_{1/2}$	0.31(7)
			$6P_{3/2}$	0.46(5)
			$4D_{5/2}$	0.60(15)
			$5D_{3/2}$	0.279(6)
			$5D_{5/2}$	0.44(5)

as a probe of the nuclear magnetization distribution. Since both states are spin-1/2, these ratios are independent of quadrupole effects that complicate the extraction of the nuclear structure information. For several francium isotopes, the ratio is presented in Fig. 5. Notice the staggered isotope behavior of $R(S/P)$ vs the even/odd isotope number. Such behavior evidences the different radial distributions of the nuclear magnetization for the even/odd number of neutrons. The ratios of the hyperfine constants of the $7^2S_{1/2}$ and $7^2P_{3/2}$ states, as well as those of the $7^2P_{1/2}$ and $7^2P_{3/2}$ ones, do not exhibit such a clear staggered dependence as the $R(S/P)$ ratio plotted in the figure. We have tested the presence of a $R(S/P)$ staggered dependence also for the Rb isotopes using the 85 and 87 data in Tables 4 and 5, and the 82 isotope ones from Zhao *et al.* (1999). This limited dataset appears to confirm the $R(S/P)$ staggered behavior.

The ratio of the hyperfine constants of the $^2P_{1/2}$ and $^2P_{3/2}$ states has been proposed in Konovalova *et al.* (2020) as an additional test of the nuclear structure, even if the nuclear quadrupole coupling is important for the latter state. This ratio calculated from the francium Table 8 data does not exhibit a clear dependence on the isotope number.

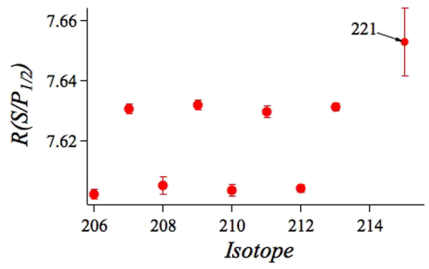

FIG. 5. $R(S/P_{1/2})$ ratio for the $7^2S_{1/2}$ and $7^2P_{1/2}$ states of francium isotopes vs the isotope number. Mean values and error bars are derived from the francium Table 8. Notice the staggered dependence of $R(S/P_{1/2})$ on the even/odd isotope number. The ^{221}Fr isotope value with a large error bar agrees with that dependence.

6. Conclusions

The previously published experimental values for the stable isotopes of the light alkali atoms and for all the nuclear-ground-configuration francium isotopes have been compiled. The tables report the most accurate data obtained before 1977 and all those published after that time. For each measured hyperfine constant, we present a recommended value. A critical examination of the most interesting cases, or of the most discording ones, is presented. For the discording cases we have calculated a w.e.e. following the procedure of the Particle Data Group in Zyla *et al.* (2020). For those cases, a comparison of our data analysis to the cluster maximum likelihood estimator introduced by Rukhin (2009, 2019), is presented in the supplementary material of this review. We encourage future reviewers of larges sets of data to look into these more recent methods that are currently gaining adepts in the community, but are not followed by those in charge of the recent redefinition of the fundamental constants of physics and chemistry Tiesinga *et al.* (2018).

The experimental interest in measuring hyperfine constants is renewed in recent years. Today, the laser sources required to excite energy levels not easily assessed at the optical pumping time are available on the market. Those sources and the associated atomic species can be important for quantum simulation and computational investigations. As in the past, the quest for higher precision spectroscopic measurement could represent an additional step for refining the experimental tools required in those areas.

Instead of concentrating the attention to a specific atomic state, the recent global theoretical analyses cover all the atomic states of a single species, possibly of all the isotopes. For this global approach, precise experimental data are required for a large set of states, stimulating the hyperfine data search in several directions.

Spectroscopic investigations of alkali atoms are also associated with the theoretical progress on the electron–nucleus hyperfine coupling. The hyperfine coupling being an important probe of the nuclear structure, the francium research by Grossman *et al.* (1999) has introduced the ratio of the S and P state hyperfine couplings as a new tool for studying nuclear properties. This has stimulated a large theoretical effort, but it has pointed out the need for more precise experimental data. The application of this ratio to lighter alkalis could be an interesting exploration direction.

The electron–nucleus interaction contains a term characterized by the nuclear magnetic octupole moment. In recent years, three different measures of that moment are reported for ^{133}Cs $6^2P_{3/2}$ by Gerginov *et al.* (2003), ^{87}Rb $5^2P_{3/2}$ in the experimental data of Ye *et al.* (1996) reexamined by Gerginov *et al.* (2009), and more recently for the ^{133}Cs $6^2D_{3/2}$ state by Chen *et al.* (2018). The parity violation search in alkali atoms may also find new life. Up until now, the most accurate data on the atomic parity-non-conserving interaction was derived from the $6^2S_{1/2} \rightarrow 7^2S_{1/2}$ transition in cesium by Wood *et al.* (1997). To obtain a more accurate value of the nuclear weak charge producing the parity-violating Hamiltonian, it would be desirable to consider other candidates. Gwinner and

Orozco (2022) with their collaborators are pursuing its measurement in the $7^2S_{1/2} \rightarrow 8^2S_{1/2}$ transition in a variety of Fr isotopes, while Aoki *et al.* (2017) have proposed to search for that violation operating on the $^7S_{1/2} \rightarrow 6^2D_{3/2}$ electric quadrupole transition in ^{210}Fr. It is expected that advances in the understanding of hyperfine interactions will continue to illuminate atomic parity nonconversion and vice versa.

As a final expectation, in the near future, a few totally new entries will be added to the above tables, counterbalanced by several refined entries.

7. Note added in proof.

The ^{133}Cs $7^2D_{3/2,5/2}$ hyperfine structures were measured using Doppler-free two-photon spectroscopy in a vapor cell in recent publications by Rahaman and Dutta (2022a, 2022b). The following hyperfine values were derived: $A = 7.3509(9)$, $B = -0.041(8)$, and $C = -0.027(530)$ for the $7^2D_{3/2}$ state, and $A = -1.708\,67(62)$, $B = 0.050(14)$, and $C = 0.4(14)$ for the $7^2D_{5/2}$ one. The ^{133}Cs $8^2P_{1/2,3/2}$ hyperfine structures were measured by optical spectroscopy experiment in an atomic beam (Quirk *et al.* 2022b). The following hyperfine values were derived: $A = 42.933(8)$ for the $8^2P_{1/2}$ state, and $A = 7.609(8)$, $B = -0.005(40)$, and $C = 0.016(4)$ for the $8^2P_{3/2}$ one.

Supplementary Material

See the supplementary material for comparison of the weighted averages and weighted enhanced errors using the unconstrained averaging of Zyla *et al.* (2020) and the clustering maximum likelihood estimator method of Rukhin (2009, 2019).

8. Acknowledgments

The authors are grateful to Marianna Safronova for a guide through the recent progress in the theoretical analyses of the hyperfine structures and a careful reading of the manuscript, and to Roberto Calabrese for hints on the francium spectroscopy. The authors are grateful and indebted to the referee for ample comments that have made this a much better review and for providing the algorithm of the CMLE approach. Hassan Jawahery, Peter J. Mohr, and William D. Phillips have helped elucidate the evaluation of the errors to report recommended values. The authors acknowledge Wang-Yau Cheng, Pierre Dubé, Johannes Deiglmayr, Randy J. Knize, Mark Lindsay, Frederic Merkt, Dieter Meschede, Priyanka Rupasinghe, and Sun Svanberg for communicating data of various atomic states. The very kind help of the librarians Armelle Michetti and Odile Richaud in Grenoble, and Massimiliano Bertelli in Pisa is also acknowledged.

9. Author Declarations

9.1. Conflict of Interest

The authors have no conflicts to disclose.

10. Data Availability

Data sharing is not applicable to this article as no new data were created or analyzed in this study.

11. References

Abele, J., "Bestimmung der g_J-Faktoren in den Zuständen $6^2P_{3/2}$ and $8^2P_{3/2}$ von ^{133}Cs," Z. Phys. A: At. Nucl. **274**, 179–184 (1975a).

Abele, J., "Untersuchung der hyperfeinstruktur des $6^2P_{1/2}$-zustandes von^{133}Cs im starken magnetfeld mit der optischen doppelresonanzmethode," Z. Phys. A: At. Nucl. **274**, 185–190 (1975b).

Agustsson, S., Bianchi, G., Calabrese, R., Corradi, L., Dainelli, A., Khanbekyan, A., Marinelli, C., Mariotti, E., Marmugi, L., Mazzocca, G., Moi, L., Ricci, L., Stiaccini, L., and Tomassetti, L., "Observation of $7p^2P_{3/2} \rightarrow 7d^2D$ optical transitions in 209 and 210 francium isotopes," Opt. Lett. **42**, 3682–3685 (2017).

Andreev, S. V., Letokhov, V. S., and Mishin, V. I., "Laser resonant photoionization detection of traces of the radioactive isotope ^{221}Fr in a sample," Sov. Phys. JETP Lett. **43**, 736–740 (1986), http://jetpletters.ru/ps/1413/article_21506.pdf.

Andreev, S. V., Letokhov, V. S., and Mishin, V. I., "Laser resonance photoionization spectroscopy of Rydberg levels in Fr," Phys. Rev. Lett. **59**, 1274–1276 (1987).

Antoni-Micollier, L., Barrett, B., Chichet, L., Condon, G., Battelier, B., Landragin, A., and Bouyer, P., "Generation of high-purity low-temperature samples of ^{39}K for applications in metrology," Phys. Rev. A **96**, 023608 (2017).

Aoki, T., Torii, Y., Sahoo, B., Das, B., Harada, K., Hayamizu, T., Sakamoto, K., Kawamura, H., Inoue, T., Uchiyama, A., Ito, S., Yoshioka, R., Tanaka, K., Itoh, M., Hatakeyama, A., and Sakemi, Y., "Parity-nonconserving interaction-induced light shifts in the $7S_{1/2}$–$6D_{3/2}$ transition of the ultracold ^{210}Fr atoms to probe new physics beyond the standard model," Appl. Phys. B: Lasers Opt. **123**, 120 (2017).

Arias, A., Lochead, G., Wintermantel, T. M., Helmrich, S., and Whitlock, S., "Realization of a Rydberg-dressed Ramsey interferometer and electrometer," Phys. Rev. Lett. **122**, 053601 (2019).

Arimondo, E., Inguscio, M., and Violino, P., "Experimental determinations of the hyperfine structure in the alkali atoms," Rev. Mod. Phys. **49**, 31–75 (1977).

Armstrong, J. L., *Theory of the Hyperfine Structure of Free Atoms*, 1st ed. (Wiley-Interscienc, New York, 1971).

Arnold, E., Borchers, W., Duong, H. T., Juncar, P., Lerme, J., Lievens, P., Neu, W., Neugart, R., Pellarin, M., Pinard, J., Vialle, J. L., Wendt, K., and ISOLDE Collaboration, "Optical laser spectroscopy and hyperfine structure investigation of the 10^2S, 11^2S, 8^2D, and 9^2D excited levels in francium," J. Phys. B: At., Mol. Opt. Phys. **23**, 3511–3520 (1990).

Arqueros, F., "Doppler-free two-photon spectroscopy of the 4S state of Na," Opt. Commun. **67**, 341–342 (1988).

Auzinsh, M., Bluss, K., Ferber, R., Gahbauer, F., Jarmola, A., Safronova, M. S., Safronova, U. I., and Tamanis, M., "Level-crossing spectroscopy of the 7, 9, and $10D_{5/2}$ states of ^{133}Cs and validation of relativistic many-body calculations of the polarizabilities and hyperfine constants," Phys. Rev. A **75**, 022502 (2007).

Banerjee, A., Das, D., and Natarajan, V., "Precise frequency measurements of atomic transitions by use of a Rb-stabilized resonator," Opt. Lett. **28**, 1579–1581 (2003).

Banerjee, A., Das, D., and Natarajan, V., "Absolute frequency measurements of the D_1 lines in ^{39}K, ^{85}Rb, and ^{87}Rb with ~0.1 ppb uncertainty," Europhys. Lett. **65**, 172–178 (2004).

Barakhshan, P., Marrs, A., Bhosale, A., Arora, B., Eigenmann, R., and Safronova, M. S., "Portal for high-precision atomic data and computation (version 2.0)" (University of Delaware, Newark, DE, 2022), https://www1.udel.edu/atom/.

Barbey, P. and Geneux, E., "Structure hyperfine de l'état $8^2P_{3/2}$ du césium 133," Helv. Phys. Acta **35**, 561–562 (1962).

Barmes, I., Witte, S., and Eikema, KS, "High-precision spectroscopy with counterpropagating femtosecond pulses," Phys. Rev. Lett. **111**, 023007 (2013).

Barwood, G. P., Gill, P., and Rowley, W. R. C., "Frequency measurements on optically narrowed Rb-stabilised laser diodes at 780 nm and 795 nm," Appl. Phys. B: Photophys. Laser Chem. **53**, 142–147 (1991).

Bayram, S. B., Arndt, P., Popov, O. I., Güney, C., Boyle, W. P., Havey, M. D., and McFarland, J., "Quantum beat spectroscopy: Stimulated emission probe of hyperfine quantum beats in the atomic Cs $8p^2P_{3/2}$ level," Phys. Rev. A **90**, 062510 (2014).

Beacham, J. R. and Andrew, K. L., "Optical study of the hyperfine structure of the rubidium resonance lines," J. Opt. Soc. Am. **61**, 231–235 (1971).

Beckmann, A., Böklen, K. D., and Elke, D., "Precision measurements of the nuclear magnetic dipole moments of ^{6}Li, ^{7}Li, ^{23}Na, ^{39}K and ^{41}K," Z. Phys. A: At. Nucl. **270**, 173–186 (1974).

Behrle, A., Koschorreck, M., and Köhl, M., "Isotope shift and hyperfine splitting of the 4s → 5p transition in potassium," Phys. Rev. A **83**, 052507 (2011).

Belin, G., Holmgren, L., Lindgren, I., and Svanberg, S., "Hyperfine interaction in excited alkali atoms," in *Summary of Contributions. Seventh Annual Conference* (Laboratoire de Spectrometrie Physique, Université Grenoble, Grenoble, 1975) p. 13.

Belin, G., Holmgren, L., Lindgren, I., and Svanberg, S., "Hyperfine interaction, Zeeman and Stark effects for excited states in potassium," Phys. Scr. **12**, 287–294 (1975b).

Belin, G., Holmgren, L., and Svanberg, S., "Hyperfine interaction, Zeeman and Stark effects for excited states in cesium," Phys. Scr. **14**, 39–47 (1976a).

Belin, G., Holmgren, L., and Svanberg, S., "Hyperfine interaction, Zeeman and Stark effects for excited states in rubidium," Phys. Scr. **13**, 351–362 (1976b).

Belin, G. and Svanberg, S., "Laser spectroscopy investigation of the hyperfine structure of highly excited $^{2}P_{3/2}$ states in alkali atoms," Phys. Lett. A **47**, 5–6 (1974).

Bellini, M., Bartoli, A., and Hänsch, T. W., "Two-photon Fourier spectroscopy with femtosecond light pulses," Opt. Lett. **22**, 540–542 (1997).

Beloy, K. and Derevianko, A., "Second-order effects on the hyperfine structure of P states of alkali-metal atoms," Phys. Rev. A **78**, 032519 (2008).

Bendali, N., Duong, H. T., and Vialle, J. L., "High-resolution laser spectroscopy on the D_1 and D_2 lines of ^{39,40,41}K using RF modulated laser light," J. Phys. B: At. Mol. Phys. **14**, 4231–4240 (1981).

Bhattacharya, M., Haimberger, C., and Bigelow, N. P., "Forbidden transitions in a magneto-optical trap," Phys. Rev. Lett. **91**, 213004 (2003).

Biraben, F. and Beroff, K., "Hyperfine interaction in the $4D_{3/2}$ and the $4D_{5/2}$ levels of sodium," Phys. Lett. A **65**, 209–212 (1978).

Bohr, A. and Weisskopf, V. F., "The influence of nuclear structure on the hyperfine structure of heavy elements," Phys. Rev. **77**, 94–98 (1950).

Bouchiat, C. and Piketty, C. A., "Nuclear spin dependent parity violating electron-nucleus interaction in heavy atoms. the anapole moment and the perturbation of the hadronic vector neutral current by the hyperfine interaction," Phys. Lett. B **269**, 195–200 (1991).

Bouchiat, M.-A., and Guéna, J., "The E2 6S-7S amplitude in cesium and its importance in a precise calibration of Epv1," J. Phys. **49**, 2037–2044 (1988).

Brandenberger, J. R. and Lindley, R. E., "Hyperfine structure in the 6 $^{2}D_{3/2}$ and 6 $^{2}D_{5/2}$ states of ^{87}Rb and ^{85}Rb," Phys. Rev. A **91**, 062505 (2015).

Brog, K. C., Eck, T. G., and Wieder, H., "Fine and hyperfine structure of the 2 ^{2}P term of Li^{6} and Li^{7}," Phys. Rev. **153**, 91–103 (1967).

Brown, R. C., Wu, S.-J., Porto, J. V., Sansonetti, C. J., Simien, C. E., Brewer, S. M., Tan, J. N., and Gillaspy, J. D., "Quantum interference and light polarization effects in unresolvable atomic lines: Application to a precise measurement of the ^{6,7}Li D_2 lines," Phys. Rev. A **87**, 032504 (2013).

Buck, P. and Rabi, I. I., "Hyperfine structure of K^{39} in the 4P state," Phys. Rev. **107**, 1291–1294 (1957).

Bucka, H., Kopfermann, H., and Minor, A., "Präzisionsmessung der hyperfeinstruktur des $6^{2}P_{3/2}$ terms des Rb I-spektrums," Z. Phys. **161**, 123–131 (1961).

Bucka, H. and von Oppen, G., "Hyperfeinstruktur und lebensdauer des $8^{2}P_{3/2}$-terms im Cs I-spektrum," Ann. Phys. **465**, 119–120 (1962).

Budick, B., Bucka, H., Goshen, R. J., Landman, A., and Novick, R., "Fine and hyperfine structure of the 3^{2}P term in lithium," Phys. Rev. **147**, 1–5 (1966).

Budinčević, I., Billowes, J., Bissell, M. L., Cocolios, T. E., de Groote, R. P., De Schepper, S., Fedosseev, V. N., Flanagan, K. T., Franchoo, S., Garcia Ruiz, R. F., Heylen, H., Lynch, K. M., Marsh, B. A., Neyens, G., Procter, T. J., Rossel, R. E., Rothe, S., Strashnov, I., Stroke, H. H., and Wendt, K. D. A., "Laser spectroscopy of francium isotopes at the borders of the region of reflection asymmetry," Phys. Rev. C **90**, 014317 (2014).

Budker, D., Kimball, D., and DeMille, D., *Atomic Physics* (Oxford University Press, Oxford, 2008).

Burghardt, B., Dubke, M., Jitschin, W., and Meisel, G., "Sub-natural linewidth laser spectroscopy of Doppler-free two-photon resonances," Phys. Lett. A **69**, 93–96 (1978).

Burghardt, B., Hoffmann, B., and Meisel, G., "The 3*d* states of ^{23}Na and ^{7}Li: Determination of unresolved hyperfine splittings and radiative lifetimes," Z. Phys. D: At., Mol. Clusters **8**, 109–118 (1988).

Bushaw, B. A., Nörtershäuser, W., Ewald, G., Dax, A., and Drake, G. W. F., "Hyperfine splitting, isotope shift, and level energy of the 3S states of ^{6,7}Li," Phys. Rev. Lett. **91**, 043004 (2003).

Campani, E., Degan, G., Gorini, G., and Polacco, E., "Measurement of the 8S hyperfine splitting in cesium," Opt. Commun. **24**, 203–206 (1978).

Carlsson, J., Jönsson, P., Sturesson, L., and Fischer, C. F., "Multi-configuration Hartree-Fock calculations and time-resolved laser spectroscopy studies of hyperfine structure constants in sodium," Phys. Scr. **46**, 394–398 (1992).

Carlsson, J. and Sturesson, L., "Accurate time-resolved laser spectroscopy on lithium atoms," Z. Phys. D: At., Mol. Clusters **14**, 281–287 (1989).

Cataliotti, F. S., Fort, C., Pavone, F. S., and Inguscio, M., "Doppler-free excitation of the weak $6S_{1/2}$–$8P_{1/2}$ cesium transition at 389 nm," Z. Phys. D: At., Mol. Clusters **38**, 31–33 (1996).

CCTF, Consultative Committee for Time and Frequency, Recommendation CCTF 1, in *Report of the 19th Meeting (13–14 September 2012) to the International Committee for Weights and Measures* (BIPM, Sèvres, 2012), p. 59.

Chang, H., Myneni, K., Smith, D. D., and Liaghati-Mobarhan, H. R., "High-precision, accurate optical frequency reference using a Fabry–Perot diode laser," Rev. Sci. Instrum. **88**, 063101 (2017).

Chen, T.-J., Chen, J.-E., Yu, H.-H., Liu, T.-W., Hsiao, Y.-F., Chen, Y.-C., Chang, M.-S., and Cheng, W.-Y., "Absolute frequency of cesium $6S_{1/2}$–$6D_{3/2}$ hyperfine transition with a precision to nuclear magnetic octupole interaction," Opt. Lett. **43**, 1954–1957 (2018).

Cheng, W.-Y., Chen, T.-J., Lin, C.-W., Chen, B.-W., Yang, Y.-P., and Hsu, H. Y., "Robust sub-millihertz-level offset locking for transferring optical frequency accuracy and for atomic two-photon spectroscopy," Opt. Express **25**, 2752–2762 (2017).

Chui, H.-C., Ko, M.-S., Liu, Y.-W., Shy, J.-T., Peng, J.-L., and Ahn, H., "Absolute frequency measurement of rubidium 5S–7S two-photon transitions with a femtosecond laser comb," Opt. Lett. **30**, 842–844 (2005).

Coc, A., Thibault, C., Touchard, F., Duong, H. T., Juncar, P., Liberman, S., Pinard, J., Carre, M., Lerme, J., Vialle, J. L., Büttgenbach, S., Mueller, A. C., Pesnelle, A., and ISOLDE Collaboration, "Isotope shifts, spins and hyperfine structures of ^{118,146}Cs and of some francium isotopes," Nucl. Phys. A **468**, 1–10 (1987).

Coc, A., Thibault, C., Touchard, F., Duong, H. T., Juncar, P., Liberman, S., Pinard, J., Lermé, J., Vialle, J. L., Büttgenbach, S., Mueller, A. C., Pesnelle, A., and ISOLDE Collaboration, "Hyperfine structures and isotope shifts of $^{207-213,220-228}$Fr; possible evidence of octupolar deformation," Phys. Lett. B **163**, 66–70 (1985).

Das, D., Banerjee, A., Barthwal, S., and Natarajan, V., "A rubidium-stabilized ring-cavity resonator for optical frequency metrology: Precise measurement of the D_1 line in ^{133}Cs," Eur. Phys. J. D **38**, 545–552 (2006a).

Das, D., Pandey, K., Wasan, A., and Natarajan, V., "Resolving closely spaced hyperfine levels in the $3P_{3/2}$ state of ^{23}Na," J. Phys. B: At., Mol. Opt. Phys. **39**, 3111–3119 (2006b).

Das, D. and Natarajan, V., "Hyperfine spectroscopy on the $6P_{3/2}$ state of ^{133}Cs using coherent control," Europhys. Lett. **72**, 740–746 (2005).

Das, D. and Natarajan, V., "Precise measurement of hyperfine structure in the $5^{2}P_{1/2}$ state of Rb," Eur. Phys. J. D **37**, 313–317 (2006a).

Das, D. and Natarajan, V., "Precise measurement of hyperfine structure in the $6P_{1/2}$ state of ^{133}Cs," J. Phys. B: At., Mol. Opt. Phys. **39**, 2013–2019 (2006b).

Das, D. and Natarajan, V., "High-precision measurement of hyperfine structure in the *D* lines of alkali atoms," J. Phys. B: At., Mol. Opt. Phys. **41**, 035001 (2008).

Deech, J. S., Luypaert, R., Pendrill, L. R., and Series, G. W., "Lifetimes, depopulation cross sections and hyperfine structures of some Rydberg S and D states of ^{133}Cs," J. Phys. B: At. Mol. Phys. **10**, L137–L141 (1977).

DeGraffenreid, W. and Sansonetti, C. J., "$2^{2}S_{1/2}$–$4^{2}S_{1/2}$ transition of atomic lithium by Doppler-free two-photon spectroscopy," Phys. Rev. A **67**, 012509 (2003).

de Groote, R. P., Budinčević, I., Billowes, J., Bissell, M. L., Cocolios, T. E., Farooq-Smith, G. J., Fedosseev, V. N., Flanagan, K. T., Franchoo, S., Garcia Ruiz, R. F., Heylen, H., Li, R., Lynch, K. M., Marsh, B. A., Neyens, G., Rossel, R. E., Rothe, S., Stroke, H. H., Wendt, K. D. A., Wilkins, S. G., and Yang, X., "Use of a continuous wave laser and Pockels cell for sensitive high-resolution collinear resonance ionization spectroscopy," Phys. Rev. Lett. **115**, 132501 (2015).

Duong, H. T., "Hyperfine structure and isotope shifts of $^{39-41}$K by rf modulated laser light," Nucl. Instrum. Methods Phys. Res. **202**, 341–342 (1982).

Duong, H. T., Ekström, C., Gustafsson, M., Inamura, T. T., Juncar, P., Lievens, P., Lindgren, I., Matsuki, S., Murayama, T., Neugart, R., Nilsson, T., Nomura, T., Pellarin, M., Penselin, S., Persson, J., Pinard, J., Ragnarsson, I., Redi, O., Stroke, H. H., Vialle, J. L, and ISOLDE Collaboration, "Atomic beam magnetic resonance apparatus for systematic measurement of hyperfine structure anomalies (Bohr-Weisskopf effect)," Nucl. Instrum. Methods Phys. Res., Sect. A **325**, 465–474 (1993).

Duong, H. T., Juncar, P., Liberman, S., Mueller, A. C., Neugart, R., Otten, E. W., Peuse, B., Pinard, J., Stroke, H. H., Thibault, C., Touchard, F., Vialle, J. L., Wendt, K., and ISOLDE Collaboration, "First observation of the blue optical lines of francium," Europhys. Lett. **3**, 175–182 (1987).

Duong, H. T., Liberman, S., Pinard, J., Coc, A., Thibault, C., Touchard, F., Carré, M., Lermé, J., Vialle, J. L., Juncar, P., Büttgenbach, S., Pesnelle, A., and ISOLDE Collaboration, "Accurate determination of ground state hyperfine structures of some radioactive alkali isotopes by r. f. magnetic resonance and laser optical pumping," J. Phys. **47**, 1903–1908 (1986).

Dzuba, V. A. and Flambaum, V. V., "Off-diagonal hyperfine interaction and parity nonconservation in cesium," Phys. Rev. A **62**, 052101 (2000).

Ewald, G., Nörtershäuser, W., Dax, A., Götte, S., Kirchner, R., Kluge, H.-J., Kühl, T., Sanchez, R., Wojtaszek, A., Bushaw, B. A., Drake, G. W. F., Yan, Z.-C., and Zimmermann, C., "Nuclear charge radii of ^{8,9}Li determined by laser spectroscopy," Phys. Rev. Lett. **93**, 113002 (2004).

Faist, A., Geneux, E., and Koide, S., "Frequency shift in magnetic transitions between hyperfine levels of $^2P_{3/2}$ states of Cs^{133}," J. Phys. Soc. Jpn. **19**, 2299–2305 (1964).

Falke, S., Tiemann, E., Lisdat, C., Schnatz, H., and Grosche, G., "Transition frequencies of the D lines of ^{39}K, ^{40}K, and ^{41}K measured with a femtosecond laser frequency comb," Phys. Rev. A **74**, 032503 (2006).

Farley, J., Tsekeris, P., and Gupta, R., "Hyperfine-structure measurements in the Rydberg S and P states of rubidium and cesium," Phys. Rev. A **15**, 1530–1536 (1977).

Farooq-Smith, G. J., Cocolios, T. E., Billowes, J., Bissell, M. L., Budinčević, I., Day Goodacre, T., de Groote, R. P., Fedosseev, V. N., Flanagan, K. T., Franchoo, S., Garcia Ruiz, R. F., Heylen, H., Li, R., Lynch, K. M., Marsh, B. A., Neyens, G., Rossel, R. E., Rothe, S., Stroke, H. H., Wendt, K. D. A., Wilkins, S. G., and Yang, X. F., "Laser and decay spectroscopy of the short-lived isotope ^{214}Fr in the vicinity of the N = 126 shell closure," Phys. Rev. C **94**, 054305 (2016a).

Farooq-Smith, G. J., Cocolios, T. E., Billowes, J., Bissell, M. L., Budinčević, I., Day Goodacre, T., de Groote, R. P., Fedosseev, V. N., Flanagan, K. T., Franchoo, S., Garcia Ruiz, R. F., Heylen, H., Li, R., Lynch, K. M., Marsh, B. A., Neyens, G., Rossel, R. E., Rothe, S., Stroke, H. H., Wendt, K. D. A., Wilkins, S. G., and Yang, X. F., "Publisher's note: Laser and decay spectroscopy of the short-lived isotope ^{214}Fr in the vicinity of the N = 126 shell closure [Phys. Rev. C **94**, 054305 (2016)]," Phys. Rev. C **94**, 059903 (2016b).

Feiertag, D., Sahm, A., and zu Putlitz, G., "Core polarization of the ^{133}Cs atom by the 7p electron," Z. Phys. A: Hadrons Nucl. **255**, 93–96 (1972).

Feiertag, D. and zu Putlitz, G., "Hyperfine structure, g_j factors and lifetimes of excited $^2P_{1/2}$ states of Rb," Z. Phys. A: Hadrons Nucl. **261**, 1–12 (1973).

Fendel, P., Bergeson, S. D., Udem, T., and Hänsch, T. W., "Two-photon frequency comb spectroscopy of the 6s–8s transition in cesium," Opt. Lett. **32**, 701–703 (2007).

Flambaum, V. V. and Khriplovich, I. B., "New bounds on the electric dipole moment of the electron and on T-odd electron-nucleon coupling," Sov. Phys. - JETP **62**, 872 (1985), http://www.jetp.ras.ru/cgi-bin/dn/e_062_05_0872.pdf.

Flanagan, K. T., Lynch, K. M., Billowes, J., Bissell, M. L., Budinčević, I., Cocolios, T. E., de Groote, R. P., De Schepper, S., Fedosseev, V. N., Franchoo, S., Garcia Ruiz, R. F., Heylen, H., Marsh, B. A., Neyens, G., Procter, T. J., Rossel, R. E., Rothe, S., Strashnov, I., Stroke, H. H., and Wendt, K. D. A., "Collinear resonance ionization spectroscopy of neutron-deficient francium isotopes," Phys. Rev. Lett. **111**, 212501 (2013).

Foot, C. J., *Atomic Physics* (Oxford University Press, Oxford, 2005).

Fort, C., Cataliotti, F. S., Raspollini, P., Tino, G. M., and Inguscio, M., "Optical double-resonance spectroscopy of trapped Cs atoms: Hyperfine structure of the 8s and 6d excited states," Z. Phys. D: At., Mol. Clusters **34**, 91–95 (1995a).

Fort, C., Inguscio, M., Raspollini, P., Baldes, F., and Sasso, A., "Doppler-free two-color spectroscopy of the $6S_{1/2}$–$8S_{1/2}$ cesium transition using semiconductor diode lasers," Appl. Phys. B: Lasers Opt. **61**, 467–472 (1995b).

Fredriksson, K., Lundberg, H., and Svanberg, S., "Fine- and hyperfine-structure investigation in the 5^2D–n^{2}F series of cesium," Phys. Rev. A **21**, 241–247 (1980).

Gabbanini, C., Ceccherini, F., Gozzini, S., and Lucchesini, A., "Resonance-enhanced ionization spectroscopy of laser-cooled rubidium atoms," Meas. Sci. Technol. **10**, 772–776 (1999).

Gangrsky, Y. P., Karaivanov, D. V., Marinova, K. P., Markov, B. N., Melnikova, L. M., Mishinsky, G. V., Zemlyanoi, S. G., and Zhemenik, V. I., "Hyperfine splitting and isotope shift in the atomic D_2 line of ^{22,23}Na and the quadrupole moment of ^{22}Na," Eur. Phys. J. A **3**, 313–318 (1998).

Georgiades, N. P., Polzik, E. S., and Kimble, H. J., "Two-photon spectroscopy of the $6S_{1/2} \rightarrow 6D_{5/2}$ transition of trapped atomic cesium," Opt. Lett. **19**, 1474–1476 (1994).

Gerginov, V., Calkins, K., Tanner, C. E., McFerran, J. J., Diddams, S., Bartels, A., and Hollberg, L., "Optical frequency measurements of $6s^2S_{1/2}$–$6p^2P_{1/2}$ (D_1) transitions in ^{133}Cs and their impact on the fine-structure constant," Phys. Rev. A **73**, 032504 (2006).

Gerginov, V., Derevianko, A., and Tanner, C. E., "Observation of the nuclear magnetic octupole moment of ^{133}Cs," Phys. Rev. Lett. **91**, 072501 (2003).

Gerginov, V., Tanner, C. E., and Johnson, W. R., "Observation of the nuclear magnetic octupole moment of ^{87}Rb from spectroscopic measurements of hyperfine intervals," Can. J. Phys. **87**, 101–104 (2009).

Gerhardt, H., Matthias, E., Schneider, F., and Timmermann, A., "Isotope shifts and hyperfine structure of the 6s-7p transitions in the cesium isotopes 133, 135, and 137," Z. Phys. A: At. Nucl. **288**, 327–333 (1978).

Gilbert, S. L., Masterson, B. P., Noecker, M. C., and Wieman, C. E., "Precision measurement of the off-diagonal hyperfine interaction," Phys. Rev. A **34**, 3509–3512 (1986).

Gilbert, S. L., Watts, R. N., and Wieman, C. E., "Hyperfine-structure measurement of the 7S state of cesium," Phys. Rev. A **27**, 581–582 (1983).

Glaser, C., Karlewski, F., Kluge, J., Grimmel, J., Kaiser, M., Günther, A., Hattermann, H., Krutzik, M., and Fortágh, J., "Absolute frequency measurement of rubidium 5S-6P transitions," Phys. Rev. A **102**, 012804 (2020).

Glodz, M. and Krainska-Miszczak, M., "Hyperfine interaction constants and lifetime of the 6^2D$_{3/2}$ and 6^2D$_{5/2}$ states of ^{39}K measured by the quantum beam method," J. Phys. B: At. Mol. Phys. **18**, 1515–1522 (1985a).

Głódó, M. and Kraińska-Miszczak, M., "Lifetime and hyperfine structure constants of the 6^2D$_{3/2}$ state in ^{41}K," Phys. Lett. A **110**, 203–205 (1985b).

Głódó, M. and Kraińska-Miszczak, M., "Magnetic-dipole and electric-quadrupole interaction constants in the 10^2D$_{5/2}$ state of ^{87}Rb," J. Phys. B: At. Mol. Phys. **20**, L541–L545 (1987).

Glodz, M. and Krainska-Miszczak, M., "Measurements of magnetic-dipole and electric-quadrupole interaction constants of the 11, 12 and 13^2D$_{5/2}$ states in ^{87}Rb by the quantum-beat method," J. Phys. B: At., Mol. Opt. Phys. **22**, 3109–3117 (1989).

Głódó, M. and Kraińska-Miszczak, M., "Magnetic-dipole and electric-quadrupole interaction constants and lifetime of the $9^2D_{5/2}$ state in Rb-87," Acta Phys. Pol. **78**, 317–322 (1990).

Głódó, M. and Kraińska-Miszczak, M., "Hyperfine interaction constants of the 10, 11 and 12 ^{2}D$_{3/2}$ states in ^{87}Rb measured by the quantum beat method," Phys. Lett. A **160**, 85–89 (1991).

Głódó, M. and Kraińska-Miszczak, M., "Hyperfine structure constants in the 10^2D$_{3/2}$ and 11^2D$_{3/2}$ states of ^{85}Rb," Acta Phys. Pol., A **83**, 161–165 (1993).

Gomez, E., Aubin, S., Orozco, L. A., and Sprouse, G. D., "Lifetime and hyperfine splitting measurements on the 7s and 6p levels in rubidium," J. Opt. Soc. Am. B **21**, 2058–2067 (2004).

Gomez, E., Aubin, S., Orozco, L. A., Sprouse, G. D., Iskrenova-Tchoukova, E., and Safronova, M. S., "Nuclear magnetic moment of ^{210}Fr: A combined theoretical and experimental approach," Phys. Rev. Lett. **100**, 172502 (2008).

Goy, P., Raimond, J. M., Vitrant, G., and Haroche, S., "Millimeter-wave spectroscopy in cesium Rydberg states. Quantum defects, fine- and hyperfine-structure measurements," Phys. Rev. A **26**, 2733–2742 (1982).

Griffith, J. A. R., Isaak, G. R., New, R., Ralls, M. P., and van Zyl, C. P., "Optical heterodyne spectroscopy using tunable dye lasers: Hyperfine structure of sodium," J. Phys. B: At. Mol. Phys. **10**, L91–L95 (1977).

Grossman, J. M., Fliller III, R. P., Mehlstäubler, T. E., Orozco, L. A., Pearson, M. R., Sprouse, G. D., and Zhao, W. Z., "Energies and hyperfine splittings of the 7D levels of atomic francium," Phys. Rev. A **62**, 052507 (2000).

Grossman, J. S., Orozco, L. A., Pearson, M. R., Simsarian, J. E., Sprouse, G. D., and Zhao, W. Z., "Hyperfine anomaly measurements in francium isotopes and the radial distribution of neutrons," Phys. Rev. Lett. **83**, 935–938 (1999).

Grove, T. T., Sanchez-Villicana, V., Duncan, B. C., Maleki, S., and Gould, P. L., "Two-photon two-color diode laser spectroscopy of the Rb $5D_{5/2}$ state," Phys. Scr. **52**, 271–276 (1995).

Grundevik, P. and Lundberg, H., "Measurement of the hyperfine structure splitting for the 4 and 5 $^2P_{1/2}$ states of sodium using radio-frequency spectroscopy," Z. Phys. A: At. Nucl. **285**, 231–233 (1978).

Grundevik, P., Lundberg, H., Martensson, A.-M., Nystrom, K., and Svanberg, S., "Hyperfine-structure study in the P sequence of ^{23}Na using quantum-beam spectroscopy," J. Phys. B: At. Mol. Phys. **12**, 2645–2654 (1979).

Grunefeld, S. J., Roberts, B. M., and Ginges, J. S. M., "Correlation trends in the hyperfine structure for Rb, Cs, and Fr, and high-accuracy predictions for hyperfine constants," Phys. Rev. A **100**, 042506 (2019).

Guéna, J., Abgrall, M., Clairon, A., and Bize, S., "Contributing to TAI with a secondary representation of the SI second," Metrologia **51**, 108–120 (2014).

Gupta, R., Happer, W., Lam, L. K., and Svanberg, S., "Hyperfine-structure measurements of excited S states of the stable isotopes of potassium, rubidium, and cesium by cascade radio-frequency spectroscopy," Phys. Rev. A **8**, 2792–2810 (1973).

Gwinner, G. and Orozco, L. A., "Studies of the weak interaction in atomic systems: Towards measurements of atomic parity non-conservation in francium," Quantum Sci. Technol. **7**, 024001 (2022).

Hagel, G., Nesi, C., Jozefowski, L., Schwob, C., Nez, F., and Biraben, F., "Accurate measurement of the frequency of the 6S–8S two-photon transitions in cesium," Opt. Commun. **160**, 1–4 (1999).

Halloran, L. J. S., Fostner, S., Paradis, E., and Behr, J. A., "Specific mass shift of potassium $5P_{1/2}$ state," Opt. Commun. **282**, 554–557 (2009).

Hawkins, R. T., Hill, W. T., Kowalski, F. V., Schawlow, A. L., and Svanberg, S., "Stark-effect study of excited states in sodium using two-photon spectroscopy," Phys. Rev. A **15**, 967–974 (1977).

He, Y.-H., Fan, J.-B., Hao, L.-P., Jiao, Y.-C., and Zhao, J.-M., "Precise measurement of hyperfine structure of cesium $7S_{1/2}$ excited state," Appl. Sci. **10**, 525 (2020).

He, Z.-S., Tsai, J.-H., Lee, M.-T., Chang, Y.-Y., Tsai, C.-C., and Whang, T.-J., "Determination of the cesium $11s^2S_{1/2}$ hyperfine magnetic coupling constant using electromagnetically induced transparency," J. Phys. Soc. Jpn. **81**, 124302 (2012).

Herd, M. T., Cook, E. C., and Williams, W. D., "Absolute frequency measurement of the $6D_{5/2}$ level of neutral ^{133}Cs using two-photon spectroscopy," Phys. Rev. A **104**, 042812 (2021).

Herrmann, P. P., Hoffnagle, J., Pedroni, A., Schlumpf, N., and Weis, A., "Doppler-free spectroscopy of the 8s state of Cs," Opt. Commun. **56**, 22–24 (1985).

Hogervorst, W. and Svanberg, S., "Stark effect investigation of D states in ^{85}Rb and ^{133}Cs using level crossing spectroscopy with a CW dye laser," Phys. Scr. **12**, 67–74 (1975).

Huang, S.-H. and Sun, Q.-F., "Calculation of the Rydberg energy levels for francium atom," Phys. Res. Int. **2010**, 203497.

Huang, Y.-C., Luo, W.-J., Kuo, Y.-T., and Wang, L.-B., "Precision measurement of hyperfine intervals in the D_1 lines of atomic ^{7}Li," J. Phys. B: At., Mol. Opt. Phys. **46**, 075004 (2013).

Inguscio, M. and Fallani, L., *Atomic Physics: Precise Measurements and Ultracold Matter* (Oxford University Press, Oxford, 2013).

Isler, R. C., Marcus, S., and Novick, R., "Hyperfine structure of the 3^2P and 4^2P states of lithium and lifetime of the 3^2P state," Phys. Rev. **187**, 76–84 (1969).

Jiang, Z.-K., Jönsson, G., and Lundberg, H., "Hyperfine-structure study of the 7, 8 and $9^2P_{3/2}$ states in ^{23}Na using quantum-beat spectroscopy," Phys. Scr. **26**, 459–461 (1982).

Jin, L., Zhang, Y.-C., Xiang, S.-S., Wang, L.-R., Ma, J., Zhao, Y.-T., Xiao, L.-T., and Jia, S.-T., "Experimental measurement of the absolute frequencies and hyperfine coupling constants of ^{133}Cs using a femtosecond optical frequency comb," Chin. Phys. Lett. **30**, 103201 (2013).

Johnson, W. R., Ho, H. C., Tanner, C. E., and Derevianko, A., "Off-diagonal hyperfine interaction between the $6p_{1/2}$ and $6p_{3/2}$ levels in ^{133}Cs," Phys. Rev. A **70**, 014501 (2004).

Johnson, W. R., Safronova, M. S., and Safronova, U. I., "Combined effect of coherent Z exchange and the hyperfine interaction in the atomic parity-nonconserving interaction," Phys. Rev. A **67**, 062106 (2003).

Johnson, W. R., Safronova, U. I., Derevianko, A., and Safronova, M. S., "Relativistic many-body calculation of energies, lifetimes, hyperfine constants, and polarizabilities in ^{7}Li," Phys. Rev. A **77**, 022510 (2008).

Kasevich, M. A., Riis, E., Chu, S., and DeVoe, R. G., "RF spectroscopy in an atomic fountain," Phys. Rev. Lett. **63**, 612–615 (1989).

Kiran Kumar, P. V., Nisheeth, B., Sankari, M., and Suryanarayana, M. V., "Precision measurement of the hyperfine structure of $8d^2D_{3/2}$ state of ^{133}Cs by the radio-frequency phase modulation technique," Opt. Commun. **320**, 77–83 (2014).

Kiran Kumar, P. V., Sankari, M., and Suryanarayana, M. V., "Hyperfine structure of the 7d $^2D_{3/2}$ level in cesium measured by Doppler-free two-photon spectroscopy," Phys. Rev. A **87**, 012503 (2013).

Kiran Kumar, P. V. and Suryanarayana, M. V., "Isotope shift and hyperfine structure measurements of $4s^2S_{1/2} \rightarrow 6s^2S_{1/2}$ two-photon transition of potassium isotopes," J. Phys. B: At., Mol. Opt. Phys. **44**, 055003 (2011).

Kiran Kumar, P. V. and Suryanarayana, M. V., "Measurement of the hyperfine splitting of the 9 $S_{1/2}$ level in cesium by Doppler-free two-photon spectroscopy," Opt. Commun. **285**, 1838–1842 (2012).

Kiran Kumar, P. V. and Suryanarayana, M. V., "Precision two-photon spectroscopy of alkali elements," Pramana **83**, 189–219 (2014).

Konovalova, E. A., Demidov, Y. A., and Kozlov, M. G., "Calculation of the hyperfine magnetic anomaly in many-electron atoms," Opt. Spectrosc. **128**, 1530–1536 (2020).

Konovalova, E. A., Demidov, Y. A., Kozlov, M. G, and Barzakh, A. E., "Calculation of francium hyperfine anomaly," Atoms **6**, 39 (2018).

Kopfermann, H., *Nuclear Moments* (Academic, New York, 1958).

Kortyna, A., Fiore, V., and Farrar, J., "Measurement of the cesium $7d^2D_{3/2}$ hyperfine coupling constants in a thermal beam using two-photon fluorescence spectroscopy," Phys. Rev. A **77**, 062505 (2008).

Kortyna, A., Masluk, N. A., and Bragdon, T., "Measurement of the $6d^2D_J$ hyperfine structure of cesium using resonant two-photon sub-Doppler spectroscopy," Phys. Rev. A **74**, 022503 (2006).

Kortyna, A., Tinsman, C., Grab, J., Safronova, M. S., and Safronova, U. I., "Experimental and theoretical study of the $6d_{3/2}$ polarizability of cesium," Phys. Rev. A **83**, 042511 (2011).

Koszorús, A., Yang, X. F., Billowes, J., Binnersley, C. L., Bissell, M. L., Cocolios, T. E., Farooq-Smith, G. J., de Groote, R. P., Flanagan, K. T., Franchoo, S., Garcia Ruiz, R. F., Geldhof, S., Gins, W., Kanellakopoulos, A., Lynch, K. M., Neyens, G., Stroke, H. H., Vernon, A. R., Wendt, K. D. A., and Wilkins, S. G., "Precision measurements of the charge radii of potassium isotopes," Phys. Rev. C **100**, 034304 (2019).

Kowalski, J., Neumann, R., Suhr, H., Winkler, K., and zu Putlitz, G., "Two-photon intracavity dye laser spectroscopy of the 4S and 3D term in ^{6,7}Li," Z. Phys. A: At. Nucl. **287**, 247–253 (1978).

Kraińska-Miszczak, M., "Decoupling in the $^2P_{3/2}$ state and D_2 fluorescence of alkali metal atoms," Opt. Commun. **38**, 255–258 (1981).

Kraińska-Miszczak, M., "Hyperfine interaction constants in the 9 $^2D_{3/2}$ state of ^{85}Rb measured by the quantum beat method," Acta Phys. Pol., A **86**, 343–347 (1994).

Kramida, A., NIST atomic energy levels and spectra bibliographic database, 2022.

Krishna, A., Pandey, K., Wasan, A., and Natarajan, V., "High-resolution hyperfine spectroscopy of excited states using electromagnetically induced transparency," Europhys. Lett. **72**, 221–227 (2005).

Krist, T., Kuske, P., Gaupp, A., Wittmann, W., and Andrä, H. J., "Improved ^{23}Na I 3^2P_{32} HFS measurement beyond the natural linewidth by beam laser quantum beats," Phys. Lett. A **61**, 94–96 (1977).

Kumar, P. and Natarajan, V., "Precise measurement of hyperfine structure in the $3S_{1/2}$ state of ^{7}Li," Sci. Rep. **7**, 13204 (2017).

Lam, L. K., Gupta, R., and Happer, W., "Hyperfine-structure measurements in the first excited D levels of potassium, rubidium, and cesium by cascade-fluorescence spectroscopy," Phys. Rev. A **21**, 1225–1234 (1980).

Lee, W.-K. and Moon, H. S., "Measurement of absolute frequencies and hyperfine structure constants of $4D_{5/2}$ and $4D_{3/2}$ levels of ^{87}Rb and ^{85}Rb using an optical frequency comb," Phys. Rev. A **92**, 012501 (2015).

Lee, W.-K., Moon, H. S., and Suh, H. S., "Measurement of the absolute energy level and hyperfine structure of the ^{87}Rb $4D_{5/2}$ state: Erratum," Opt. Lett. **40**, 2111 (2015).

Lee, W.-K., Seb Moon, H., and Suhng Suh, H., "Measurement of the absolute energy level and hyperfine structure of the ^{87}Rb $4D_{5/2}$ state," Opt. Lett. **32**, 2810–2812 (2007).

Lee, Y.-C., Chang, Y.-H., Chang, Y.-Y., Chen, Y.-Y., Tsai, C.-C., and Chui, H.-C., "Hyperfine coupling constants of cesium 7D states using two-photon spectroscopy," Appl. Phys. B **105**, 391–397 (2011).

Li, R., Wu, Y., Rui, Y., Li, B., Jiang, Y., Ma, L., and Wu, H., "Absolute frequency measurement of ^{6}Li D lines with kHz-level uncertainty," Phys. Rev. Lett. **124**, 063002 (2020).

Li, R., Wu, Y.-L., Rui, Y., and Wu, H.-B., "Observation of subnatural-linewidth spectra in cold ^{6}Li atoms," Phys. Rev. A **103**, 032823 (2021).

Li, W.-H., Mourachko, I., Noel, M. W., and Gallagher, T. F., "Millimeter-wave spectroscopy of cold Rb Rydberg atoms in a magneto-optical trap: Quantum defects of the *ns*, *np*, and *nd* series," Phys. Rev. A **67**, 052502 (2003).

Liberman, S., Pinard, J., Duong, H. T., Juncar, P., Pillet, P., Vialle, J.-L., Jacquinot, P., Touchard, F., Büttgenbach, S., Thibault, C., de Saint-Simon, M., Klapisch, R., Pesnelle, A., and Huber, G., "Laser optical spectroscopy on francium D_2 resonance line," Phys. Rev. A **22**, 2732–2737 (1980).

Lien, Y.-H., Lo, K.-J., Chen, H.-C., Chen, J.-R., Tian, J.-Y., Shy, J.-T., and Liu, Y.-W., "Absolute frequencies of the ^{6,7}Li $2S\ ^2S_{1/2} \rightarrow 3S\ ^2S_{1/2}$ transitions," Phys. Rev. A **84**, 042511 (2011).

Liu, Y.-W., and Baird, P. E. G., "Measurement of the caesium $6S_{1/2} - 8P_{1/2}$ transition frequency," Appl. Phys. B **71**, 567–572 (2000).

Lorenzen, C.-J. and Niemax, K., "Level isotope shifts of ^{6,7}Li," J. Phys. B: At. Mol. Phys. **15**, L139–L145 (1982).

Lorenzen, C.-J. and Niemax, K., "Quantum defects of the $n^2P_{1/2,3/2}$ levels in ^{39}K I and ^{85}Rb I," Phys. Scr. **27**, 300–305 (1983).

Lorenzen, C.-J. and Niemax, K., "Precise quantum defects of nS, nP and nD Levels in Cs I," Z. Phys. A: At. Nucl. **315**, 127–133 (1984).

Lou, B.-Q., Li, F., Wang, P.-Y., Wang, L.-M., and Tang, Y.-B., "*Ab initio* calculation of hyperfine-structure constant *A* of Fr and evaluation of magnetic dipole moments of Fr isotopes," Acta Phys. Sin. **68**, 093101 (2019).

Lu, Z.-T., Corwin, K. L., Vogel, K. R., Wieman, C. E., Dinneen, T. P., Maddi, J., and Gould, H., "Efficient collection of ^{221}Fr into a vapor cell magneto-optical trap," Phys. Rev. Lett. **79**, 994–997 (1997).

Lundberg, H., Mårtensson, A.-M., and Svanberg, S., "Hyperfine structure in the sequence of sodium S states," J. Phys. B: At. Mol. Phys. **10**, 1971–1978 (1977).

Lynch, K. M., Billowes, J., Bissell, M. L., Budinčević, I., Cocolios, T. E., de Groote, R. P., De Schepper, S., Fedosseev, V. N., Flanagan, K. T., Franchoo, S., Garcia Ruiz, R. F., Heylen, H., Marsh, B. A., Neyens, G., Procter, T. J., Rossel, R. E., Rothe, S., Strashnov, I., Stroke, H. H., and Wendt, K. D. A., "Decay-assisted laser spectroscopy of neutron-deficient francium," Phys. Rev. X **4**, 011055 (2014).

Lynch, K. M., Cocolios, T. E., Billowes, J., Bissell, M. L., Budinčević, I., Day Goodacre, T., de Groote, R. P., Farooq-Smith, G. J., Fedosseev, V. N., Flanagan, K. T., Franchoo, S., Garcia Ruiz, R. F., Heylen, H., Li, R., Marsh, B. A., Neyens, G., Rossel, R. E., Rothe, S., Stroke, H. H., Wendt, K. D. A., Wilkins, S. G., and Yang, X., "Combined high-resolution laser spectroscopy and nuclear decay spectroscopy for the study of the low-lying states in ^{206}Fr, ^{202}At, and ^{198}Bi," Phys. Rev. C **93**, 014319 (2016).

Lyons, J. D. and Das, T. P., "Theoretical analysis of level crossing in a ^{2}P atomic state," Phys. Rev. A **2**, 2250–2259 (1970).

Mack, M., Karlewski, F., Hattermann, H., HöckhS., Jessen, F., Cano, D., and Fortágh, J., "Measurement of absolute transition frequencies of ^{87}Rb to nS and nD Rydberg states by means of electromagnetically induced transparency," Phys. Rev. A **83**, 052515 (2011).

Marcassa, L. G., Muniz, S. R., Telles, G. D., Zilio, S. C., and Bagnato, V. S., "Measurement of Na $5S_{1/2}$ hyperfine splitting by ionization using a sample of cold atoms," Opt. Commun. **155**, 38–42 (1998).

Marian, A., Stowe, M. C., Felinto, D., and Ye, J., "Direct frequency comb measurements of absolute optical frequencies and population transfer dynamics," Phys. Rev. Lett. **95**, 023001 (2005).

Maric, M., McFerran, J. J., and Luiten, A. N., "Frequency-comb spectroscopy of the D_1 line in laser-cooled rubidium," Phys. Rev. A **77**, 032502 (2008).

McLaughlin, C., Ayachitula, R., Lindsay, M., and Knize, R., "Hyperfine splittings and isotope shift of the Rb 5S–6S two-photon transition," in 53rd Annual Meeting of the APS Division of Atomic, Molecular and Optical Physics, Bulletin of the American Physical Society, 2022, abstract: N01.00124.

Meschede, D., "Centimeter-wave spectroscopy of highly excited rubidium atoms," J. Opt. Soc. Am. B **4**, 413–419 (1987).

Metcalf, H. J. and van der Straten, P., *Laser Cooling and Trapping of Neutral Atoms* (Springer-Verlag, New York, 1999).

Moon, H. S., Lee, W.-K., and Suh, H. S., "Hyperfine-structure-constant determination and absolute-frequency measurement of the Rb $4D_{3/2}$ state," Phys. Rev. A **79**, 062503 (2009).

Morgenweg, J., Barmes, I., and Eikema, K. S. E., "Ramsey-comb spectroscopy with intense ultrashort laser pulses," Nat. Phys. **10**, 30–33 (2014).

Morzyński, P., Wcisło, P., Ablewski, P., Gartman, R., Gawlik, W., Masłowski, P., Nagórny, B., Ozimek, F., Radzewicz, C., Witkowski, M., Ciuryło, R., and Zawada, M., "Absolute frequency measurement of rubidium 5S–7S two-photon transitions," Opt. Lett. **38**, 4581–4584 (2013).

Morzyński, P., Wcisło, P., Ablewski, P., Gartman, R., Gawlik, W., Masłowski, P., Nagórny, B., Ozimek, F., Radzewicz, C., Witkowski, M., Ciuryło, R., and Zawada, M., "Line shape measurements of rubidium 5S–7S two-photon transition," J. Phys.: Conf. Ser. **548**, 012023 (2014).

Nagourney, W., Happer, W., and Lurio, A., "Level-crossing study of the hyperfine structure of lithium," Phys. Rev. A **17**, 1394–1407 (1978).

Nakayama, S., Kelly, F. M., and Series, G. W., "Hyperfine structures, lifetimes and collisional cross sections of some Rydberg D states of ^{133}Cs," J. Phys. B: At. Mol. Phys. **14**, 835–838 (1981).

Neugart, R., Billowes, J., Bissell, M. L., Blaum, K., Cheal, B., Flanagan, K. T., Neyens, G., Nörtershäuser, W., and Yordanov, D. T., "Collinear laser spectroscopy at ISOLDE: New methods and highlights," J. Phys. G: Nucl. Part. Phys. **44**, 064002 (2017).

Neuzner, A., Körber, M., Dürr, S., Rempe, G., and Ritter, S., "Breakdown of atomic hyperfine coupling in a deep optical-dipole trap," Phys. Rev. A **92**, 053842 (2015).

Ney, J., "Hyperfeinstrukturuntersuchung der 4*p* und $5p\ ^2P_{3/2}$-terme im K I-spektrum durch resonanzstreuung von licht zur bestimmung der kernquadrupolmomente von K^{39} und K^{41}," Z. Phys. A: Hadrons Nucl. **223**, 126–138 (1969).

Ney, J., Repnow, R., Bucka, H., and Svanberg, S., "Untersuchung des $4p\ ^2P_{3/2}$ und $5p\ ^2P_{3/2}$-terms des *KI*-spektrums durch resonanzstreuung von licht zur bestimmung des kernquadrupolmoments von K^{40}," Z. Phys. A: Hadrons Nucl. **213**, 192–201 (1968).

Nez, F., Biraben, F., Felder, R., and Millerioux, Y., "Optical frequency determination of the hyperfine components of the $5S_{1/2}$-$5D_{3/2}$ two-photon transitions in rubidium," Opt. Commun. **102**, 432–438 (1993).

Nez, F., Biraben, F., Felder, R., and Millerioux, Y., "Erratum: Optical frequency determination of the hyperfine components of the $5S_{1/2}$-$5D_{3/2}$ two-photon transitions in rubidium," Opt. Commun. **110**, 731 (1993).

Noble, G. A., Schultz, B. E., Ming, H., and van Wijngaarden, W. A., "Isotope shifts and fine structures of ^{6,7}Li D lines and determination of the relative nuclear charge radius," Phys. Rev. A **74**, 012502 (2006).

Nörtershäuser, W., Sánchez, R., Ewald, G., Dax, A., Behr, J., Bricault, P., Bushaw, B. A., Dilling, J., Dombsky, M., Drake, G. W. F., Götte, S., Kluge, H.-J., Kühl, T., Lassen, J., Levy, C. D. P., Pachucki, K., Pearson, M., Puchalski, M., Wojtaszek, A., Yan, Z.-C., and Zimmermann, C., "Isotope-shift measurements of stable and short-lived lithium isotopes for nuclear-charge-radii determination," Phys. Rev. A **83**, 012516 (2011).

Nyakang'o, E. O., Shylla, D., Natarajan, V., and Pandey, K., "Hyperfine measurement of the $6P_{1/2}$ state in ^{87}Rb using double resonance on blue and IR transition," J. Phys. B: At., Mol. Opt. Phys. **53**, 095001 (2020).

Ohtsuka, T., Nishimiya, N., Fukuda, T., and Suzuki, M., "Doppler-free two-photon spectroscopy of $6S_{1/2}$–$6D_{3/2,5/2}$ transition in cesium," J. Phys. Soc. Jpn. **74**, 2487–2491 (2005).

Orson, S. T., McLaughlin, C. D., Lindsay, M. D., and Knize, R. J., "Absolute hyperfine energy levels and isotope shift of Rb 5S–6S two-photon transition," J. Phys. B: At., Mol. Opt. Phys. **54**, 175001 (2021).

Orth, H., Ackermann, H., and Otten, E. W., "Fine and hyperfine structure of the 2^2P term of ^{7}Li; determination of the nuclear quadrupole moment," Z. Phys. A: At. Nucl. **273**, 221–232 (1975).

Orth, H., Veil, R., Ackermann, H., and Otten, E. W., "Fine and hyperfine structure of the 2^2P term of ^{6}Li and ^{7}Li; determination of the ^{7}Li quadrupole moment," in *Abstracts of Contributed Papers to the Fourth International Conference on Atomic Physics*, edited by J. Kowalski and H. G. Weber (Heidelberg, 1974), p. 93.

Otto, P., Gamperling, M., Hofacker, M., Meyer, T., Pagliari, V., Stifter, A., Krauss, M., and Hüttner, W., "Level magnetizabilities of the alkaline metal atoms," Chem. Phys. **282**, 289–304 (2002).

Ovchinnikov, Y. B., Szymaniec, K., and Edris, S., "Measurement of rubidium ground-state hyperfine transition frequency using atomic fountains," Metrologia **52**, 595–599 (2015).

Pal, R., Safronova, M. S., Johnson, W. R., Derevianko, A., and Porsev, S. G., "Relativistic coupled-cluster single-double method applied to alkali-metal atoms," Phys. Rev. A **75**, 042515 (2007).

Papuga, J., Bissell, M. L., Kreim, K., Barbieri, C., Blaum, K., De Rydt, M., Duguet, T., Garcia Ruiz, R. F., Heylen, H., Kowalska, M., Neugart, R., Neyens, G., Nörtershäuser, W., Rajabali, M. M., Sánchez, R., Smirnova, N., Somà, V., and Yordanov, D. T., "Shell structure of potassium isotopes deduced from their magnetic moments," Phys. Rev. C **90**, 034321 (2014).

Peper, M., Helmrich, F., Butscher, J., Agner, J. A., Schmutz, H., Merkt, F., and Deiglmayr, J., "Precision measurement of the ionization energy and quantum defects of ^{39}K I," Phys. Rev. A **100**, 012501 (2019).

Pérez Galván, A., Zhao, Y., and Orozco, L. A., "Measurement of the hyperfine splitting of the $6S_{1/2}$ level in rubidium," Phys. Rev. A **78**, 012502 (2008).

Pérez Galván, A., Zhao, Y., Orozco, L. A., Gómez, E., Lange, A. D., Baumer, F., and Sprouse, G. D., "Comparison of hyperfine anomalies in the $5S_{1/2}$ and $6S_{1/2}$ levels of ^{85}Rb and ^{87}Rb," Phys. Lett. B **655**, 114–118 (2007).

Persson, J. R., "Extraction of hyperfine anomalies without precise values of the nuclear magnetic dipole moment," Eur. Phys. J. A **2**, 3–4 (1998).

Persson, J. R., "Table of hyperfine anomaly in atomic systems," At. Data Nucl. Data Tables **99**, 62–68 (2013).

Pescht, K., Gerhardt, H., and Matthias, E., "Isotope shift and HFS of D_1 lines in Na-22 and 23 measured by saturation spectroscopy," Z. Phys. A: At. Nucl. **281**, 199–204 (1977).

Puchalski, M. and Pachucki, K., "Fine and hyperfine splitting of the 2P state in Li and Be^+," Phys. Rev. A **79**, 032510 (2009).

Quirk, J. A., Damitz, A., Tanner, C. E., and Elliott, D. S., "Measurement of the hyperfine coupling constants and absolute energies of the $12s^2S_{1/2}$, $13s^2S_{1/2}$, and $11d^2D_J$ levels in atomic cesium," Phys. Rev. A **105**, 022819 (2022a).

Quirk, J. A., Sherman, L.,Damitz, A., Tanner, C. E., and Elliott, D. S., "Measurement of the hyperfine coupling constants and absolute energies of the $8p\ ^2P_{1/2}$ and $8p\ ^2P_{3/2}$ levels in atomic cesium," arXiv:2209.08142 [physics.atom-ph] (2022b).

Rafac, R. J. and Tanner, C. E., "Measurement of the ^{133}Cs $6p^2P_{1/2}$ state hyperfine structure," Phys. Rev. A **56**, 1027–1030 (1997).

Raghavan, P., "Table of nuclear moments," At. Data Nucl. Data Tables **42**, 189–291 (1989).

Rahaman, B. and Dutta, S. "Hyperfine coupling constants of the cesium $7D_{5/2}$ state measured up to the octupole term," Opt. Lett. **47**, 4612–4615 (2022a).

Rahaman, B. and Dutta, S. "High precision measurement of the hyperfine splitting and ac Stark shift of the $7d^2D_{3/2}$ state in atomic cesium," Phys. Rev. A **106**, 042811 (2022b).

Raimond, J. M., Goy, P., Vitrant, G., and Haroche, S., "Millimeter-wave spectroscopy of cesium Rydberg states and possible applications to frequency metrology," J. Phys. Colloq. **42**, C8-37–C8-43 (1981).

Ramos, A., Cardman, R., and Raithel, G., "Measurement of the hyperfine coupling constant for $nS_{1/2}$ Rydberg states of ^{85}Rb," Phys. Rev. A **100**, 062515 (2019).

Ramsey, N. F., *Molecular Beams* (Oxford University Press, New York, 1956).

Rapol, U. D., Krishna, A., and Natarajan, V., "Precise measurement of hyperfine structure in the $5P_{3/2}$ state of ^{85}Rb," Eur. Phys. J. D **23**, 185–188 (2003).

Ren, Y.-N., Yang, B.-D., Wang, J., Yang, G., and Wang, J.-M., "Measurement of the magnetic dipole hyperfine constant A_{hfs} of cesium $7S_{1/2}$ state," Act. Phys. Sin. **65**, 073103 (2016).

Roberts, B. M. and Ginges, J. S. M., "Nuclear magnetic moments of francium-207–213 from precision hyperfine comparisons," Phys. Rev. Lett. **125**, 063002 (2020).

Rui, Y., Wu, Y.-L., Li, R., and Wu, H.-B., "Precise absolute frequency measurement of three-electron Li^6 atom D-line transitions," Sci. Sin. **51**, 074209 (2021).

Rukhin, A. L., "Weighted means statistics in interlaboratory studies," Metrologia **46**, 323–331 (2009).

Rukhin, A. L., "Homogeneous data clusters in interlaboratory studies," Metrologia **56**, 035002 (2019).

Rupasinghe, P., Wee, F., Bullock, T., and Liu, J.-X., "Measurement of hyperfine constants and the isotope shift of rubidium $5P^2P_{1/2}$ excited-state using saturated absorption spectroscopy," arXiv:2208.04244 (2022).

Rydberg, S. and Svanberg, S., "Investigation of the $np\ ^2P_{3/2}$ level sequence in the Cs I spectrum by level crossing spectroscopy," Phys. Scr. **5**, 209–212 (1972).

Ryschka, M. and Marek, J., "Observation of quantum beats in superradiance on the $5^2D_{3/2}$–$6^2P_{1/2}$ transition in cesium vapours," Phys. Lett. A **86**, 98–100 (1981).

Safronova, M. S., Budker, D., DeMille, D., Kimball, D. F. J., Derevianko, A., and Clark, C. W., "Search for new physics with atoms and molecules," Rev. Mod. Phys. **90**, 025008 (2018).

Safronova, M. S., Johnson, W. R., and Derevianko, A., "Relativistic many-body calculations of energy levels, hyperfine constants, electric-dipole matrix elements, and static polarizabilities for alkali-metal atoms," Phys. Rev. A **60**, 4476–4487 (1999).

Safronova, M. S. and Safronova, U. I., "Critically evaluated theoretical energies, lifetimes, hyperfine constants, and multipole polarizabilities in ^{87}Rb," Phys. Rev. A **83**, 052508 (2011).

Safronova, U. I. and Safronova, M. S., "High-accuracy calculation of energies, lifetimes, hyperfine constants, multipole polarizabilities, and blackbody radiation shift in ^{39}K," Phys. Rev. A **78**, 052504 (2008).

Sagle, J. and van Wijngaarden, W. A., "Excited state hyperfine structures in ^{133}Cs using quantum beat spectroscopy," Can. J. Phys. **69**, 808–812 (1991).

Sahoo, B. K., Nandy, D. K., Das, B. P., and Sakemi, Y., "Correlation trends in the hyperfine structures of ^{210,212}Fr," Phys. Rev. A **91**, 042507 (2015).

Sansonetti, C. J., Simien, C. E., Gillaspy, J. D., Tan, J. N., Brewer, S. M., Brown, R. C., Wu, S., and Porto, J. V., "Absolute transition frequencies and quantum interference in a frequency comb based measurement of the ^{6,7}Li D lines," Phys. Rev. Lett. **107**, 023001 (2011).

Sansonetti, J. E., "Spectroscopic data for neutral francium (Fr I)," J. Phys. Chem. Ref. Data **36**, 497–507 (2007).

Saßmannshausen, H., Merkt, F., and Deiglmayr, J., "High-resolution spectroscopy of Rydberg states in an ultracold cesium gas," Phys. Rev. A **87**, 032519 (2013).

Scherf, W., Khait, O., Jäger, H., and Windholz, L., "Re-measurement of the transition frequencies, fine structure splitting and isotope shift of the resonance lines of lithium, sodium and potassium," Z. Phys. D: At., Mol. Clusters **36**, 31–33 (1996).

Shimizu, F., Shimizu, K., Gomi, Y.-i., and Takuma, H., "Direct observation of hyperfine splittings of the ^{7}Li $2P_{3/2}$ state by subnatural linewidth spectroscopy," Phys. Rev. A **35**, 3149–3151 (1987).

Shiner, A. D., Madej, A. A., Dubé, P., and Bernard, J. E., "Absolute optical frequency measurement of saturated absorption lines in Rb near 422 nm," Appl. Phys. B **89**, 595–601 (2007).

Sieradzan, A., Kulatunga, P., and Havey, M., "Hyperfine-structure measurements in the $4p^2P_{3/2}$ state of ^{41}K using polarization quantum-beat spectroscopy," Phys. Rev. A **52**, 4447–4450 (1995).

Sieradzan, A., Stoleru, R., Yei, W., and Havey, M. D., "Measurement of hyperfine coupling constants in the $3d^2D_j$ levels of ^{39}K, ^{40}K, and ^{41}K by polarization quantum-beat spectroscopy," Phys. Rev. A **55**, 3475–3483 (1997).

Simsarian, J. E., Ghosh, A., Gwinner, G., Orozco, L. A., Sprouse, G. D., and Voytas, P. A., "Magneto-optic trapping of ^{210}Fr," Phys. Rev. Lett. **76**, 3522–3525 (1996).

Simsarian, J. E., Zhao, W. Z., Orozco, L. A., and Sprouse, G. D., "Two-photon spectroscopy of the francium $8S_{1/2}$ level," Phys. Rev. A **59**, 195–199 (1999).

Sinclair, A. G., McDonald, B. D., Riis, E., and Duxbury, G., "Double resonance spectroscopy of laser-cooled Rb atoms," Opt. Commun. **106**, 207–212 (1994).

Singh, A. K., Muanzuala, L., and Natarajan, V., "Precise measurement of hyperfine structure in the $2P_{1/2}$ state of ^{7}Li using saturated-absorption spectroscopy," Phys. Rev. A **82**, 042504 (2010).

Singh, Y., Nandy, D. K., and Sahoo, B. K., "Reexamination of nuclear quadrupole moments in $^{39-41}$K isotopes," Phys. Rev. A **86**, 032509 (2012).

Snadden, M. J., Bell, A. S., Riis, E., and Ferguson, A. I., "Two-photon spectroscopy of laser-cooled Rb using a mode-locked laser," Opt. Commun. **125**, 70–76 (1996).

Stalnaker, J. E., Ayer, H. M. G., Baron, J. H., Nuñez, A., and Rowan, M. E., "Measurement of the $4S_{1/2} \rightarrow 6S_{1/2}$ transition frequency in atomic potassium via direct frequency-comb spectroscopy," Phys. Rev. A **96**, 012504 (2017).

Stalnaker, J. E., Mbele, V., Gerginov, V., Fortier, T. M., Diddams, S. A., Hollberg, L., and Tanner, C. E., "Femtosecond frequency comb measurement of absolute frequencies and hyperfine coupling constants in cesium vapor," Phys. Rev. A **81**, 043840 (2010).

Stevens, G. D., Iu, C.-H., Williams, S., Bergeman, T., and Metcalf, H., "Hyperfine splitting of the $3\,^2S$ state of ^{7}Li measured using Stark spectroscopy of Rydberg states," Phys. Rev. A **51**, 2866–2869 (1995).

Stoicheff, B. P. and Weinberger, E., "Doppler-free two-photon absorption spectrum of rubidium," Can. J. Phys. **57**, 2143–2154 (1979).

Stone, N. J., "Table of nuclear magnetic dipole and electric quadrupole moments," At. Data Nucl. Data Tables **90**, 75–176 (2005).

Svanberg, S. and Belin, G., "Determination of hyperfine structure and g_j factors in the sequences of ^{2}D states in alkali atoms using a tunable dye laser," J. Phys. B: At. Mol. Phys. **7**, L82–L86 (1974).

Svanberg, S. and Tsekeris, P., "Hyperfine-structure investigation of highly excited ^{2}D levels in ^{87}Rb and ^{133}Cs using a cw tunable dye laser in a two-step excitation scheme," Phys. Rev. A **11**, 1125–1137 (1975).

Svanberg, S., Tsekeris, P., and Happer, W., "Hyperfine-structure studies of highly excited D and F levels in alkali atoms using a cw tunable dye laser," Phys. Rev. Lett. **30**, 817–820 (1973).

Tai, C., Gupta, R., and Happer, W., "Hyperfine structure of the $8^2P_{1/2}$ state of Cs^{133}," Phys. Rev. A **8**, 1661–1665 (1973).

Tai, C., Happer, W., and Gupta, R., "Hyperfine structure and lifetime measurements of the second-excited D states of rubidium and cesium by cascade fluorescence spectroscopy," Phys. Rev. A **12**, 736–747 (1975).

Tang, Y.-B., Lou, B.-Q., and Shi, T.-Y., "*Ab initio* studies of electron correlation effects in magnetic dipolar hyperfine interaction of Cs," J. Phys. B: At., Mol. Opt. Phys. **52**, 055002 (2019).

Tanner, C. E. and Wieman, C., "Precision measurement of the hyperfine structure of the ^{133}Cs $6P_{3/2}$ state," Phys. Rev. A **38**, 1616–1617 (1988).

Tauschinsky, A., Newell, R., van Linden van den Heuvell, H. B., and Spreeuw, R. J. C., "Measurement of ^{87}Rb Rydberg-state hyperfine splitting in a room-temperature vapor cell," Phys. Rev. A **87**, 042522 (2013).

Tetu, M., Fortin, R., and Savard, J.-Y., "A new determination of the Rb85 unperturbed hyperfine transition frequency," IEEE Trans. Instrum. Meas. **IM-25**, 477–480 (1976).

Thibault, C., Touchard, F., Büttgenbach, S., Klapisch, R., De Saint Simon, M., Duong, H. T., Jacquinot, P., Juncar, P., Liberman, S., Pillet, P., Pinard, J., Vialle, J. L., Pesnelle, A., Huber, G., and the Isolde Collaboration, "Hyperfine structure and isotope shift of the D_2 line of $^{118-145}$Cs and some of their isomers," Nucl. Phys. A **367**, 1–12 (1981a).

Thibault, C., Touchard, F., Büttgenbach, S., Klapisch, R., de Saint Simon, M., Duong, H. T., Jacquinot, P., Juncar, P., Liberman, S., Pillet, P., Pinard, J., Vialle, J. L., Pesnelle, A., and Huber, G., "Hyperfine structure and isotope shift of the D_2 line of $^{76-98}$Rb and some of their isomers," Phys. Rev. C **23**, 2720–2729 (1981b).

Thompson, D. C., O'Sullivan, M. S., Stoicheff, B. P., and Xu, G.-X., "Doppler-free two-photon absorption spectrum of potassium," Can. J. Phys. **61**, 949–955 (1983).

Tian, Y.-L., Yang, P.-F., Wu, W., Li, S.-K., Li, G., Zhang, P.-F., and Zhang, T.-C., "Precision measurement of cesium 6S–7S two-photon spectra with single trapped atoms," Jpn. J. Appl. Phys. **58**, 042002 (2019).

Tiesinga, E., Mohr, P. J., Newell, D. B., and Taylor, B. N., "CODATA recommended values of the fundamental physical constants: 2018," Rev. Mod. Phys. **93**, 025010 (2021).

Touchard, F., Guimbal, P., Büttgenbach, S., Klapisch, R., De Saint Simon, M., Serre, J. M., Thibault, C., Duong, H. T., Juncar, P., Liberman, S., Pinard, J., and Vialle, J. L., "Isotope shifts and hyperfine structure of $^{38-47}$K by laser spectroscopy," Phys. Lett. B **108**, 169–171 (1982).

Truong, G.-W., Anstie, J. D., May, E. F., Stace, T. M., and Luiten, A. N., "Accurate lineshape spectroscopy and the Boltzmann constant," Nat. Commun. **6**, 8345 (2015).

Tsekeris, P., Farley, J., and Gupta, R., "Measurement of the hyperfine structure of the $8^2P_{1/2}$ state of ^{87}Rb and the $9^2P_{1/2}$ state of ^{133}Cs," Phys. Rev. A **11**, 2202–2203 (1975).

Tsekeris, P. and Gupta, R., "Measurement of hyperfine structure of the $8^2S_{1/2}$ and $9^2S_{1/2}$ states of rubidium, and $12^2S_{1/2}$ state of cesium by stepwise dye-laser spectroscopy," Phys. Rev. A **11**, 455–459 (1975).

Tsekeris, P., Gupta, R., Happer, W., Belin, G., and Svanberg, S., "Determination of hyperfine structure of highly excited S states in alkali atoms using a CW dye laser," Phys. Lett. A **48**, 101–102 (1974).

TsekerisP., Liao, K. H., and Gupta, R., "Radiofrequency spectroscopy of the $5^2S_{1/2}$ state of ^{23}Na: Hyperfine-structure measurement," Phys. Rev. A **13**, 2309–2310 (1976).

Udem, T., Reichert, J., Holzwarth, R., and Hänsch, T. W., "Absolute optical frequency measurement of the cesium D_1 line with a mode-locked laser," Phys. Rev. Lett. **82**, 3568–3571 (1999).

Umfer, C., Windholz, L., and Musso, M., "Investigations of the sodium and lithium D-lines in strong magnetic fields," Z. Phys. D: At., Mol. Clusters **25**, 23–29 (1992).

Vadla, C., Obrebski, A., and Niemax, K., "Isotope shift of the $3s^2S_{1/2}$ and $3p^2P_J$ levels in ^{6,7}Li," Opt. Commun. **63**, 288–292 (1987).

van Wijngaarden, W. A., Bonin, K. D., and Happer, W., "Observation of quantum beats in the $6D_{3/2} \rightarrow 5P_{1/2}$ transition in ^{85}Rb," Phys. Rev. A **33**, 77–81 (1986).

van Wijngaarden, W. A., Li, J., and Koh, J., "Hyperfine-interaction constants of the $8D_{3/2}$ state in ^{85}Rb using quantum-beat spectroscopy," Phys. Rev. A **48**, 829–831 (1993).

van Wijngaarden, W. A. and Sagle, J., "Hyperfine structure of excited alkali states using quantum beat spectroscopy," J. Phys. B: At., Mol. Opt. Phys. **24**, 897–903 (1991a).

van Wijngaarden, W. A. and Sagle, J., "Magnetic-field decoupling of an alkali-metal excited-state hyperfine structure," Phys. Rev. A **43**, 2171–2178 (1991b).

van Wijngaarden, W. A. and Li, J., "Measurement of hyperfine structure of sodium $3P_{1/2,3/2}$ states using optical spectroscopy," Z. Phys. D: At., Mol. Clusters **32**, 67–71 (1994).

Volz, U., Majerus, M., Liebel, H., Schmitt, A., and Schmoranzer, H., "Precision lifetime measurements on NaI $3p^2P_{1/2}$ and $3p^2P_{3/2}$ by beam-gas-laser spectroscopy," Phys. Rev. Lett. **76**, 2862–2865 (1996).

Voss, A., Buchinger, F., Cheal, B., Crawford, J. E., Dilling, J., Kortelainen, M., Kwiatkowski, A. A., Leary, A., Levy, C. D. P., Mooshammer, F., Ojeda, M. L., Pearson, M. R., Procter, T. J., and Tamimi, W. A., "Nuclear moments and charge radii of neutron-deficient francium isotopes and isomers," Phys. Rev. C **91**, 044307 (2015).

Voss, A., Pearson, M. R., Billowes, J., Buchinger, F., Cheal, B., Crawford, J. E., Kwiatkowski, A. A., Levy, C. D. P., and Shelbaya, O., "First use of high-frequency intensity modulation of narrow-linewidth laser light and its application in determination of ^{206,205,204}Fr ground-state properties," Phys. Rev. Lett. **111**, 122501 (2013).

Walls, J., Ashby, R., Clarke, J. J., Lu, B., and van Wijngaarden, W. A., "Measurement of isotope shifts, fine and hyperfine structure splittings of the lithium D lines," Eur. Phys. J. D **22**, 159–162 (2003).

Wang, J., Liu, H.-F., Yang, B.-D., He, J., and Wang, J.-M., "Determining the hyperfine structure constants of caesium $8S_{1/2}$ state aided by atomic coherence," Meas. Sci. Technol. **25**, 035501 (2014a).

Wang, J., Liu, H.-F., Yang, G., Yang, B.-D., and Wang, J.-M., "Determination of the hyperfine structure constants of the ^{87}Rb and ^{85}Rb $4D_{5/2}$ state and the isotope hyperfine anomaly," Phys. Rev. A **90**, 052505 (2014b).

Wang, J., Wang, J.-M., Liu, H.-F., Yang, B.-D., and He, J., "Measurement of hyperfine splitting and determination of hyperfine structure constant of cesium $8S_{1/2}$ state by using of ladder-type EIT," Proc. SPIE **8773**, 877311 (2013).

Wang, Q., Zhang, N., Guang, W., Zhang, S.-G., Wang, W.-L., Wei, R., and Wang, Y.-Z., "Precision measurements of the ground-state hyperfine splitting of ^{85}Rb using an atomic fountain clock," Phys. Rev. A **100**, 022510 (2019).

Wang, S.-D., Yuan, J.-P., Wang, L.-R., Xiao, L.-T., and Jia, S.-T., "Investigation on the Cs $6S_{1/2}$ to 7D electric quadrupole transition via monochromatic two-photon process at 767 nm," Front. Phys. **16**, 12502 (2021).

Wang, Z., Zhang, J., Zeng, Z., Yan, K., Zhou, H., and Yang, B., "Hyperfine energy level splitting structure measurement of the excited state $6D_{5/2}$ for cesium atom," Laser Optoelectron. Prog. **57**, 030202 (2020a).

Wang, Z.-R., Hou, X.-K., Bai, J.-D., and Wang, J.-M., "Measuring the hyperfine splitting and deriving the hyperfine interaction constants of the cesium $5p^6 7d^2 D_{5/2}$ excited state," Appl. Sci. **10**, 8178 (2020b).

Wilkins, S. G., Lynch, K. M., Billowes, J., Binnersley, C. L., Bissell, M. L., Cocolios, T. E., Goodacre, T. D., de Groote, R. P., Farooq-Smith, G. J., Flanagan, K. T., Franchoo, S., Ruiz, R. F. G., Gins, W., Heylen, H., Koszorús, A., Neyens, G., Stroke, H. H., Vernon, A. R., Wendt, K. D. A., and Yang, X. F., "Quadrupole moment of ^{203}Fr," Phys. Rev. C **96**, 034317 (2017).

Williams, W. D., Herd, M. T., and Hawkins, W. B., "Spectroscopic study of the $7p_{1/2}$ and $7p_{3/2}$ states in cesium-133," Laser Phys. Lett. **15**, 095702 (2018).

Windholz, L., Jäger, H., Musso, M., and Zerza, G., "Laserspectroscopic investigations of the lithium-*D*-lines in magnetic fields," Z. Phys. D: At., Mol. Clusters **16**, 41–47 (1990).

Wood, C. S., Bennett, S. C., Cho, D., Masterson, B. P., Roberts, J. L., Tanner, C. E., and Wieman, C. E., "Measurement of parity nonconservation and an anapole moment in cesium," Science **275**, 1759–1763 (1997).

Wu, C.-M., Liu, T.-W., Wu, M.-H., Lee, R.-K., and Cheng, W.-Y., "Absolute frequency of cesium 6*S*–8*S* 822 nm two-photon transition by a high-resolution scheme," Opt. Lett. **38**, 3186–3189 (2013).

Wu, Y.-L., Li, R., Rui, Y., Jiang, H.-F., and Wu, H.-B., "Precise measurement of ^{6}Li transition frequencies and hyperfine splitting," Acta Phys. Sin. **67**, 163201 (2018).

Yang, G., Wang, J., and Wang, J.-M., "Determination of the hyperfine coupling constants of the $5D_{5/2}$ of ^{85}Rb atoms by using high signal-to-noise ratio electromagnetically-induced transparency spectra," Acta Phys. Sin. **66**, 103201 (2017).

Yan, G., Wang, J., Yang, B.-D., and Wang, J.-M., "Determination of the hyperfine coupling constant of the cesium $7S_{1/2}$ state," Laser Phys. Lett. **13**, 085702 (2016).

Ye, J., Swartz, S., Jungner, P., and Hall, J. L., "Hyperfine structure and absolute frequency of the ^{87}Rb $5P_{3/2}$ state," Opt. Lett. **21**, 1280–1282 (1996).

Yei, W., Sieradzan, A., Cerasuolo, E., and Havey, M. D., "Measurement of hyperfine coupling constants of the $5d^2D_j$ levels in Cs using polarization quantum-beat spectroscopy," Phys. Rev. A **57**, 3419–3424 (1998).

Yei, W., Sieradzan, A., and Havey, M. D., "Delayed-detection measurement of atomic Na $3p\ ^2P_{3/2}$ hyperfine structure using polarization quantum-beat spectroscopy," Phys. Rev. A **48**, 1909–1915 (1993).

Zhang, J., Tandecki, M., Collister, R., Aubin, S., Behr, J. A., Gomez, E., Gwinner, G., Orozco, L. A., Pearson, M. R., and Sprouse, G. D., and FrPNC Collaboration, "Hyperfine anomalies in Fr: Boundaries of the spherical single particle model," Phys. Rev. Lett. **115**, 042501 (2015).

Zhang, S.-N., Zhang, X.-G., Jiang, Z.-J., Shang, H.-S., Chang, P.-Y., Chen, J.-B., Lian, J.-Q., Tu, J.-H., and Yang, S.-Y., "Precision measurement of the hyperfine structure of the ^{85}Rb $6P_{3/2}$ state," in *2017 Joint Conference of the European Frequency and Time Forum and IEEE International Frequency Control Symposium (EFTF/IFCS)* (IEEE, New York, 2017), pp. 762–764.

Zhao, X., Crane, S. G., Guckert, R., and Vieira, D. J., "Hyperfine structure and isotope shift of ^{82}Rb D_1 and D_2 transitions," Phys. Rev. A **60**, 4730–4733 (1999).

Zhu, M., Oates, C. W., and Hall, J. L., "Improved hyperfine measurements of the Na 5*p* excited state through frequency-controlled Dopplerless spectroscopy in a Zeeman magneto-optic laser trap," Opt. Lett. **18**, 1186–1188 (1993).

zu Putlitz, G. and Venkataramu, K. V., "Hyperfeinstruktur und lebensdauer des $8^2P_{3/2}$-terms von rubidium," Z. Phys. A: Hadrons Nucl. **209**, 470–473 (1968).

Zyla, P. *et al.*, "Review of particle physics," Prog. Theor. Exp. Phys. **2020**, 083C01 (2020).